DOCTORAL THESIS

Osteoblastic PLEKHO1 contributes to joint inflammation in rheumatoid arthritis

Dang, Lei

Date of Award:
2019

HONG KONG BAPTIST UNIVERSITY

Doctor of Philosophy

THESIS ACCEPTANCE

DATE: June 14, 2019

STUDENT'S NAME: DANG Lei

THESIS TITLE: Osteoblastic PLEKHO1 Contributes to Joint Inflammation in Rheumatoid Arthritis

This is to certify that the above student's thesis has been examined by the following panel members and has received full approval for acceptance in partial fulfillment of the requirements for the degree of Doctor of Philosophy.

Chairman:	Prof Yu Zhiling Professor, Chinese Medicine - Teaching and Research Division, HKBU (Designated by Dean of School of Chinese Medicine)
Internal Members:	Dr Han Simon Q B Associate Professor, Chinese Medicine - Teaching and Research Division, HKBU (Designated by Director of Chinese Medicine - Teaching and Research Division)
	Prof Chen Hubiao Professor, Chinese Medicine - Teaching and Research Division, HKBU
External Members:	Prof Pan Xiaohua Professor Department of Orthopaedics and Traumatology Shenzhen Bao'an People's Hospital
	Dr Peng Songlin Associate Professor Department of Spine Surgery Jinan University Second Medical College
In-attendance:	Prof Zhang Ge Professor, Chinese Medicine - Teaching and Research Division, HKBU

Issued by Graduate School, HKBU

Osteoblastic PLEKHO1 Contributes to Joint Inflammation in Rheumatoid Arthritis

Dang Lei

A thesis submitted in partial fulfilment of the requirements for the degree of Doctor of Philosophy

Principal Supervisor:

Prof. Zhang Ge (Hong Kong Baptist University)

June 2019

DECLARATION

I hereby declare that this thesis represents my own work which has been done after registration for the degree of PhD at Hong Kong Baptist University, and has not been previously included in a thesis or dissertation submitted to this or any other institution for a degree, diploma or other qualifications.

I have read the University's current research ethics guidelines, and accept responsibility for the conduct of the procedures in accordance with the University's Research Ethics Committee (REC). I have attempted to identify all the risks related to this research that may arise in conducting this research, obtained the relevant ethical and/or safety approval (where applicable), and acknowledged my obligations and the rights of the participants.

Signature: Danglei

Date: June 2019

Abstract

Background: Osteoblasts participating in the inflammation regulation gradually obtain concerns. However, its role in joint inflammation of rheumatoid arthritis (RA) is largely unknown. Here, we investigated the role of osteoblastic pleckstrin homology domain-containing family O member 1 (PLEKHO1), a negative regulator of osteogenic lineage activity, in regulating joint inflammation in RA.

Methods: The level of osteoblastic PLEKHO1 in RA patients and collagen-induced arthritis (CIA) mice was examined. The role of osteoblastic PLEKHO1 in joint inflammation was evaluated by a CIA mice model which was induced in osteoblast-specific *Plekho1* conditional knockout mice and mice expressing high *Plekho1* exclusively in osteoblasts, respectively. The effect of osteoblastic PLEKHO1 inhibition was explored in a CIA mice model. The mechanism of osteoblastic PLEKHO1 in regulating joint inflammation was performed by a series of *in vitro* studies.

Results: PLEKHO1 was highly expressed in osteoblasts from RA patients and CIA mice. Osteoblastic *Plekho1* deletion ameliorated joint inflammation, whereas overexpressing *Plekho1* only within osteoblasts exacerbated local inflammation in CIA mice. PLEKHO1 was required for TNF receptor-associated factor 2 (TRAF2)-mediated the ubiquitination of receptor-interacting serine/threonine-protein kinase 1 (RIP1) to activate nuclear factor kappa-light-chain-enhancer of activated B (NF-kB) pathway for inducing inflammatory cytokines production in osteoblasts. Moreover, osteoblastic PLEKHO1 inhibition improved joint inflammation and attenuated bone formation reduction in CIA mice.

Conclusions: These data strongly suggest that highly expressed PLEKHO1 in osteoblasts mediates joint inflammation in RA. Targeting osteoblastic PLEKHO1 may exert dual therapeutic action of alleviating joint inflammation and promoting bone repair in RA.

Acknowledgements

I would like to take this opportunity to greatly thank my supervisors Prof. Ge Zhang, Prof. Aiping Lyu, and Dr. Zhijun Yang for their guidance, support, patience, and encouragement during my Ph.D. study, not only in my research project, but also in my life. I also really appreciate the enormous amount of time and attention they have given to me during writing and revising my paper, as well as the thesis.

I would also like to express my gratitude to all my labmates, Dr. Xiaojuan He, Dr. Fangfei Li, Dr. Yuanyuan Yu, Dr. Jin Liu, Dr. Chao Liang, Dr. Jun Lu, Dr. Shaikh Atik Badshah, Dr. Daogang Guan, Dr. Shuaijian Ni, Dr. Shengzheng Wang, Mr. Kang Zheng, Ms. Qingqing Guo, Ms. Xiaoqiu Wu, Ms. Luyao Wang, Ms. Qing Ren, Ms. Duoli Xie, Mr. Rongcheng Dai, Mr. Huarui Zhang, Mr. Chuanxin Zhong, Mr. Dijie Li, and Mr. Xuekun Fu for their valuable suggestions and kind help on my project as well as the happy time they brought to me during these years. Thank Ms. Hilda Cheung and Mr. Chileung Chan in School of Chinese Medicine, Hong Kong Baptist University for their technical support during experiments. Last but not the least, my greatest gratitude goes to my friends and family for their love, support, and encouragement in my life.

This study was support by the Hong Kong General Research Fund (HKBU479111, HKBU478312, HKBU 12114416, HKBU262913, HKBU261113, HKBU12122516), the Natural Science Foundation Council of China (81272045, 81470072, 81700780), the Research Grants Council & Natural Science Foundation Council of China (N_HKBU435/12), the Hong Kong Baptist University Strategic Development Fund (SDF15-0324-P02), and the National Key R&D Program of China (2018YFC1705205).

Table of Contents

List of Figures

List of Tables

List of Abbreviation

ACPA	Anti-citrullinated protein antibody
Ang1	Angiopoietin 1
ANOVA	One-way analysis of variance
APC	Antigen-presenting cells
APRIL	A proliferation‑inducing ligand
BFR/BS	Bone formation rate/bone surface
BLyS	B lymphocyte stimulator
BMD	Bone mineral density
BMP	Bone morphogenetic protein
BSA	Bovine serum albumin
BV/TV	Bone volume fraction
cBMD	Cortical BMD
cBV/TV	Cortical BV/TV
CFA	Complete Freund’s adjuvant
c-Fms	Macrophage colony-stimulating factor receptor
CIA	Collagen-induced arthritis
CKIP-1	Casein kinase-2 interacting protein-1
CRP	C-reactive protein
CTLA-8	Cytotoxic T-lymphocyte-associated antigen 8
EDTA	Ethylenediaminetetraacetic acid
ELISA	Enzyme-linked immunosorbent assay
FBS	Fetal bovine serum
FGF	Fibroblast growth factor
FLS	Fibroblast-like synoviocyte
G-CSF	Granulocyte-colony stimulating factor
GMCSF	Granulocyte-macrophage colony-stimulating factor
H&E	Hematoxylin and eosin

hTERT	Human telomerase reverse transcriptase
IB	Immunoblotting
IFN-γ	Interferon gamma
IL-1	Interleukin 1
IL-2	Interleukin 2
IL-6	Interleukin 6
IL-8	Interleukin 8
IL-15	Interleukin 15
IL-16	Interleukin 16
IL-17	Interleukin 17
IL-18	Interleukin 18
IL-33	Interleukin 33
ILGF-1	Insulin like growth factor-1
IP	Immunoprecipitation
LCM	Laser capture micro-dissection
MAR	Mineral apposition rate
M-CSF	Macrophage colony-stimulating factor
MHC	Major histocompatibility complex
MicroCT	Micro computed tomography
MMP	Matrix metalloproteinases
MSC	Mesenchymal stem cells
NF-kB	Nuclear factor kappa-light-chain-enhancer of activated B
NK	Nature killer
Ob.N/B.Pm	Osteoblast number per bone perimeter
Ob.S/BS	Osteoblast surface/bone surface
Ocn	Osteocalcin
Oc.N/B.Pm	Osteoclast number per bone perimeter
Oc.S/BS	Osteoclast surface/bone surface
PADI4	Peptidyl arginine deiminase, type IV

PBS	Phosphate-buffered saline
PCR	Polymerase chain reaction
PDGF	Platelet derived growth factor
PGE_2	Prostaglandin E2
PLEKHO1	Pleckstrin homology domain-containing family O member 1
PTPN22	Protein tyrosine phosphatase, non-receptor type 22
PVDF	Polyvinylidene difluoride
RA	Rheumatoid arthritis
RANK	Receptor activator of nuclear factor κB
RANKL	Receptor activator of nuclear factor κB ligand
RF	Rheumatoid factor
RIP1	Receptor-interacting serine/threonine-protein kinase 1
STA	K/BxN serum-transfer arthritis
STAT4	Signal transducer and activator of transcription 4
TCR	T-cell receptor
tBMD	Trabecular BMD
Tb.N	Trabecular number
Tb.Th	Trabecular thickness
tBV/TV	Trabecular BV/TV
Th	T helper cells
TNF-α	Tumor necrosis factor alpha
TNFAIP3	TNF alpha induced protein 3
TRADD	TNFR1-associated death domain protein
TRAF1-C5	Tumor necrosis factor-receptor associated factor 1/complement component 5
TRAF2	TNF receptor-associated factor 2
Tregs	Regulatory T cells
VEGF	Vascular endothelial growth factor

WT	Wild-type

Chapter One

Introduction

1. Clinical Challenge in Rheumatoid Arthritis

Rheumatoid arthritis (RA) is a chronic, progressive, inflammatory autoimmune disease. RA affects over 1.3 million Americans and more than 1% of the population in the whole world (Freeman and J., 2018). Although some patients have controlled the RA in the mild to moderate stage of diseases, many finally experience severe physical disability, joint destruction, and established multiple co-morbidities, such as diabetes mellitus, hypertension, and bronchial asthma (Al-Herz et al., 2016). The progression of RA has reduced the quality of life among patients (Haroon et al., 2007). Moreover, the morality was 54% higher in RA patients than in the general population. The mortality rate was also higher in the patients with RA compared to those with cardiovascular, respiratory, musculoskeletal, and digestive diseases (van den Hoek et al., 2017). The current available agents unmet the need in the RA treatment. A better understanding of how the pathological mechanisms drive the RA progress is urgently required in order to develop effective therapeutics for RA patients.

RA is classically regarded as an “autoimmune disease of unknown aetiology”. Therefore, genes and the environment were considered to be the risk factors of RA. After the trigger of RA by genetic susceptibility and environmental factors, T cells, B cells and the orchestrated interaction of pro-inflammatory cytokines participated in the maturation stage of RA (Guo et al., 2018). At this stage, the pro-inflammation cytokines, tumor necrosis factor alpha (TNF-α), Interleukin 6 (IL-6), Interleukin 1 (IL-1), and Interleukin 17 (IL-17), played important roles in the disease progression (Smolen and Steiner, 2003). At the progressive and late stage of RA, the resulting

inflammation attacked the joints, caused the swelling of the knuckle joints and wrists, leaded to severe pain and stiffness, and finally damaged cartilage and bone. Then, the joints were irreversibly destroyed and fused without appropriate treatment. Although there has been success with anti-inflammatory therapy, the repair of arthritic bone loss is one of most challenging goals in the treatment of RA.

The bone loss in RA suggested the dysregulation of bone homeostasis in inflammation conditions. It required the urgent need for understanding the alternations of functional bone cells in the inflammation environment. Recently, the inflammatory effector cells and their mediators involving in modulating bone cells related to bone homeostasis were reported (Loi et al., 2016). Whether the function cells in bone and their associated factors play the roles in the inflammation environment still remains elusive. Therefore, it is necessary to explore the changes and roles of functional bone cells and their mediators in the inflammation conditions. These findings might offer a novel therapeutic strategy for stimulating bone repair in RA.

In this part, the complex epidemiology and pathobiology of RA will be summarized as currently understood, highlighting the role of effector cells and functions of inflammatory modulators in RA development. In addition, bone loss is the central symptom of RA. The increased understanding of the bone pathology in RA will be introduced. We also focused on the new findings and potential effective treatments of bone loss in RA.

2. Epidemiology of Rheumatoid Arthritis

The population-based studies have released that the RA affected 0.5–1.0% of adults in developed countries. The occurrence of RA was more in women than men. The prevalence of RA rose with age and was highest in women

older than 65 years, suggesting hormonal factors played a pathogenic role in RA progression (Symmons et al., 2002); (Carbonell et al., 2008, Pedersen et al., 2009). Prevalence of RA varied geographically (Costenbader et al., 2008, Biver et al., 2009). The disease was common in north America and northern Europe compared with the rural west Africa (Kalla and Tikly, 2003). These variations were indicative of different genetic risks and environmental exposures.

2.1 Genetic Risk Factors

Recent findings suggested that the RA development was on basis of gene (Smolen and Steiner, 2003). There were more than 80% of RA patients containing the epitope of the HLA-DRB1*04 cluster (Smolen et al., 2007). Among these patients, the ones expressing two HLA-DRB1*04 alleles were at high risk for the development of nodular disease, major organ involvement and surgery related to joint destruction (Weyand et al., 1992). HLADRB1 alleles, with the epitope sequence (QRRAA or KRRAA or RRRAA) at 70~74 position, have a high risk for RA development or close association with the presence of rheumatoid factors (RF) (Klareskog et al., 2008). These findings could be supported by the finding that the amino acid sequence on the HLADR β-chain alleles conferred binding of specific peptides and affected antigen presentation to T-cell receptors (TCR) (Smolen et al., 2007). Disease-associated HLADR alleles might present the arthritis-related peptides. These peptides could stimulate and expand autoantigen-specific T cells in the lymph nodes and joints at the beginning stage of RA (Smolen et al., 2007).

In addition, the results from the single-nucleotide polymorphism genotyping have demonstrated that the polymorphism across the major histocompatibility complex (MHC) was related to the development of RA

(Plenge, 2009). It has contributed to the genetic susceptibility to RA in some ethnic groups. The locus, such as peptidyl arginine deiminase, type IV (PADI4), protein tyrosine phosphatase, non-receptor type 22 (PTPN22), signal transducer and activator of transcription 4 (STAT4), TNF alpha induced protein 3 (TNFAIP3), and tumor necrosis factor-receptor associated factor 1/complement component 5 (TRAF1-C5), was also associated with RA, but they only have a few contribution to the risk of RA (Plenge, 2009).

2.2 Environmental Risk Factors

Smoking was regarded as the dominant environmental risk factor for RA. The smokers with more than 40 packs of cigarette per year have double risk of RA development than nonsmokers, which still continued after quitting smoking (Ludvigsson et al., 2014). The effect of smoking has a strong relation to the production of anti-citrullinated protein antibody (ACPA), one of pathological incentives in RA. Because the smoking has great impact on the changing genetic background to induce ACPAs (Klareskog et al., 2006).

Other potential environmental risk factors, including alcohol intake, coffee intake, low socioeconomic status, oral contraceptive use, vitamin D status, the bronchial stressor such as silica, and infectious agents, were linked to RA development, although supporting evidence for some factors was barely strong (Liao et al., 2009).

3. Stages of Rheumatoid Arthritis

There are four distinct stages in RA progression, and each stage has their own pathological characteristics (**Figure 1-1**).

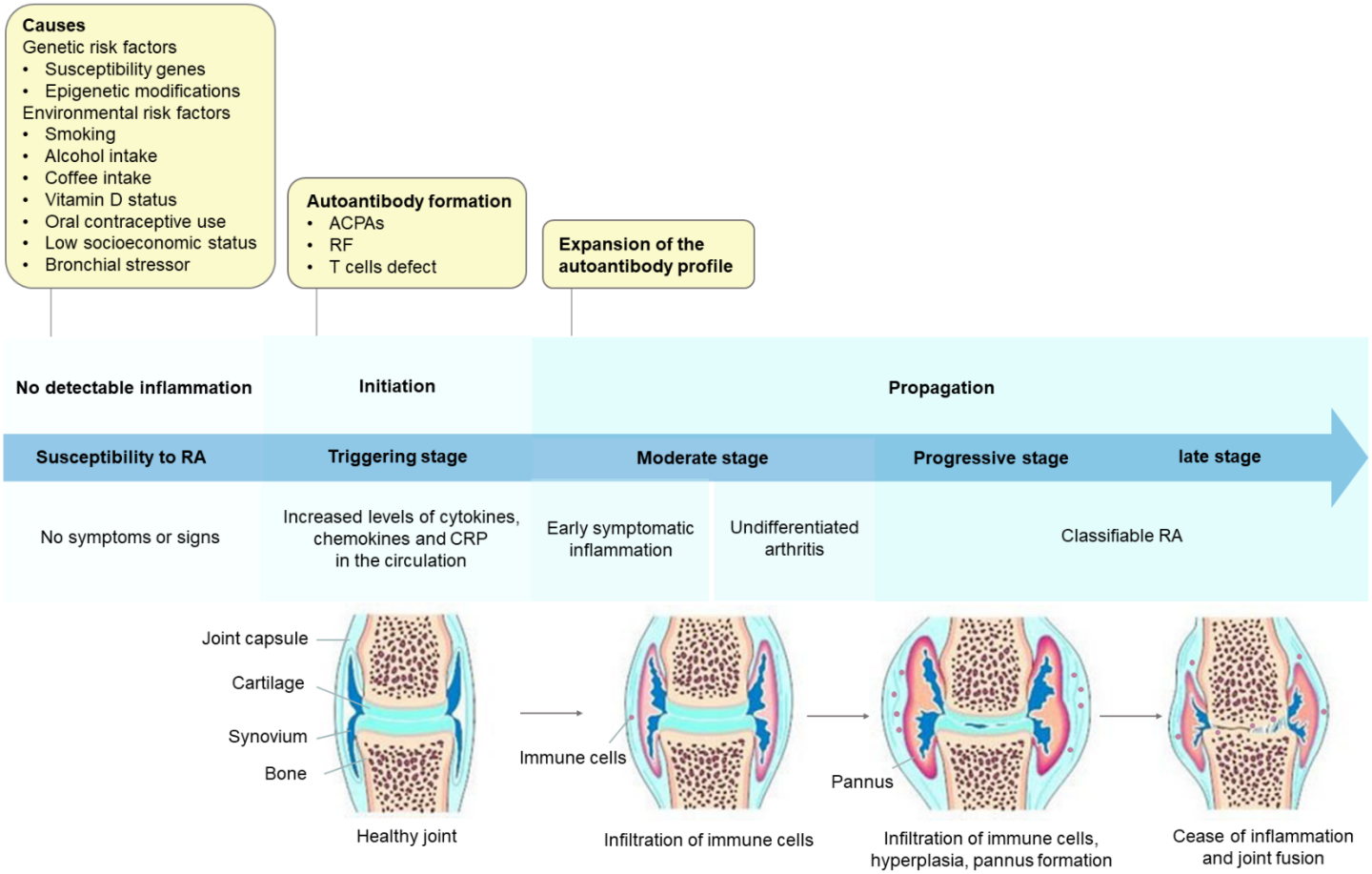

Figure 1-1 Development and progression of four stages in the rheumatoid arthritis (RA). ACPA, anti-citrullinated protein antibody; RF, rheumatoid factor; CRP, C-reactive protein.

3.1 Triggering Stage of Rheumatoid Arthritis

In this stage of RA, the ACPAs are identified to be most specific incentives today. The stimulation of ACPAs suggested the loss of tolerance to post-translational citrullination (Iobagiu et al., 2011). In more detail, PADI4 acted on the citrullinated posttranslational modifications of proteins. The smoking might stimulate the polymorphism in PADI4. Its polymorphism influenced the citrullination and formed the citrullinated antigens, further leading to the production of ACPAs. The production of ACPAs could stimulate RA (Auger et al., 2009).

The infection is another inducer of RA. These infectious agents stimulated the formation of immune complexes, leading to the triggering autoimmune system (Boissier et al., 2012).

In addition, T cells from RA patients have a faster pace of telomere shortening, which was a senescent phenotype. The weak telomere repair and the transcriptional repression of the human telomerase reverse transcriptase (hTERT) increased apoptosis of T cells (Fujii et al., 2009). The apoptosis of T cells could cause the immune attacks, which stimulated the development of organ-specific autoimmune diseases.

3.2 Moderate Stage of Rheumatoid Arthritis

RA has more than 10-year latency period before clinical onset after initial exposure to ACPAs or other RFs (Rantapaa-Dahlqvist et al., 2003). During the latency period, the serum levels of the CRP, Interleukin 15 (IL-15), Interleukin 16 (IL-16), and the type II TNFα receptor (a naturally occurring TNF inhibitor), were abnormally elevated (Karlson et al., 2009).

After the sufficient activation of innate immunity by autologous antigens and

exogenous material, the dendritic cells were firstly activated to stimulate immune response (Smolen and Steiner, 2003, Smolen et al., 2007). Then, the antigen-presenting cells (APCs), including activated B cells, dendritic cells, and macrophages, could display antigen complexed with MHCs on their surfaces, and the T cells recognized them by their TCRs (Smolen and Steiner, 2003, Smolen et al., 2007).

After the TCR received the stimulation from APCs, the T cells differentiated into mature help T cell ($CD4^+$ T cells). The $CD4^+$ T cells helped the activity of other immune cells by releasing T-cell cytokines, such as Interferon gamma (IFN-γ), IL-17, and Interleukin 2 (IL-2), in the synovial membrane to infiltrate the joints (Smolen and Steiner, 2003, Smolen et al., 2007). T-cell activation resulted in the stimulated production of cytokines and chemokines, leading to a feedback loop for additional B-cell, macrophage, and T-cell interactions (Smolen and Steiner, 2003, Smolen et al., 2007).

Moreover, B cells not only presented antigen presentation, but also produced the antibodies, autoantibodies and cytokines in contribution to the RA pathogenesis (Smolen and Steiner, 2003, Smolen et al., 2007). B cells expressed immunoglobulin and differentiation antigens (Smolen et al., 2007). The autoantibodies from B cells could form larger immune complexes that further stimulated the production of pro-inflammatory cytokines through complement and Fc-receptor activation (Smolen et al., 2007).

The stimulation of innate and adaptive immunity paved the way for the RA development (Choy, 2012). For a long-term inflammatory condition in joint, the pathophysiology of RA became deteriorated.

3.3 Progressive Stage of Rheumatoid Arthritis

At this stage, the significant changes of bone and cartilage in the inflamed joints were observed. Although RFs were expressed in the synovial membrane, they were also found in many other organs. Why the immune response took place within local synovial membrane and joint, as well as induced the joint inflammation and destruction at the progressive stage?

Some findings gave the explanation to this phenomenon. There were lymphoid follicles in the synovium. These follicles were the same as those in lymph nodes, and the synovium could connect to the secondary lymphoid organ for activating T and B cells (Weyand et al., 2001). In addition, it has found that the $CD3^{-}TCR\zeta^{dim}$ T cells were accumulated in the synovial fluid than those in the peripheral blood from the RA patients, which suggested the selective migration of these effector cells to inflamed joints and their exit from the circulating pool. These $CD3^{-}TCR\zeta^{dim}$ T cells had the characteristics of differentiated effector T cells. But these specific T cells used accessory pathways for transducing the gene expression of inflammatory cytokine and activate monocytes by the cell-cell contacts. The T-cell–monocyte interactions probably played a vital role in promoting the chronic and excessive cytokines in the inflamed joints (Zhang et al., 2007b). These findings might explain these pathological changes in the local synovium and joints during the progression of RA.

Other key factor for the arthritis in the synovial membrane during RA was the formation of synovial angiogenesis. Vascular endothelial growth factor (VEGF) was the most important proangiogenic factor. The stimuli, such as the cellular proliferation, cellular apoptosis, inflammation, and hypoxia, in the rheumatoid synovium could stimulate the expression of VEGF (Semerano et al., 2011). The VEGF could increase the permeability of blood

vessel, as well as migration and proliferation of endothelial cells (Ferrara, 2001, Eklund and Olsen, 2006). The VEGF could bind to the cognate receptors on endothelial cells for activating the production of matrix metalloproteinases (MMP)s. Then, the basement membrane was degraded by the released MMPs, resulting in migration and proliferation of endothelial cells to form vascular tubules. Finally, blood vessels were stabilized by pro-angiogenic factors such as Angiopoietin 1 (Ang1), followed by the connecting through the pericytes into the new basement membrane to drive the blood flow (Koch, 1998, Folkman and Klagsbrun, 1987, Szekanecz and Koch, 2005). The new formation of blood vessel by angiogenesis could help the inflammatory cells infiltration into the synovium and joints (Szekanecz and Koch, 2008, Koch, 1998, Veale and Fearon, 2006, Lainer-Carr and Brahn, 2007).

The normal synovium consists of a lining layer containing both fibroblast-like synoviocytes (FLSs) and macrophage-like synoviocytes that overlined a sublining layer of the spaces of joints. The newly formed blood vessels mentioned above could facilitate the increase of FLS number. This increase of FLS was also stimulated by the inflammatory microenvironment established by the macrophage-like synoviocytes. This inflammatory microenvironment could amply, resulting in high levels of inflammatory cytokines and MMPs in the synovium and joints (Amano et al., 2003). Then, the lining layer of synovium was markedly thickened to form the pannus, which was caused by the macrophage infiltration.

The pannus was characterized by a heavily infiltrated subintimal region, containing T cells, B cells, and macrophages. And the function of pannus was linked to the stromal oedema and proliferation of blood vessels in the synovium and joints. The pannus could produce the fibroblast growth factor

(FGF), insulin like growth factor-1 (ILGF-1), and platelet derived growth factor (PDGF), which contributed to the vessel remodeling and stability in the VEGF-induced angiogenesis for exacerbating the joint inflammation and destruction (Boissier et al., 2012).

The pannus also contained rich osteoclast precursors (Choy, 2012). These osteoclast precursors in the pannus were from local macrophage-like synoviocytes and inflow macrophages. These macrophages were involved in both the antigen presentation in the synovium infiltration and also osteoclastic bone resorption (Smolen and Steiner, 2003, Smolen et al., 2007). The accumulated evidence demonstrated that osteoclast activation in the pannus was a key process to induce bone erosion. Because it has demonstrated that the specific inhibition of osteoclast activation could reduce joint destruction in RA (Cohen et al., 2008).

Finally, the incorporation of synoviocytes with inflammatory cells finally destroyed the cartilage and bone (Smolen et al., 2007, Amano et al., 2003, McCARTY and D., 1980). The diseased synovial tissue became unrecognizable lining structure.

On the other hand, a more recently mechanism was described about the migration of synovial cells among joints (Lefevre et al., 2009). Cadherin-11 could mediate the FLSs to organize themselves by the cell-cell interactions inside synovial tissue. The absence of cadherin-11 in the FLSs could reduce the disorganization of the synovium in the K/BxN serum-transfer arthritis (STA) model (Lee et al., 2007). This might another mechanism in the synergistic effects of FLSs movement in RA progression.

3.4 Late Stage of Rheumatoid Arthritis

The inflammatory process ceased, and joints fused altogether at the late stage of RA (Freeman and J., 2018). It may not necessarily lead to the late stage of RA after appropriate treatment, although it is difficult to maintain the mobility and range of joint motion.

At this stage, the pro-inflammatory cytokines could stimulate the development of systemic effects. There are cardiovascular diseases, osteoporosis, and the disorders in the hypothalamic-pituitary-adrenal axis (Choy, 2012).

4. Involvement of Critical Cytokines in Rheumatoid Arthritis

The inflammatory cells as well as their secretory cytokines regulate the immune inflammation. The involvement of cytokines in RA aided the cell-cell communication in immune responses and stimulated the cell movement towards inflammatory and infectious sites (McInnes et al., 2016).

Among the cytokines in RA, TNF-α, IL-1, IL-6, and IL-17 are key mediators of cell movement and inflammation in RA (Alunno et al., 2017, Firestein, 2003) (**Table 1-1**).

Table 1-1 Function of relevant pro-inflammatory cytokines in rheumatoid arthritis

Name	Source	Function	Reference
TNF-α	Macrophages/monocytes, T cells	Induce the secretion of secondary cytokines Stimulate the nature killer (NK) cells and macrophages/monocytes Induce fever and apoptosis	(Neunaber et al., 2011, Ferguson et al., 1997)
IL-1	Activated macrophages	Increase bone resorption Stimulate the production of MMPs Stimulate plasminogen activators Stimulate prostaglandin synthesis	(Okada and Murakami, 1998, Svoboda et al., 1994, Dinarello, 1988)
IL-6	T cells, endothelial cells, macrophages/monocytes	Induce fever Regulate growth and differentiation of T cells and B cells Induce the release of soluble TNF receptors and IL-1 Induce acute phase response Inhibit neutrophil apoptosis	(Neunaber et al., 2011, Svoboda et al., 1994)
IL-17	Th 17 cells	Induce inflammation Regulate Cartilage damage Induce bone erosion	(Kawaguchi et al., 2004)

4.1 TNF-α

The activated macrophages and T cells produced the TNF-α. TNF-α exerted pro-inflammatory effects via connecting with its receptors, p75 on immune system cells or p55 in most tissues (Neunaber et al., 2011, Ferguson et al., 1997). These receptors could convert to the natural TNF inhibitors when they were secreted and then cleaved by enzyme in the bloodstream. Although TNF-α exerted pro-inflammatory effects in RA, recent evidence suggested its anti-inflammatory effects (Sfikakis, 2010).

Most of RA patients were responsive to the inhibition of TNF-α. Because the inhibition of TNF-α in RA could directly influence its stimulation of other pro-inflammatory cytokines, and MMPs, as well as modulate the regulatory T cells (Tregs) (Nadkarni et al., 2007, Biton et al., 2011)

It has reported that the TNF-α exerted anti-inflammatory effects through mediating Tregs (Chen et al., 2007). TNF-α connected to the p75 expressed on the surface of Tregs for activating the Tregs development to suppress the immune response (Biton et al., 2012).

4.2 IL-1

IL-1a, IL-1b, Interleukin 18 (IL-18), and Interleukin 33 (IL-33) are members in the IL-1 family, which were highly expressed in RA. The IL-1 is the prototype in these inflammatory cytokine family. The leukocytes, endothelial cells, osteoclasts, and chondrocytes are their target cells in RA (Okada and Murakami, 1998, Svoboda et al., 1994, Dinarello, 1988). IL-1RI and IL-1RII are two receptors of IL-1. Unlike the transmitting IL-1 signals by IL-RI, the IL-RII could act as a decoy receptor by binding and inhibiting IL-1 at the cell membrane (Bessis et al., 2000). Therefore, these two IL-1 receptors

regulated the bioavailability of the IL-1 in the serum.

And the IL-1 has its own antagonist, IL-1Ra, to prevent the activation of these two receptors. The IL-1Ra was produced by the monocytes after the stimulation by the anti-inflammatory cytokines (Bessis et al., 2000).

4.3 IL-6

IL-6 activated the leukocytes and antibody production at the local synovium (Neunaber et al., 2011, Svoboda et al., 1994). It has demonstrated that the IL-6 also contributed to systemic manifestations of RA, such as asthenia, and anemia (Assier et al., 2010). There are two types of IL-6 receptor, IL-6Ra and gp130. The IL-6Ra is a specific receptor for IL-6, while the IL-6 shared the gp130 with other cytokines. Both IL-6 receptors induced trans-signaling. Because both receptors existed in a soluble form, which could act as antagonists to IL-6 (Knupfer and Preiss, 2008).

4.4 IL-17

IL-17 is originally termed as cytotoxic T-lymphocyte-associated antigen 8 (CTLA-8), which was first identified in 1993 (Rouvier et al., 1993). The recombinant IL-17 activated the NF-κB pathway, resulting in the increase of IL-6 production in fibroblasts and also induction of the T cell proliferation as other pro-inflammatory cytokines (Yao et al., 2011, Fossiez et al., 1996).

Murine $CD4^+$ T cells were divided into Th1 and Th2 subtypes on basis of their production of cytokines (Mosmann et al., 2005). However, the finding of IL-17 challenged the previous bipolar classification of helper T cells (Steinman, 2007). Because its amino acid sequence was significantly different from other cytokines previously described in this part, and the its receptor barely meet those of above cytokine receptor families. It suggested

that IL-17 was a distinctive molecule in this signaling. In the infection stimulation, the naïve T cells could differentiate into a subset of T cells with markable production of IL-17. Without the classification into the cytokines from Th1 or Th2, it leaded to the discovery of Th17 cells as a new $CD4^+$ T cell population from the production of IL-17 (Infante-Duarte et al., 2000).

Then, accumulated studies have released the physiological role of IL-17 and Th17 cells, as well as their contribution in the pathological conditions of RA. IL-17 induced the production of granulocyte-colony stimulating factor (G-CSF), prostaglandin E2 (PGE_2), Interleukin 8 (IL-8), and IL-6, in a concentration-dependent manner during the coculture of RA synovial fibroblasts (Chabaud et al., 1999). The high IL-17 levels were found in synovial fluids from RA patients compared to those from osteoarthritis patients (Chabaud et al., 1999). And exogenous IL-17 increased the expression of IL-6 in the culture of synovial tissues. These observations indicated that IL-17 has a significant role in the pathogenesis of RA through the production of pro-inflammatory cytokines (Kawaguchi et al., 2004, Chabaud et al., 1999).

IL-17 also activated the osteoclastogensis at the progressive stage of RA (Kim et al., 2015). The treatment of IL-17 increased the osteoclastogenesis of osteoclast precursors in the coculture with the hematopoietic cells from the synovial fluids of RA patients (Kotake et al., 1999). It has also reported that IL-17 promoted osteoclastogenesis in the $CD14^+$ osteoclast precursors from healthy donors by the upregulation of the receptor activator of NF-κB (RANK) (Adamopoulos et al., 2010).

There are many other cytokines involving in RA synovitis, including granulocyte-macrophage colony-stimulating factor (GMCSF), B lymphocyte

stimulator (BLyS), and A proliferation‐inducing ligand (APRIL). Their interactions in the synovial environment were complex and different at different RA stages (Klareskog et al., 2006).

5. Challenges and Opportunities

Because the inflammation cytokines are essential to RA development and progression. Thus, the current clinical therapeutics of RA was to inhibit inflammatory responses by disruption of inflammation cytokines (Guo et al., 2018). Although the anti-inflammation medications could inhibit inflammation symptoms in RA, the established bone destruction barely repaired even after treatment. Thus, the inhibition of bone erosion in RA remains as a clinical challenge, emphasizing the need to better understand the bone homeostasis in the inflammation conditions (Loi et al., 2016).

During the RA development, the chronic inflammation in the synovial membrane contributes to the progressive bone damage (Koyama and Tanaka, 2016). Accumulating evidences have demonstrated the inflammatory cytokines from inflammatory effector cells regulated the functions of bone-resorptive osteoclasts and bone-forming osteoblasts.

5.1 Osteoclasts in the Inflammation

Osteoporosis is a well-known co-morbidity in RA (Dimitroulas et al., 2013). The arthritic bone loss in RA suggested the dysregulation of the balance between bone-formation osteoblasts and bone-resorptive osteoclasts (Goldring and Gravallese, 2000). The genetic depletion or blockade of osteoclasts or their function improved the bone erosion in various models of inflammatory arthropathy (Redlich et al., 2002b, Pettit et al., 2001). It indicated that the osteoclasts played an essential role for the structural damage in such inflammation conditions.

Macrophages have osteoclast commitment potential, which migrated to inflamed joints by the induction of pro-inflammatory cytokines (Cohen et al., 2008). It has demonstrated that the osteoclast differentiation from macrophages required the receptor activator of NF-κB ligand (RANKL), binding to its receptor RANK, and macrophage-colony stimulating factor (M-CSF), engaging its receptor CD115 (c-Fms) on the surface of their precursors. Above factors were abundant in the synovial membrane of RA, where provided the prerequisite milieu for osteoclastogenesis (Firestein et al., 1988, Gravallese et al., 2000, Shigeyama et al., 2000). It has found that the RANKL was increased in the synovium of RA patients (Redlich et al., 2002a, Romas et al., 2002, Kong et al., 1999). In addition, the FLS approximated to osteoclast precursors in the inflamed synovium of RA, which produced the M-CSF and RANKL. They were likely to primary contributors to promote osteoclastogenesis in RA (Takayanagi et al., 2000).

TNF-α and IL-1 were major participants in inflammatory osteolysis. TNF-a recruited macrophages in the inflamed joints and then stimulated their differentiation to osteoclasts (Lam et al., 2000, Li et al., 2004). In addition, TNF-α also exerted its osteoclastogenic effects by either directly targeting their precursors or promoting the expression of RANKL and M-CSF. IL-1 induced the RANKL and RANK expression to increase osteoclast formation (Zwerina et al., 2007, Wei et al., 2005). The deficiency of IL-1 in mice could abrogate the osteolysis in TNF-α-stimulated synovial inflammation, suggesting that TNF triggered bone erosion through induction of IL-1 (Zwerina et al., 2007). And current findings have shown that IL-17 exerted the osteoclastogenic properties through stimulating RANKL expression from the mesenchymal stem cells (MSCs) (Sato et al., 2006, Kotake et al., 1999). Thus, the inflammation microenvironment in RA induced the pathological

osteoclast differentiation, leading to excessive bone erosion.

5.2 Osteoblasts in the Inflammation

The inflammation promotes osteoclastogenesis, as well as diminishes osteoblast differentiation and function. It has reported that the inflammation decreased the osteoblast differentiation and function. And it further contributed to the arthritic bone loss and the inhibition of bone regeneration capacity. (Baum and Gravallese, 2016, Karmakar et al., 2010). Recently, an interesting finding has reported that the osteoblasts directly regulated inflammation and progressive bone damage by the production of inflammatory molecules in the bacterial challenge (Marriott et al., 2004). Therefore, the role of osteoblasts in the inflammation regulation caught our attention.

5.3 The PLEKHO1 and its Role in the Osteoblasts during Inflammation Condition

Pleckstrin homology domain-containing family O member 1 (PLEKHO1, also known as casein kinase-2 interacting protein-1 (CKIP-1)) plays an important role in the bone formation. The effect of PLEKHO1 on bone formation is a negative regulator of the bone morphogenetic protein (BMP) pathway (Nie et al., 2013).

Recent studies have found that PLEKHO1 involved in cytokine signaling during the inflammation (Zhang et al., 2007a, Sakamoto et al., 2014). Therefore, we wonder whether the osteoblastic PLEKHO1 regulated the local joint inflammation and bone-formation reduction in inflammation conditions of RA.

6. Objective of Present Study

The findings of monocyte/macrophage-osteoclast lineages in the inflammation are accumulated. However, the role of MSC-osteoblasts lineages and their associated factors in the inflammation has not been clearly known. Further understanding of the role of osteoblasts in the inflammation conditions will provide new therapeutic strategies in RA. Thus, we explored the role of osteoblastic PLEKHO1 in the inflammation conditions during RA pathology.

Chapter Two

Osteoblastic PLEKHO1 contributes to Joint Inflammation in Rheumatoid Arthritis

1. Materials and Methods

1.1 Human joint bone tissue preparation

Tibial plateau samples from knee joint of subjects with RA (fulfilled the 1987 revised American College of Rheumatology criteria) were obtained at knee joint replacement surgery and provided by Shanghai Guanghua Hospital (China). Subjects with malignancy, diabetes or other severe diseases in the previous 5 years were excluded from our study. For non-RA control, we selected age- and sender-matched subjects who diagnosed as severe trauma (TM) and underwent knee joint replacement surgery in Shanghai Guanghua Hospital and Shenzhen 8th People Hospital (China). Half of the bone samples were fixed with 4% buffered formalin before decalcification, the other half were stored in liquid nitrogen until use. All the clinical procedures were approved by the Committees of Clinical Ethics in the Shanghai Guanghua Hospital and Shenzhen 8th People Hospital. All subjects gave informed consent prior to surgery.

1.2 Cells

Murine osteoblastic cell line, MC3T3E1, was purchased from the Cell Resource Center, Peking Union Medical College (China) and cultured in α-MEM (Thermo Fisher Scientific) containing 10% fetal bovine serum (FBS, Thermo Fisher Scientific) and 1% penicillin-streptomycin (Thermo Fisher Scientific) at 37°C in a humidified 5% CO2 incubator. Human osteoblast–like cell line, MG-63, was purchased from ATCC and cultured in EMEM (Thermo Fisher Scientific) containing 10% FBS and 1% penicillin-

streptomycin at 37°C in a humidified 5% CO2 incubator. Human embryonic kidney HEK293T cell was purchased from ATCC and cultured in DMEM (Thermo Fisher Scientific) containing 10% FBS and 1% penicillin-streptomycin at 37°C in a humidified 5% CO2 incubator. Primary osteoblast precursor cells were isolated from the calvarial bone of newborn C57BL/6 mice (1- to 2-day-old) through enzymatic digestion with α-MEM containing 0.1% collagenase (Life technologies, Grand Island, NY, USA) and 0.2% dispase II (Life Technologies, Grand Island, NY, USA). The isolated osteoblast precursor cells were promoted with osteogenic α-MEM medium with 10% FBS, 1% penicillin-streptomycin, 5mM β-glycerol phosphate (Sigma-Aldrich, St. Louis, MO, USA), 0.1mg/ml ascorbic acid (Sigma-Aldrich, St. Louis, MO, USA) and 10nM dexamethasone (Sigma-Aldrich, St. Louis, MO, USA) for 9 days and culture medium was replaced every 2–3 days (Zhou et al., 2010). Primary FLSs were isolated from the ankle joints of C57BL/6 mice by collagenase digestion (Hardy et al., 2013). Isolated FLSs were grown in DMEM high glucose, GlutaMAX (Life Technologies, Grand Island, NY, USA) supplemented with 10% FBS and 1% penicillin-streptomycin. As no bone marrow-derived lineage cells were detected after passage 3, cultured FLSs were used between passages 4-8. $CD4^+$ T lymphocytes were isolated from the spleen single-cell suspension of C57BL/6 mice by specific magnetic beads-based negative-selection (Miltenyi Biotec, Bergisch Gladbach, Germany). Neutrophils were isolated from peripheral blood of C57BL/6 mice by specific magnetic beads sorting (Miltenyi Biotec, Bergisch Gladbach, Germany) (Berger et al., 2012). Before use, osteoblasts were confirmed to express osteocalcin, synovial fibroblasts were confirmed to express vascular cell adhesion molecule 1 and not F4/80 or CD45, $CD4^+$ T lymphocytes were confirmed to express CD3 and CD4, and neutrophils were confirmed to express Gr-1 and CD11b.

1.3 Co-culture and migration experiment

For osteoblasts-FLS co-culture: FLSs were grown in co-culture with osteoblasts from *Plekho1*$_{osx}^{-/-}$ mice, *Plekho1*$_{osx}$ *Tg* mice or WT littermates. Co-culture experiments were conducted in 6-well transwell coculture plates (Millipore, Billerica, MA, USA). The primary osteoblasts (5×10^5/well) were placed in the lower well and FLSs (5×10^5/well) in the inserts. TNF-α was added for 24 h. After experiment, the inserts were removed from the transwell coculture plates. FLSs in the inserts were collected and firstly detected the osteocalcin mRNA expression by quantitative real-time polymerase chain reaction (PCR) to exclude the possible contamination of osteoblasts in the same co-culture system. Then, the mRNA levels of IL-1β and IL-6 in FLSs were detected by quantitative real-time PCR. For osteoblasts-CD4$^+$ T cells co-culture: Isolated CD4$^+$ T lymphocytes were grown in co-culture with osteoblasts from *Plekho1*$_{osx}^{-/-}$ mice, *Plekho1*$_{osx}$ *Tg* mice or WT littermates. Coculture experiments were conducted in 6-well transwell coculture plates (Millipore, Billerica, MA, USA). The primary osteoblasts (5×10^5/well) were placed in the lower well and CD4$^+$ T lymphocytes (1×10^6/well) in the inserts. TNF-α was added for 24 h. After experiment, CD4$^+$ T lymphocytes were collected and firstly detected the osteocalcin mRNA expression by quantitative real-time PCR to exclude the possible contamination of osteoblasts. Then, the mRNA levels of IL-1β and IL-6 in CD4$^+$ T lymphocytes were detected by quantitative real-time PCR. For osteoblasts-neutrophils co-culture: Isolated neutrophils were plated onto 3.0μm pore polycarbonate membrane transwell inserts, which were placed into the osteoblasts culture wells in the presence of TNF-α. Neutrophils were allowed to migrate through the membrane for 2 h. Migrated cells attached to the bottom of the well were stained by chloroacetate esterase and positive cells were counted to determine changes in chemotactic activity of osteoblasts.

1.4 siRNA inhibition

Plekho1 siRNA and non-sense siRNA (random siRNA) were purchased from GenePharma (Shanghai, China). Transfection was performed with Lipofectamine™ 2000 (Invitrogen Life Technologies, Carlsbad, CA, USA) according to the manufacturer's instructions. Briefly, murine osteoblastic cells MC3T3E1 were seeded in a 6-well plate. Then, 4 ul of 20 uM *Plekho1* siRNA and 2.5 ul of Lipofectamine™ 2000 were diluted in 0.25 ml of Opti-MEM separately for each well. After 5 min of incubation at room temperature, the diluted *Plekho1* siRNA and Lipofectamine™ 2000 were mixed gently and allowed to stand for 20 min at room temperature. Then, cells were washed by PBS. And 1.5 ml MEM without serum and antibiotics was added to each well. Followed by adding 0.5 ml of Opti-MEM containing the Lipofectamine™ 2000-siRNA complex and incubated for 6 h at 37 °C. Non-sense siRNAs transfected by Lipofectamine™ 2000 were used as negative control. Then, the Lipofectamine™ 2000-siRNA complex was removed and replaced with fresh complete MEM. Next, the cells were stimulated by 10 ng/ml TNF-α for another 45 min. The supernatant and the cell lysis were collected for ELISA and western blot analysis, respectively.

1.5 Plasmid construction and transfection

HEK293T cells were cultured and used for transfection. Plasmids of different epitope-tagged human PLEKHO1 and TRAF2, including both full-length proteins and truncated mutants, as well as human RIP1 were constructed by PCR, followed by subcloning into expression vector pcDNA3.1 (Hoeflich et al., 1999, Wang et al., 2012, Zhang et al., 2006, Takeuchi et al., 1996). Plasmid of HA-tagged human ubiquitin-K63 was from Addgene. Transfection was performed using Lipofectamine™ 2000 (Invitrogen) according to the manufacturer's instructions (Lu et al., 2008).

1.6 Immunoprecipitation and immunoblotting

At 36 h after the transfection, HEK293T cells were lysed in HEPES lysis buffer (20 mM HEPES pH 7.2, 50 mM NaCl, 0.5% Triton X-100, 1 mM NaF, 1 mM dithiothreitol) supplemented with protease inhibitor cocktail (Roche) and phosphatase inhibitors (10mM NaF and 1mM Na_3VO_4). Immunoprecipitations were performed using anti-Flag or anti-Myc antibody and protein A/G-agarose (Santa Cruz Biotechnology) at 4 °C. PLEKHO1 and TRAF2, including full-length proteins and truncated mutants, in lysates or immunoprecipitates were examined by anti-Myc (Cell Signaling Technology) and anti-Flag (Sigma) primary antibodies, respectively, and the appropriate secondary antibodies in immunoblotting, followed by detection with SuperSignal chemiluminescence kit (Thermo Fisher Scientific) (Zhang et al., 2014, Lu et al., 2008, Sondarva et al., 2010).

1.7 *In vitro* ubiquitylation assay

HEK293T cells were transfected with Myc-RIP1, HA-Ub-K63, Flag-PLEKHO1 or Flag-ΔLZ and Flag-TRAF2 or Flag-ΔTRAF C. At 36 h after the transfection, cells were lysed in HEPES lysis buffer and then incubated with anti-Myc antibody (Sigma) for 3 h and protein A/G-agarose beads (Santa Cruz Biotechnology) for a further 8 h at 4 °C. After three washes, ubiquitination of RIP1 was detected by immunoblotting with an anti-HA antibody (Cell Signaling Technology) (Lu et al., 2008, Alvarez et al., 2010).

1.8 Animals

Osteoblast-specific *Plekho1* knockout mice (*Plekho1*$_{osx}^{-/-}$ mice), *Plekho1* knockout mice (*Plekho1*$^{-/-}$ mice) and osteoblast-specific *Plekho1* overexpressing (*Plekho1*$_{osx}$ *Tg*) mice were prepared according to our previous reports (Liu et al., 2017). We generated the *Plekho1*$_{osx}^{-/-}$ mice

based on the Cre-loxP strategy. Briefly, we created the heterozygous mice carrying the mutant allele with LoxP sites harboring exon 3 to exon 6 of Plekho1 gene (*Plekho1*$^{fl/-}$), which were then crossed with Osx-Cre mice (Beijing Biocytogen Co., Ltd, China) to generate the *Plekho1*$_{osx}^{-/-}$ mice. To generate *Plekho1*$^{-/-}$ mice, *Plekho1*$^{fl/+}$ mice were crossed with CMV-Cre mice (Beijing Biocytogen Co., Ltd, China). To generate *Plekho1*$_{osx}$ *Tg* mice, we created a mouse strain carrying the ROSA26-PCAG-STOP^{fl}-Plekho1-eGFP allele, and crossed them with the Osx-Cre mice to generate the *Plekho1*$_{osx}$ *Tg* mice that overexpressing Plekho1 in osteoblasts. DBA/1 mice and C57BL/6J mice were from Vital River Laboratory Animal Technology Co., Ltd. (Beijing, China). The human TNF transgenic (hTNFtg) mice (strain Tg197; genetic background, C57BL/6) were obtained from Dr. G. Kollias (Institute of Immunology, Biomedical Sciences Research Center "Alexander Fleming," Vari, Greece). Male *Plekho1*$_{osx}^{-/-}$ mice were bred with female hTNFtg mice to obtain *Plekho1*$_{osx}^{-/-}$/hTNFtg mice. Male *Plekho1*$^{-/-}$ mice were bred with female *Plekho1*$_{osx}$ *Tg* mice to generate offspring (*Plekho1*$^{-/-}$/*Plekho1*$_{osx}$ *Tg* mice) that express high PLEKHO1 exclusively in osteoblasts. All mice data were generated from age- and sex-matched littermates. All the animals were maintained under standard animal housing conditions (12-h light, 12-h dark cycles and free access to food and water). All procedures were approved by the Ethical Animal Care and Use Committee in China Academy of Chinese Medical Sciences and Hong Kong Baptist University.

1.9 Collagen-induced arthritis (CIA) mice model

The induction of CIA was performed as previously described with slight modification (Brand et al., 2007). Briefly, type II collagen (bovine type II collagen for DBA/1 mice, chicken type II collagen for C57BL/6J mice) (Sigma-Aldrich, St. Louis, MO, USA) was dissolved at a concentration of 2 mg/ml in 0.05 M acetic acid and emulsified with complete Freund's adjuvant

(CFA) (Sigma-Aldrich, St. Louis, MO, USA). To induce CIA in C57BL/6J mice, 100mg of desiccated killed *Mycobacterium tuberculosis* H37Ra (BD Biosciences) was suspended in 30ML of CFA (Inglis et al., 2007). On day 0, the CIA mice were immunized with 0.1 mL of collagen by intradermal injection at the base of the tail. On day 21, mice were given a booster dose of collagen through the same route.

1.10 Treatment

For mice siRNA treatment experiment: DBA/1 mice were induced by type II collagen. After CIA was successfully established (day 28 after primary immunization, a mouse with a score of one or above was regarded as arthritic), parts of the mice were sacrificed before treatment as CIA baseline (CIA-BL). The remaining CIA mice were divided into $(AspSerSer)_6$-liposome-*Plekho1* siRNA group, $(AspSerSer)_6$-liposome-non sense siRNA group, $(AspSerSer)_6$-liposome group, and vehicle control group. The mice in each group received six periodic intravenous injections of $(AspSerSer)_6$-liposome-*Plekho1* siRNA, $(AspSerSer)_6$-liposome-non sense siRNA, $(AspSerSer)_6$-liposome, and PBS, respectively, with a siRNA dose of 5.89 mg/kg at an interval of one week.

1.11 Evaluation of arthritis severity

Clinical severity of arthritis in mice was evaluated according to the following visual scoring system (Brand et al., 2007): 0 = no swelling or erythema; 1 =Erythema and mild swelling confined to the tarsals or ankle joint; 2 = Erythema and mild swelling extending from the ankle to the tarsals; 3 = Erythema and moderate swelling extending from the ankle to metatarsal joints; 4 = Erythema and severe swelling encompass the ankle, foot and digits, or ankylosis of the limb. Each limb was assigned a score of 0 to 4, with a maximum possible score of 16 for each mouse.

1.12 Enzyme-linked immunosorbent assay (ELISA)

Ankle joints of mice were pulverized using a mortar and pestle filled with liquid nitrogen. Tissue was transferred to 15 ml tubes, placed on dry ice and resuspended in 1 ml PBS /200 mg of tissue and homogenized using a tissue homogeniser. Joint homogenates were centrifuged for 10 min at 500g at 4°C. Supernatants were transferred to 1.5 ml tubes, centrifuged at 15,000 g for 5 min and collected for analysis. IL-1β and IL-6 quantifications were determined by ELISA according the instructions of the manufacturer (eBioscience), data was multiplied by a dilution factor for conversion from pg/ml to pg/g (Rioja et al., 2004).

1.13 Total RNA isolation, reverse transcription and quantitative real-time PCR

Total RNA was isolated from cultured cells and isolated cells using the RNeasy® Mini Kit (QIAGEN, Dusseldorf, Germany). The concentration of total RNA was determined using a spectrophotometer. cDNA was synthesized from 0.5 μg of total RNA using a commercial first-strand cDNA synthesis kit (QIAGEN, Dusseldorf, Germany). Real-time PCR reactions were performed using SYBR Green in a 7900HT Fast Real-Time PCR System (Applied Biosystems, Foster City, California, USA). The employed primer sequences in the study were listed in **Table 2-1**. The amplification conditions were as follows: 50°C for 2 minutes, 95°C for 10 minutes, 40 cycles of 95°C for 15 seconds, and 60°C for 1 minute. The fluorescence signal emitted was collected by ABI PRISM® 7900HT Sequence Detection System and the signal was converted into numerical values by SDS 2.1 software (Applied Biosystems). The mRNA expression level of the target gene was first calculated from the Relative Standard Curve Method by the SDS 2.1 software. The threshold cycle (CT) value, which represented the relative expression of

each target gene, was determined from the corresponding curve. Then, the relative expression of mRNA was determined by dividing the target amount by endogenous control amount to obtain a normalized target value. The relative mRNA expression was calculated using the $2^{-\triangle\triangle Ct}$ method as follow: $\triangle\triangle Ct = (Ct_{\text{target gene}} - Ct_{\text{reference gene}})_{\text{experimental group}} - (Ct_{\text{target gene}} - Ct_{\text{reference gene}})_{\text{WT-OB group}}$) (Zhang et al., 2012).

Table 2-1 Real-time PCR Primers

Gene	Primers (5'-3')		Size	Tm	Accession No.
	Forward	Reverse	(bp)		
Human Plekho1	ACCCGAGCCAAGAACCGTAT	TGGAAGCCACAGCCATTAGG	139	60	NM_016274.4
Human GAPDH	GGCATGGACTGTGGTCATGAG	TGCACCACCAACTGCTTAGC	87	60	NM_002046.3
Human β-actin	CTGGGACGACATGGAGAAAA	AAGGAAGGCTGGAAGAGTGC	144	60	NM_001101.3
Mouse Plekho1	AACCGCTATGTGGTGCTGAA	CAGGGTGAACTTGCTGTGATT	165	60	NM_023320.2
Mouse IL-1β	AGTTGACGGACCCCAAAAG	CTTCTCCACAGCCACAATGA	145	60	NM_008361.4
Mouse IL-6	CGGAGAGGAGACTTCACAGAG	ATTTCCACGATTTCCCAGAG	104	60	NM_031168.2
Mouse GAPDH	TGCACCACCAACTGCTTAG	GGATGCAGGGATGATGTTC	177	60	NM_008084.2
Mouse β-actin	ATATCGCTGCGCTGGTCGTC	AGGATGGCGTGAGGGAGAGC	174	60	NM_007393.5

1.14 Western blot analysis

The bone specimens and cells were snap-frozen in liquid nitrogen and mechanically homogenized in lysis buffer. Protein fractions were collected by centrifugation at 15,000g at 4 °C for 10 min and then subjected to SDS-PAGE and transferred to polyvinylidene difluoride (PVDF) membranes. The membranes were blocked with 5% bovine serum albumin (BSA) and incubated with specific antibodies overnight. A horseradish peroxidase–labeled secondary antibody (Abcam) was added and visualized using an enhanced chemiluminescence kit (Pierce). Antibodies to the following proteins were used: GAPDH (Sigma), PLEKHO1 (Santa Cruz, sc-50227), IKKβ (Cell Signaling Technology, #8943), p-IKKα/β (Cell Signaling Technology, #2078), p65 (Cell Signaling Technology) and p-p65 (Abcam, ab106129). The relative amounts of the transferred proteins were quantified by scanning the auto-radiographic films with a gel densitometer (Bio-Rad, USA) and normalized to the corresponding GAPDH level (Zhang et al., 2009).

1.15 Laser capture micro-dissection (LCM)

For LCM, the hind paw of mice was decalcified in 10% ethylenediaminetetraacetic acid (EDTA) and embedded in OCT. Then, the series frozen sections (5μm) were prepared in a cryostat (CM3050; Leica Microsystems, Wetzlar, Germany) at -20˚C. Adjacent sections were mounted on either glass slides or polyethylene membrane–equipped slides (P.A.L.M., Bernried, Germany). The sections mounted on glass slides were performed immunostaining to identify the osteocalcin-positive cells. Briefly, the cryosections were air dried at room temperature, fixed in ice-cold acetone for 10 min, permeabilized in 0.1% Triton X-100 at room temperature for 20 min, and blocked in 5% donkey serum in PBS. The sections were

incubated overnight at 4 °C with rabbit polyclonal anti-osteocalcin antibody (1:50 dilution; Santa Cruz Biotechnology, Inc.). After three washes in PBS, the sections were incubated with Alexa Fluor 488-conjugated donkey anti-rabbit IgG (1:400 dilution; Invitrogen). Finally, the sections were mounted with medium containing (4',6-diamidinole-2-phenolindole) DAPI (Vector laboratories) and examined under a fluorescence microscope to identify the osteocalcin-positive staining cells. The adjacent sections mounted on membrane-coated slides were stained with neutral red for 1 min at room temperature. After brief rinsing in water, the sections were air-dried. Osteocalcin-positive staining cells in adjacent sections were isolated by microdissection with an upgraded laser pressure catapulting microdissection system (P.A.L.M.) using a pulsed 355 nm diode laser in the Leica LMD 7000 Laser Microdissection System. About 100~200 identified cells were collected in reaction tube containing 5μl lysis buffer for RNA extraction and subsequent real-time PCR analysis following above mentioned protocols (Zhang et al., 2009).

1.16 Immunofluorescence staining

The bone specimens were fixed with 4% buffered formalin and embedded with O.C.T. after decalcification with 10% EDTA. The frozen sections (5 μm thickness) were cut in a freezing cryostat at -20°C. The sections were air dried at room temperature, fixed in ice-cold acetone for 10 min, permeablilized with 0.1% Triton X-100 at room temperature for 20 min, and blocked in 5% donkey serum in PBS. The sections were then incubated overnight at 4°C with the mixture of goat polyclonal osteocalcin antibody (1:50; Santa Cruz Biotechnology, Inc.), and rabbit polyclonal PLEKHO1 antibody (1:50; Santa Cruz Biotechnology, Inc.). Following three washes in PBS, the sections were incubated with the mixture of Alexa Fluor 488-conjugated donkey anti-goat antibody, and Alexa Fluor 568-conjugated

donkey anti-rabbit antibody (1:300; Invitrogen) for 1 h. Negative control experiments were done by omitting the primary antibodies. The sections were mounted with the medium containing DAPI (Vector Laboratories) and then examined under a fluorescence microscope (DM6000B, Leica image analysis system) (Zhang et al., 2009, Walsh et al., 2009).

1.17 Micro computed tomography (MicroCT) analysis

MicroCT analysis was performed using a high-speed μCT (viva CT 40, Scanco Medical, Switzerland) at energy of 70 kVp and intensity of 114 μA with high resolution and voxel size of 15 μm of 10.5 μm (mouse). In mouse studies, the hind limbs were scanned and the proximal tibia was selected for analysis. 3D reconstruction analysis was performed with SCANCO software (SCANCO Medical, Switzerland). Standard image analysis procedures were used to determine trabecular and cortical parameters. The following parameters were determined: bone mineral density (BMD), bone volume fraction (BV/TV), trabecular number (Tb.N) and trabecular thickness (Tb.Th) (Poliachik et al., 2010).

1.18 Histology evaluation

The hind paw of mice was fixed in 4% formaldehyde, decalcified with EDTA and embedded in paraffin. The serial sections of the paw and hand were examined for inflammation using hematoxylin and eosin (H&E) staining. Inflammation was scored according to the following criteria: 0 = normal; 1 = minimal infiltration of inflammatory cells in perijoint area; 2 = mild infiltration; 3 = moderate infiltration; and 4 = marked infiltration (Guma et al., 2009). Scoring was executed blindly by two investigators and mean values were calculated.

1.19 Bone histomorphometric analysis

To assess bone formation, the animals were administered with xylenol orange (90 mg/kg) and calcein green (10 mg/kg) for labeling bone formation surface on day 12 and day 2 before sacrifice by intraperitoneal injection, respectively. The hind paw of mice was fixed in 70% ethanol. The samples were trimmed from surrounding soft tissues, dehydrated in a series of ethanol solutions (70%, 80%, 90%, 95% and 100%), and embedded in methyl methacrylate. Non-decalcified histological sections (10μm thick) were made using a diamond saw microtome. The sections for light microscopic observations were performed by the modified Goldner's trichrome, while unstained sections were prepared for fluorescent microscope observations. In mice study, the calcaneus area within the hind paw was chosen for histomorphometric analysis. All the measurements were performed using the professional image software (ImageJ, NIH, USA and BIOQUANT OSTEO, Version 13.2.6, Nashville, TN, USA). The following bone histomorphometric parameters for bone remodeling activity were analyzed, including mineral apposition rate (MAR), bone formation rate/bone surface (BFR/BS), osteoblast surface/bone surface (Ob.S/BS), osteoblast number per bone perimeter (Ob.N/B.Pm), osteoclast surface / bone surface (Oc.S/BS) and osteoclast number per bone perimeter (Oc.N/B.Pm) (Zhang et al., 2012).

1.20 Statistical analysis

For statistical analysis, data were expressed as the mean ± standard deviation. In general, statistical differences among groups were analyzed by one-way analysis of variance (ANOVA) with a Tukey's multiple comparisons test to determine group differences in the study parameters. Especially, the dynamic detection data were compared by means of two-way ANOVA with subsequent Bonferroni posttests. All statistical analyses were performed using Graphpad Prism Software, 6.05 (Graph Pad

Software Inc., San Diego, CA). P values less than 0.05 were considered significant.

2. Experimental Design and Results

2.1 Upregulation of osteoblastic PLEKHO1 in RA patients and CIA mice

2.1.1 Experimental design

We collected the bone samples from the knee joint of fifteen RA patients and eight age- and sender-matched severe trauma (TM) patients underwent knee joint replacement surgery in the study on human bone samples. The bone samples were divided to perform western blot and immunofluorescence analysis, respectively. On one hand, the protein was extracted from the bone samples, which was used to detect the expression of PLEKHO1 by western blot analysis. On the other hand, the bone samples were decalcified for cry-sectioning to examine the protein expression of PEKHO1 within Osteocalcin-positive (Ocn^+) cells (osteoblasts) by immunofluorescence analysis.

In the study on the inflammatory arthritis mice, we applied the rodent model with collage-induced arthritis (CIA). Ten DBA/1 mice were sacrificed at day 0 as baseline. Another forty DBA/1 mice were immunized with 0.1 mL of collagen by intradermal injection at the base of the tail on day 0. These mice were given a booster dose of collagen through the same route on the day 21 and sacrificed at day 28, 35, 42, and 49 after the primary immunization (n=10 for each time point). The forty age-matched DBA/1 mice were sacrificed at day 28, 35, 42, and 49 as normal controls. After sacrifice, the bone tissues of ankle joints from hind paws were dissected to downstream processing and analysis, respectively. The protein was extracted from the bone tissues of ankle joints from left hind paws to quantify the levels of PLEKHO1 within osteoblasts. And the bone tissues of ankle joints from right hind paws were subjected for decalcification followed by cry-sectioning. The sections were performed to immunofluorescence analysis to examine the PLEKHO1 expression within Ocn^+ cells. And the Ocn^+ cells of ankle joint

from CIA mice and their normal controls were collected by laser capture micro-dissection (LCM) at different time point after primary immunization and then performed to quantify the mRNA levels of *Plekho1* within Ocn^+ cells by real-time PCR.

2.1.2 Result

We observed high levels of PLEKHO1 in knee joint bone tissues from RA patients when compared to those from TM controls **(Fig. 2-1a, 2-1b)**. The immunofluorescence staining results showed an increase of colocalization of PLEKHO1 positive with osteocalcin (Ocn) positive in knee joint bone tissues from RA patients **(Fig. 2-1c)**. Quantitatively, the percentage of cells co-expressing PLEKHO1 and Ocn in Ocn positive (Ocn^+) cells of bone tissues from knee joint was also remarkably higher in RA patients compared to TM patients **(Fig. 2-1d)**.

In addition, we observed the time course changes in PLEKHO1 expression within osteoblasts in CIA mice. In line with the above findings in RA patients' bone specimens, we also found the percentage of cells co-expressing PLEKHO1 and Ocn in Ocn^+ cells was higher in bone tissues of ankle joint in the hind paws from CIA mice on day 49 after primary immunization compared to those normal controls **(Fig. 2-1e, 2-1f)**. Further real-time PCR analysis showed that the *Plekho1* mRNA level in Ocn^+ cells of ankle joint from CIA group was increased over time from day 28 and significantly higher than that in control group on day 35, 42 and 49, respectively **(Fig. 2-1g)**. **These data suggested that local inflammatory environment might lead to the aberrant upregulation of PLEKHO1 in osteoblasts of joint bone tissues.**

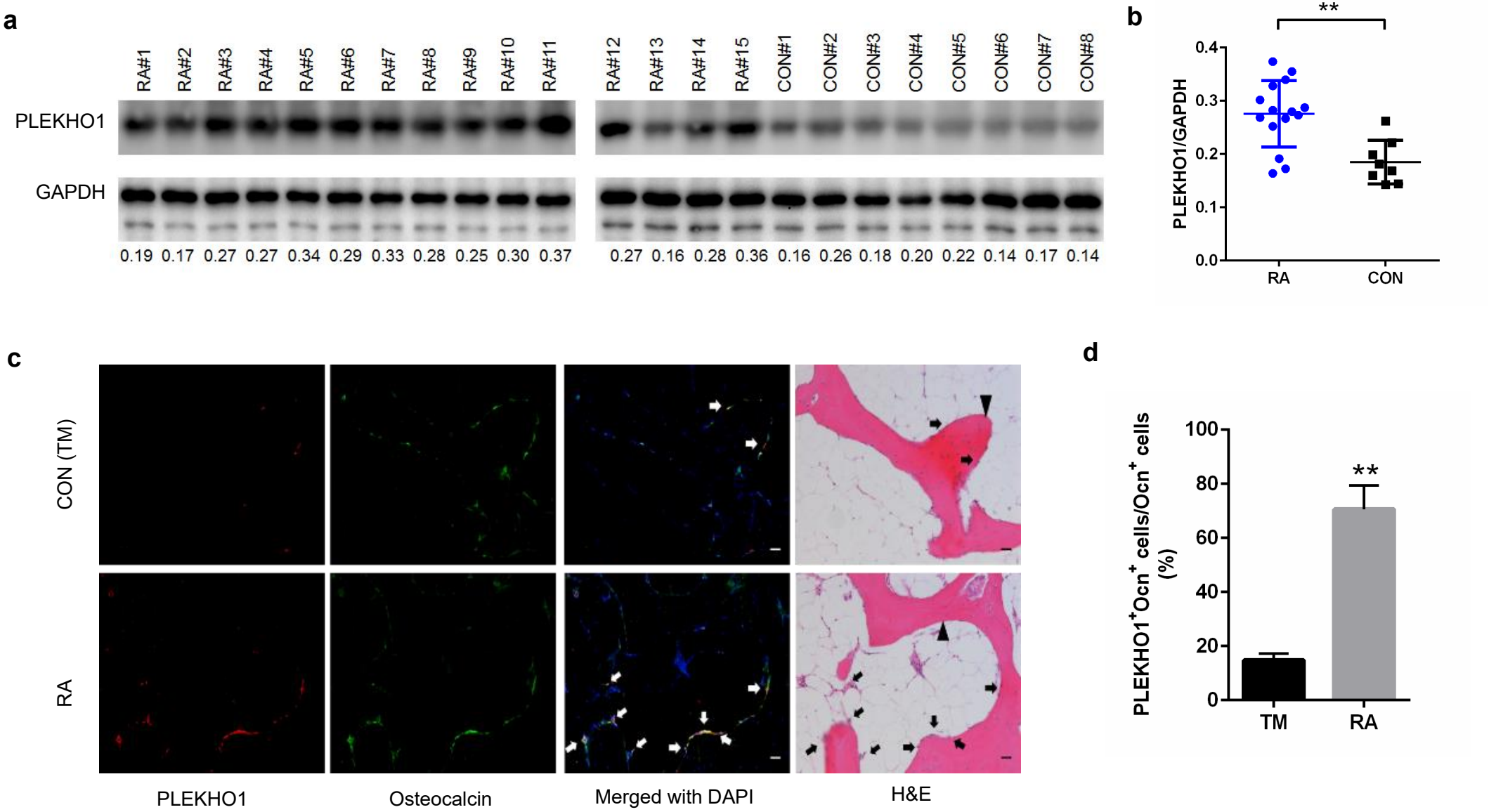
a
RA#1
RA#2
RA#3
RA#4
RA#5
RA#6
RA#7
RA#8
RA#9
RA#10
RA#11
RA#12
RA#13
RA#14
RA#15
CON#1
CON#2
CON#3
CON#4
CON#5
CON#6
CON#7
CON#8
PLEKHO1
GAPDH
0.19 0.17 0.27 0.27 0.34 0.29 0.33 0.28 0.25 0.30 0.37
0.27 0.16 0.28 0.36 0.16 0.26 0.18 0.20 0.22 0.14 0.17 0.14
b
**
PLEKHO1/GAPDH
0.4
0.3
0.2
0.1
0.0
RA
CON
c
CON (TM)
RA
PLEKHO1
Osteocalcin
Merged with DAPI
H&E
d
PLEKHO1+Ocn+ cells/Ocn+ cells (%)
100
80
60
40
20
0
**
TM
RA

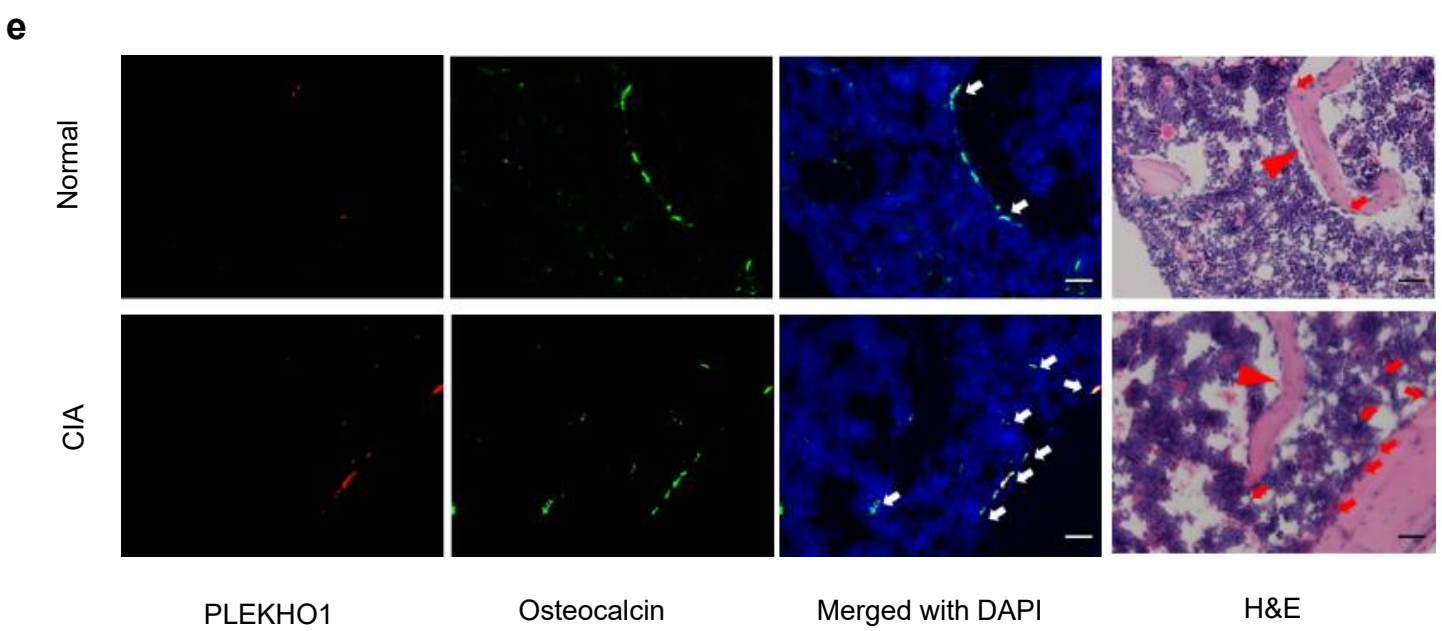
e
Normal
CIA
PLEKHO1
Osteocalcin
Merged with DAPI
H&E

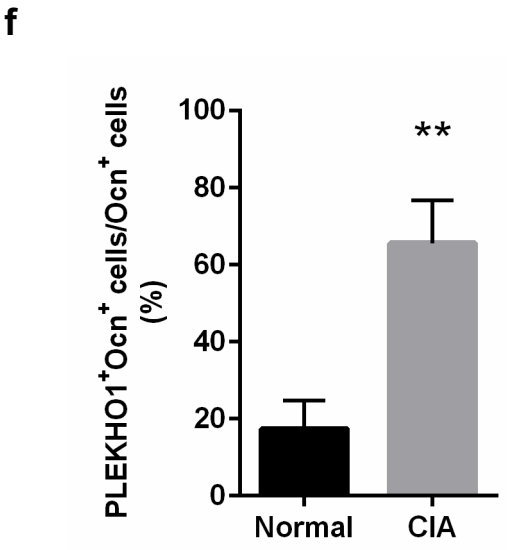
f
PLEKHO1+Ocn+ cells/Ocn+ cells (%)
100
80
60
40
20
0
**
Normal
CIA

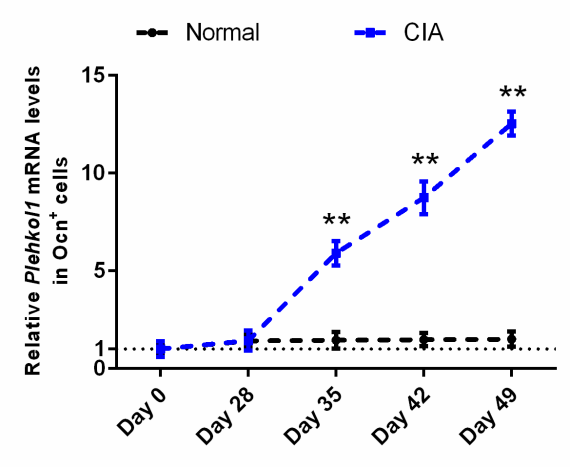
g
Normal
CIA
Relative Plehkol1 mRNA levels in Ocn+ cells
15
10
5
1
0
**
**
**
Day 0
Day 28
Day 35
Day 42
Day 49

Figure 2-1 Highly expressed PLEKHO1 in osteoblasts of RA patients and CIA mice. (**a,b**) Comparison of PLEKHO1 levels in bone tissues from knee joint between RA and TM patients underwent knee joint replacement surgery by western blot. **a**, Representative electrophoretic bands of the samples from fifteen RA patients and eight TM patients are shown. The numbers below the bands represent a semiquantitative value. **b**, The semiquantitative data of the protein levels. (**c,d**) Comparison of PLEKHO1 expression (red) within osteocalcin positive (Ocn^+) osteoblasts (green) in bone tissues from knee joint between RA and TM patients by immunofluorescence analysis. **c**, Representative fluorescent micrographs of the samples from five RA patients and five TM patients are shown. Merged images with DAPI staining show co-staining of PLEKHO1 and Ocn^+ osteoblasts (arrows, yellow). H&E staining of the same sections is shown, and black arrowheads point to bone-formation surfaces, enriched by those cells with pink, which is a merged color of green (osteoblast marker) and blue (DAPI staining for nuclei) in the immunofluorescence staining. Scale bars, 20 μm. **d**, Comparison of the percentage of cells co-expressing Ocn and PLEKHO1 in Ocn^+ cells from bone tissues of knee joint between RA patients and TM patients. (**e,f**) Comparison of PLEKHO1 expression (red) within Ocn^+ osteoblasts (green) in bone tissues of ankle joint from hind paws of CIA and normal mice on day 49 after primary immunization by immunofluorescence analysis. **e**, Representative fluorescent micrographs of the bone samples from ten CIA mice and ten normal mice are shown. Merged images with DAPI staining show co-staining of PLEKHO1 and Ocn^+ osteoblasts (arrows, yellow). H&E staining of the same sections is shown, and red arrowheads point to bone-formation surfaces. Scale bars: 20 μm. **f,** Comparison of the percentage of cells co-expressing Ocn and PLEKHO1 in Ocn^+ cells from bone tissues of ankle joint from hind paws between CIA mice and normal mice on day 49 after primary immunization. (**g**) Time course changes of *Plekho1* mRNA level in Ocn^+ osteoblasts from CIA and normal mice by LCM combined with real-time PCR. Note: RA, rheumatoid arthritis;

TM: severe trauma. All data are the mean ± s.d. **P < 0.01. Two-way ANOVA with Bonferroni posttests is performed. Comparisons between two groups are performed using a Student’s t test.

2.2 Inflammation-related increase in osteoblastic PLEKHO1 expression

2.2.1 Experimental design

The human osteoblast–like cell line MG-63 and mouse osteoblast–like cell line MC3T3E1 at passage 3 (P3) were stimulated with different concentrations of IL-1β (0 ng/mL, 1 ng/mL, 2 ng/mL, and 3 ng/mL), IL-6 (0 ng/mL, 5 ng/mL, 10 ng/mL, and 15 ng/mL), and TNF-α (0 ng/mL, 10 ng/mL, 20 ng/mL, and 30 ng/mL) for 24 hours, respectively. Then, the cells were harvested for real-time PCR to examine the mRNA levels of *Plekho1*.

2.2.2 Result

We found that the recombinant pro-inflammatory cytokines, IL-1β, IL-6, and TNF-α were stimulated high levels of *Plekho1* mRNA in human osteoblast–like cell line MG-63 and mouse osteoblast–like cell line MC3T3E1 and the levels of *Plekho1* mRNA were increased in a dose-dependent manner in these cells after stimulation **(Fig. 2-2)**. **It indicated that the local inflammation contributed to the aberrantly increased expression of PLEKHO1 within osteoblasts.**

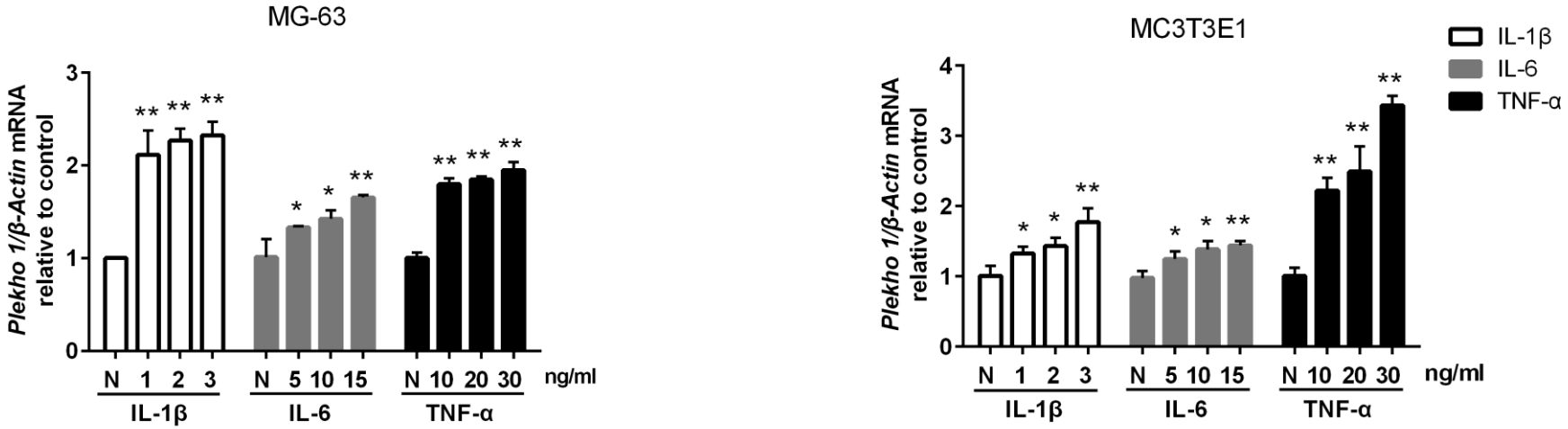

Figure 2-2 Highly expressed PLEKHO1 in osteoblast-like cells after pro-inflammatory stimulation. Levels of *Plekho1* mRNA induced by pro-inflammatory cytokines (IL-1β, IL-6, and TNF-α) in human osteoblast–like cell line MG-63 (left) and mouse osteoblast–like cell line MC3T3E1 (right) by real-time PCR analysis. N: no cytokines, served as control. All data are the mean ± s.d. *P < 0.05, **P < 0.01. Two-way ANOVA with Bonferroni posttests is performed. Comparisons between two groups are performed using a Student's t test.

2.3 Attenuation of joint inflammation in CIA mice by the osteoblastic *Plekho1* deletion

2.3.1 Experiment design

Both the *Plekho1*$_{osx}^{-/-}$ mice and WT mice in the C57BL/6J background were immunized with type II chicken collagen in CFA, and followed by a boost of type II chicken collagen at day 21 after the first injection. The clinical severity of arthritis in mice was scored during the CIA development. In addition, the *Plekho1*$_{osx}^{-/-}$ mice and WT mice were sequentially sacrificed at day 0 and day 49 at the primary immunization (n=10 for each genotype at each time point), respectively. And the ankle joints of hid paws were collected for the MicroCT analysis, dynamic bone histomorphometric analysis, histological evaluation of inflammation, as well as the protein levels of IL-1β and IL-6 by ELISA examination.

2.3.2 Result

2.3.2.1 The genotyping of *Plekho1*$_{osx}^{-/-}$ mice

We generated the heterozygous mice carrying the mutant allele with LoxP sites harboring exon 3 to exon 6 of *Plekho1* gene (*Plekho1*$^{fl/-}$). These mice were then crossed with *Osx-Cre* mice to generate the osteoblast-specific *Plekho1* conditional knockout (*Plekho1*$_{osx}^{-/-}$) mice **(Fig. 2-3a-b)**. Real-time PCR analysis showed that the *Plekho1* mRNA level was hardly detected in Ocn^{+} cells (osteoblasts) from *Plekho1*$_{osx}^{-/-}$ mice when compared to control littermates (hereafter wild-type (WT) mice, including *Plekho1*$^{fl/fl}$ mice, *Osx*$^{+/-}$; *Plekho1*$^{fl/-}$ mice, and *Osx*$^{+/-}$ mice), whereas no significant difference in *Plekho1* mRNA level within Ocn^{-} cells (non-osteoblasts) was found between *Plekho1*$_{osx}^{-/-}$ mice and WT mice **(Fig. 2-3c)**.

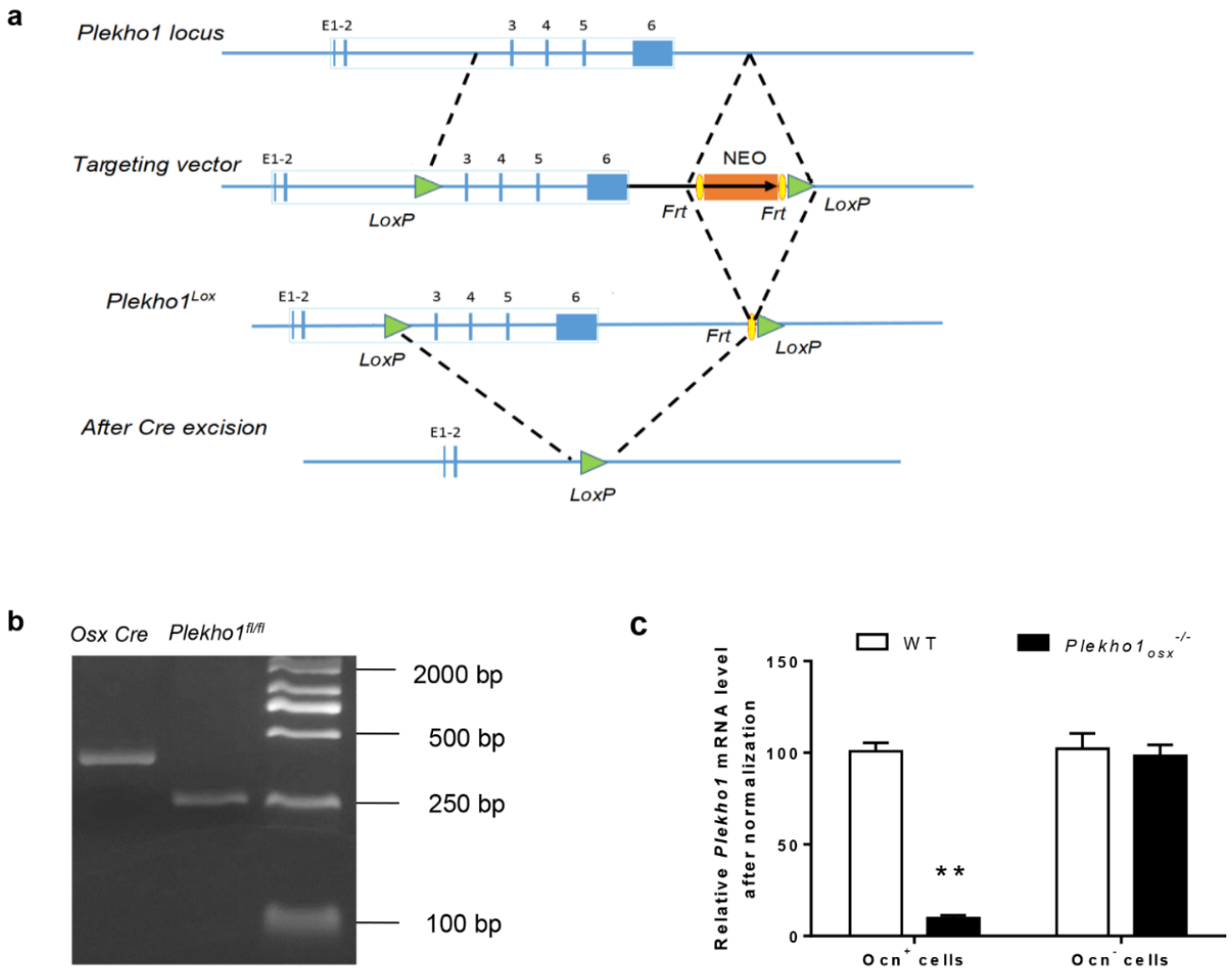
a
Plekho1 locus
E1-2
3
4
5
6
Targeting vector
NEO
LoxP
Frt
Frt
LoxP
Plekho1Lox
After Cre excision
b
Osx Cre
Plekho1fl/fl
2000 bp
500 bp
250 bp
100 bp
c
WT
Plekho1osx-/-
Relative Plekho1 mRNA level after normalization
150
100
50
0
**
Ocn+ cells
Ocn- cells

Figure 2-3 Characterization of the osteoblast-specific *Plekho1* conditional knockout (*Plekho1*$_{osx}^{-/-}$) mice. (**a**) Schematic diagram for development strategy to generate *Plekho1*$^{floxp/-}$ mice. (**b**) Identification of *Plekho1*$_{osx}^{-/-}$ mice by PCR analysis. *Plekho1*$^{fl/fl}$(271bp), *Osx Cre*(445bp). (**c**) Real-time PCR analysis for *Plekho1* mRNA in Ocn^{+} cells isolated from WT mice (including *Plekho1*$^{fl/fl}$ mice, *Osx*$^{+/-}$;*Plekho1*$^{fl/-}$ mice, and *Osx*$^{+/-}$ mice) and *Plekho1*$_{osx}^{-/-}$ mice (*n*=8 subjects each). **P<0.01, compared to WT mice.

2.3.2.2 The decreased joint inflammation in *Plekho1*$_{osx}^{-/-}$ mice during CIA

We found that *Plekho1*$_{osx}^{-/-}$-CIA mice showed obvious attenuation in joint inflammation. The arthritis score in *Plekho1*$_{osx}^{-/-}$-CIA mice was significantly lower than that in WT mice from day 37 to day 49 after first immunization **(Fig. 2-4a)**. Histological evaluation showed that the score for inflammation in ankle joint from the hind paws was significantly lower in *Plekho1*$_{osx}^{-/-}$-CIA mice than that in WT-CIA mice on day 49 after primary immunization **(Fig. 2-4b-c)**. Moreover, IL-1β and IL-6 levels in ankle joint of hind paws from *Plekho1*$_{osx}^{-/-}$-CIA mice were also remarkably lower on day 49 when compared with the WT-CIA mice **(Fig. 2-4d)**. **These results implied that osteoblastic PLEKHO1 negatively regulated local joint inflammation.**

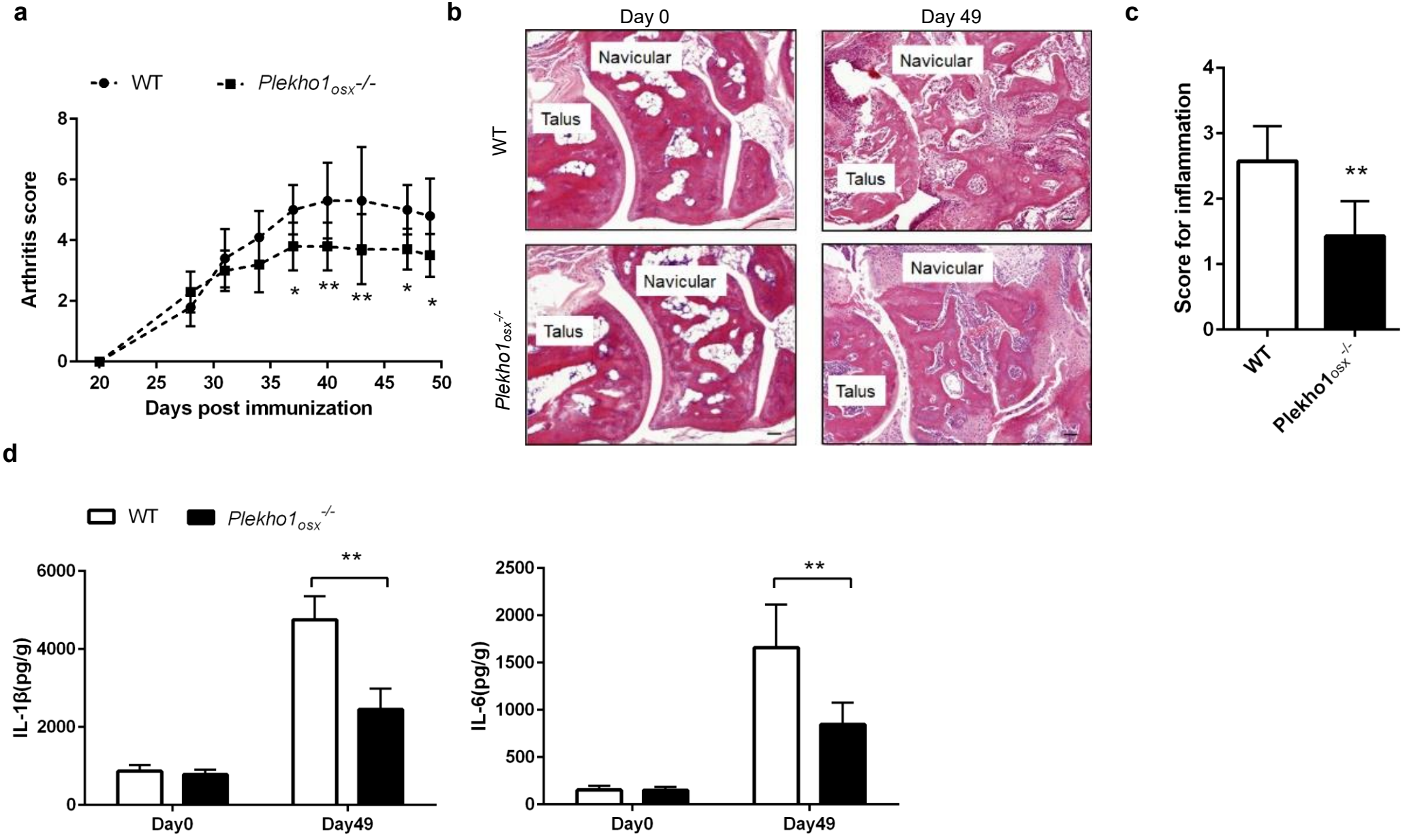
a
WT
Plekho1osx-/-
Arthritis score
Days post immunization
b
Day 0
Day 49
WT
Plekho1osx-/-
Navicular
Talus
c
Score for inflammation
WT
Plekho1osx -/-
d
WT
Plekho1osx -/-
IL-1β(pg/g)
IL-6(pg/g)
Day0
Day49

Figure 2-4 Genetic deletion of osteoblastic *Plekho1* leads to amelioration of joint inflammation in CIA mice. (**a**) Time course changes in arthritis score from $Plekho1_{osx}^{-/-}$ mice and WT mice (including $Plekho1^{fl/fl}$ mice, $Osx^{+/-};Plekho1^{fl/-}$ mice, and $Osx^{+/-}$ mice) after induction with type II chicken collagen. (**b**) Representative histological images in the ankle joint of hind paws from $Plekho1_{osx}^{-/-}$-CIA mice and WT-CIA mice on day 49 after primary immunization. Scale bars, 50μm. (**c**) Histological inflammation score in the ankle joint of hind paws from $Plekho1_{osx}^{-/-}$-CIA mice and WT-CIA mice on day 49 after primary immunization. (**d**) Time course changes of IL-1β and IL-6 levels in the ankle joint of hind paws from $Plekho1_{osx}^{-/-}$-CIA mice and WT-CIA mice by ELISA examination. All data are the mean ± s.d. $n = 10$ per group. *P < 0.05, **P < 0.01. For **a**, Two-way ANOVA with subsequent Bonferroni posttests is performed. For **c & d**, a Student's t test is performed.

2.3.2.3 The improved bone structure in *Plekho1$_{osx}^{-/-}$* mice during CIA

As our previous studies demonstrated that osteoblastic PLEKHO1 negatively regulated bone formation during aging-related bone loss and osteoporosis (Zhang et al., 2012, Liu et al., 2017), we consistently examined the bone phenotypes of *Plekho1*$_{osx}^{-/-}$ -CIA mice. MicroCT analysis showed a better organized architecture and a higher bone mass in *Plekho1*$_{osx}^{-/-}$-CIA mice compared to WT-CIA mice on day 49 after primary immunization, both in cortical bone and trabecular bone **(Fig. 2-5a)**. The values of BMD, BV/TV, Tb.Th, and Tb.N of the tibial bones were gradually decreased from baseline (day 0) in WT-CIA mice and *Plekho1*$_{osx}^{-/-}$-CIA mice. However, *Plekho1*$_{osx}^{-/-}$-CIA mice showed a slow decrease in these parameters on day 49 compared to the rapid decrease in the control mice **(Fig. 2-5b)**. Dynamic bone histomorphometric analysis showed a larger width between the xylenol and the calcein labeling bands in *Plekho1*$_{osx}^{-/-}$-CIA mice compared to WT-CIA mice **(Fig. 2-5c)**. The values of MAR, BFR/BS, Ob.S/BS, and Ob.N/B.Pm were also decreased slower in *Plekho1*$_{osx}^{-/-}$-CIA mice than those in WT-CIA mice on day 49 after primary immunization. The values of Oc.S/BS and Oc.N/B.Pm showed a slower increase in *Plekho1*$_{osx}^{-/-}$-CIA mice than those in WT-CIA mice on day 49 after primary immunization **(Fig. 2-5d)**. **These results demonstrated that osteoblastic PLEKHO1 indeed negatively regulated bone formation in CIA mice as well.**

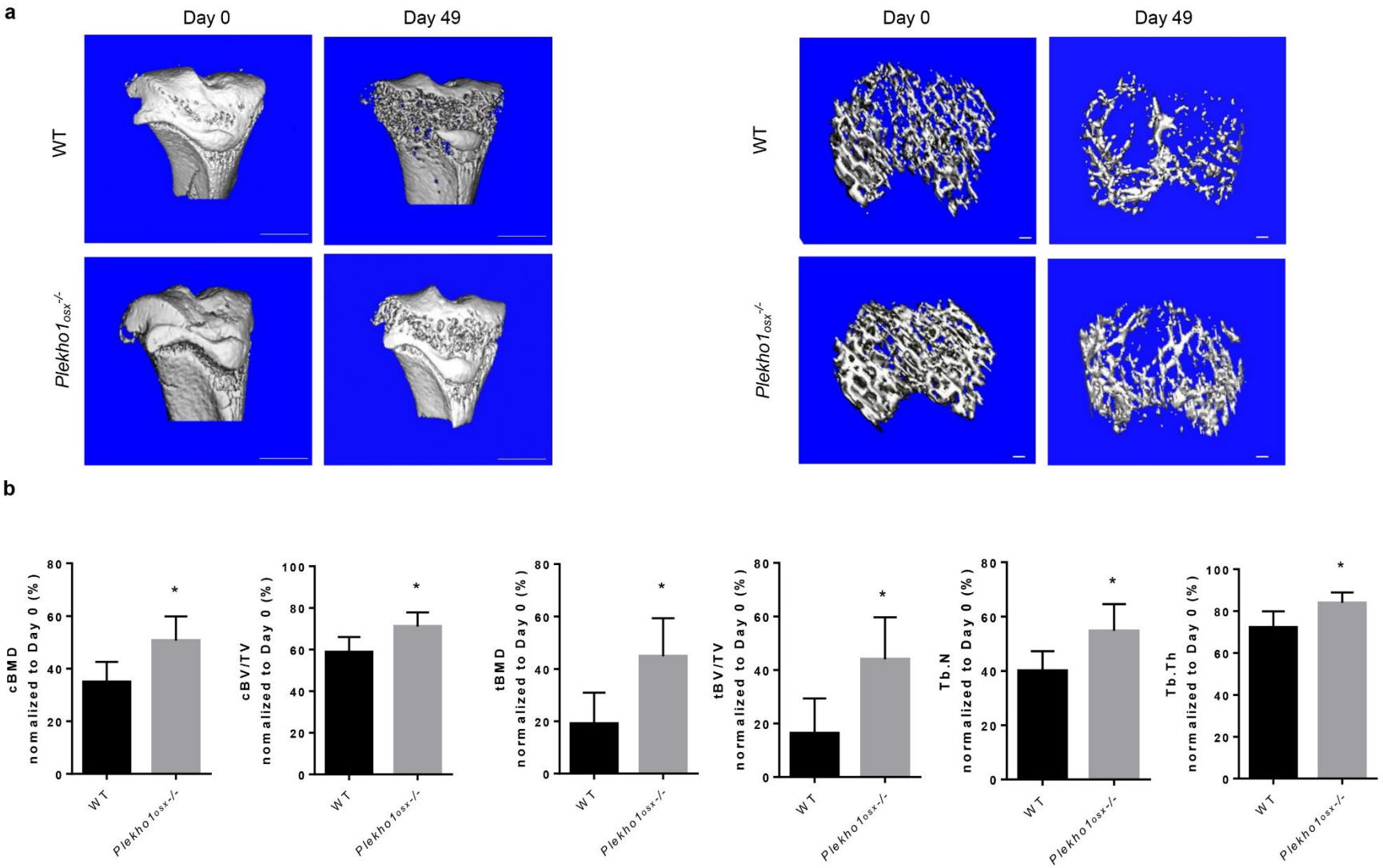
a
Day 0
Day 49
WT
Plekho1osx-/-
Day 0
Day 49
WT
Plekho1osx-/-
b
cBMD nomalized to Day 0 (%)
cBV/TV nomalized to Day 0 (%)
tBMD normalized to Day 0 (%)
tBV/TV normalized to Day 0 (%)
Tb.N normalized to Day 0 (%)
Tb.Th normalized to Day 0 (%)
WT
Plekho1osx-/-
*

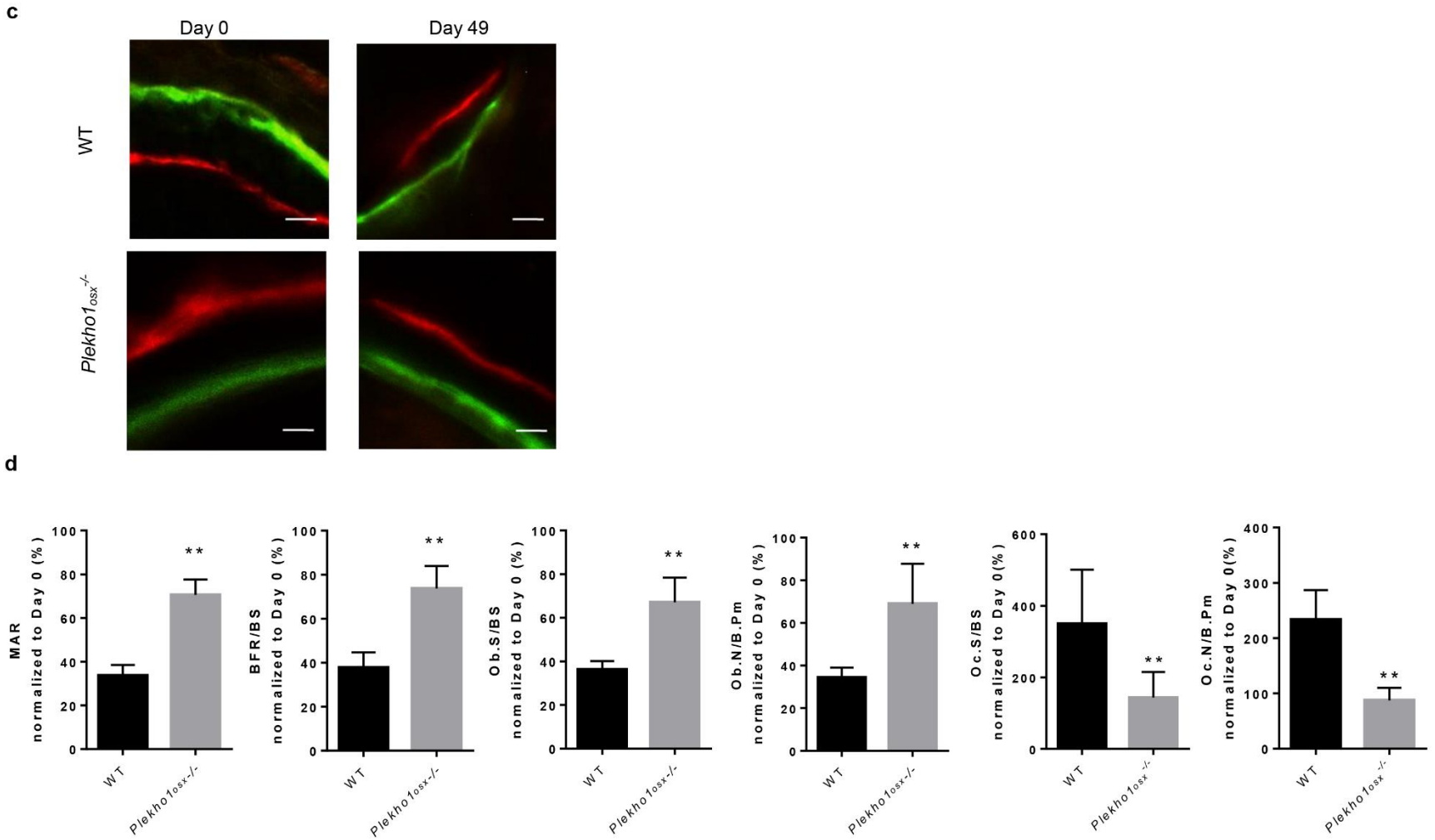
c
Day 0
Day 49
WT
Plekho1osx-/-
d
MAR
normalized to Day 0 (%)
BFR/BS
normalized to Day 0 (%)
Ob.S/BS
normalized to Day 0 (%)
Ob.N/B.Pm
normalized to Day 0 (%)
Oc.S/BS
normalized to Day 0(%)
Oc.N/B.Pm
normalized to Day 0(%)
**
WT
Plekho1osx-/-

Figure 2-5 Bone phenotype changes in *Plekho1*$_{osx}^{-/-}$ mice with CIA. (**a**) Representative 3D microarchitecture of the proximal tibia from *Plekho1*$_{osx}^{-/-}$-CIA mice and WT-CIA mice, obtained by microCT examination. Left: Cortical bone, Scale bars,1mm. Right: Trabecular bone, Scale bars,100μm. (**b**) Comparison of the microCT parameters (BMD, BV/TV, Tb.N and Tb.Th) between *Plekho1*$_{osx}^{-/-}$-CIA mice and WT-CIA mice. (**c**) Bone formation examined by sequential labeling with fluorescent dye in non-decalcified bone sections. Representative fluorescent micrographs in the hind paws from *Plekho1*$_{osx}^{-/-}$-CIA mice and WT-CIA mice showing xylenol (red) and calcein (green) labeling. Scale bar, 10μm. (**d**) Comparison of the bone histomorphometry parameters (MAR, BFR/BS, Ob.S/BS, Ob.N/B.Pm, Oc.S/BS and Oc.N/B.Pm) between *Plekho1*$_{osx}^{-/-}$-CIA mice and WT-CIA mice. *P < 0.05, **P < 0.01. Comparisons between two groups are performed using a Student's t test. Note: BMD, bone mineral density; BV/TV, relative bone volume; Tb.Th, trabecular thickness, Tb.N, trabecular number, MAR, mineral apposition rate; BFR/BS, bone formation rate/bone surface; Ob.S/BS: osteoblast surface/bone surface; Ob.N/B.Pm: osteoblast number per bone perimeter; Oc.S/BS: osteoclast surface/bone surface; Oc.N/B.Pm: osteoclast number per bone perimeter; tBMD, trabecular BMD; tBV/TV, trabecular BV/TV; cBMD, cortical BMD, cBV/TV, cortical BV/TV.

2.4 Exacerbation of joint inflammation in CIA mice by the osteoblastic *Plekho1* overexpression

2.4.1 Experiment design

The *Plekho1*$^{-/-}$*/Plekho1*$_{osx}$ *Tg* mice, *Plekho1*$_{osx}$$^{-/-}$ mice, and WT mice in the C57BL/6J background were immunized with type II chicken collagen in CFA, and followed by a boost of type II chicken collagen at day 21 after the first injection. The clinical severity of arthritis in mice was scored during the CIA establishment. The *Plekho1*$^{-/-}$*/Plekho1*$_{osx}$ *Tg* mice*, Plekho1*$_{osx}$$^{-/-}$ mice, and WT mice were sequentially sacrificed at day 0 and day 49 at the primary immunization (n=10 for each genotype at each time point), respectively. And the ankle joints of hid paws were collected for the histological evaluation of inflammation, as well as the protein levels of IL-1β and IL-6 by ELISA examination.

2.4.2 Result

2.4.2.1 The genotyping of *Plekho1*$^{-/-}$*/Plekho1*$_{osx}$ *Tg* mice

To exclude the interference of PLEKHO1 in other cells, we created another mouse strain carrying the ROSA26-PCAG-STOP^{fl}-*Plekho1*-eGFP allele, and crossed them with the Osx-Cre mice to generate the osteoblast-specific *Plekho1* overexpressing (*Plekho1*$_{osx}$ *Tg*) mice that overexpressing PLEKHO1 in osteoblasts. Then, we crossed *Plekho1*$^{-/-}$ mice with *Plekho1*$_{osx}$ *Tg* mice to obtain mice that express high Plekho1 exclusively in osteoblasts (*Plekho1*$^{-/-}$*/Plekho1*$_{osx}$ *Tg* mice) (**Figure 2-6a-b**). Real-time PCR analysis showed that *Plekho1*$^{-/-}$*/Plekho1*$_{osx}$ *Tg* mice had remarkably higher *Plekho1* mRNA levels in Ocn^{+} cells (osteoblasts), at the same time, had little *Plekho1* mRNA levels in Ocn^{-} cells (non-osteoblasts) when compared to control littermates (hereafter WT mice, including *Osx*$^{+/-}$*;Plekho1*$^{fl/-}$ mice and *Osx*$^{+/-}$*;Plekho1*$^{fl/fl}$ mice). *Plekho1*$^{-/-}$ mice had hardly detected *Plekho1* mRNA levels in both Ocn^{+} cells and Ocn^{-} cells (**Figure 2-6c**).

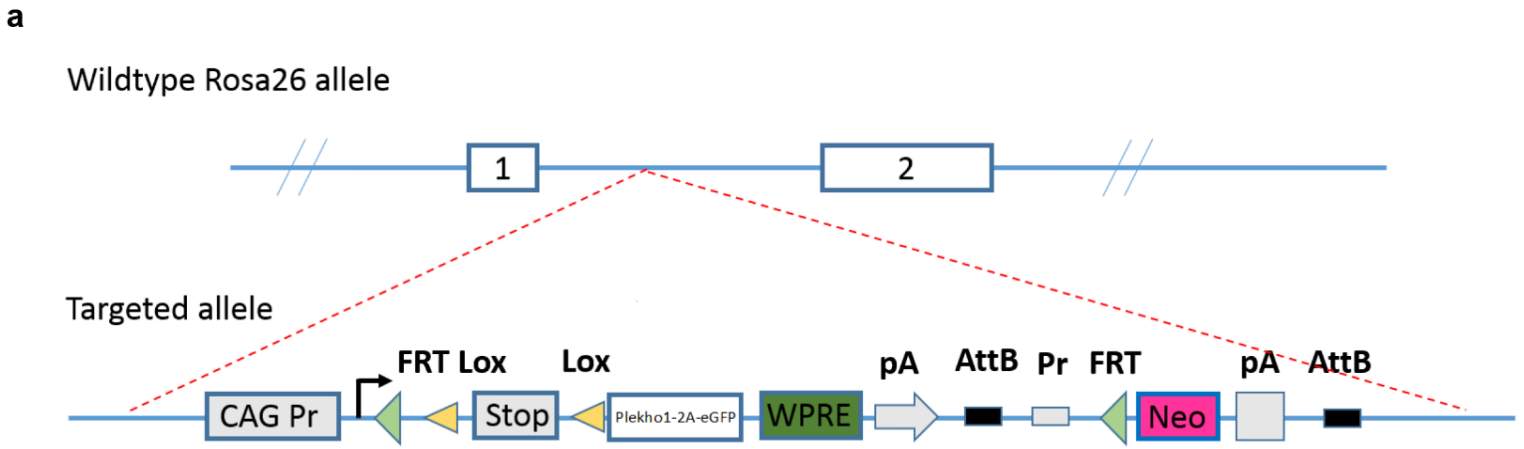
a
Wildtype Rosa26 allele
1
2
Targeted allele
FRT Lox
Lox
pA
AttB
Pr
FRT
pA
AttB
CAG Pr
Stop
Plekho1-2A-eGFP
WPRE
Neo

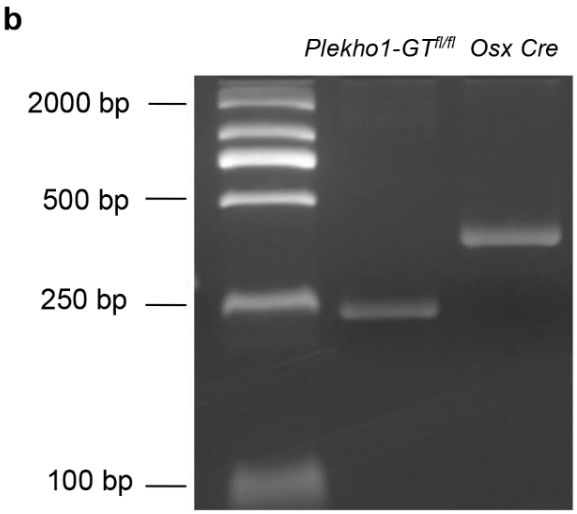
b
Plekho1-GTfl/fl Osx Cre
2000 bp
500 bp
250 bp
100 bp

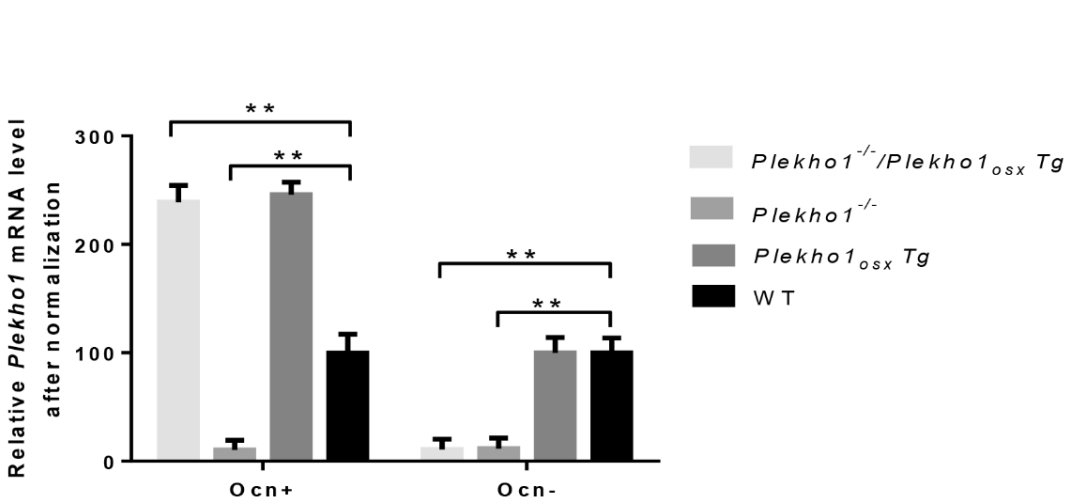
c
Relative Plekho1 mRNA level after normalization
300
200
100
0
**
**
**
**
Ocn+
Ocn-
Plekho1-/-/Plekho1osx Tg
Plekho1-/-
Plekho1osx Tg
WT

Figure 2-6 Establishment of *Plekho1*$^{-/-}$/*Plekho1*$_{osx}$*Tg* mice. (**a**) Schematic diagram for development strategy to generate ROSA26-PCAG-STOP^{fl}-*Plekho1*-eGFP knock-in mice. (**b**) Identification of *Plekho1*$_{osx}$*Tg* mice by PCR analysis. *Plekho1-GT*$^{fl/fl}$ (236bp), *Osx Cre* (445bp). (**c**) Real-time PCR analysis for *Plekho1* mRNA in Ocn^{+} cells isolated from *Plekho1*$^{-/-}$/*Plekho1*$_{osx}$*Tg* mice, *Plekho1*$^{-/-}$ mice, *Plekho1*$_{osx}$*Tg* mice, and WT mice. **P<0.01, compared to WT mice (including *Osx*$^{+/-}$; *Plekho1*$^{fl/-}$ mice and *Osx*$^{+/-}$;*Plekho1*$^{fl/fl}$ mice).

2.4.2 The increased severity of joint inflammation in *Plekho1*$^{-/-}$*/Plekho1*$_{osx}$*Tg* mice during CIA

We found that exclusively high PLEKHO1 expression in osteoblasts exacerbated the disease severity and joint inflammation progression, which were shown by increased arthritis score from day 35 after primary immunization and higher pathological inflammation score of ankle joint form the hind paws in *Plekho1*$^{-/-}$*/Plekho1*$_{osx}$ *Tg*-CIA mice compared to WT-CIA mice on day 49 after primary immunization **(Fig. 2-7a, 2-7b, 2-7c)**. IL-1β and IL-6 levels in ankle joint of hind paws from *Plekho1*$^{-/-}$*/Plekho1*$_{osx}$ *Tg*-CIA mice were also obviously higher when compared to WT-CIA mice on day 49 after primary immunization **(Fig. 2-7d)**. **These results further demonstrated that osteoblastic PLEKHO1 negatively regulated local joint inflammation.**

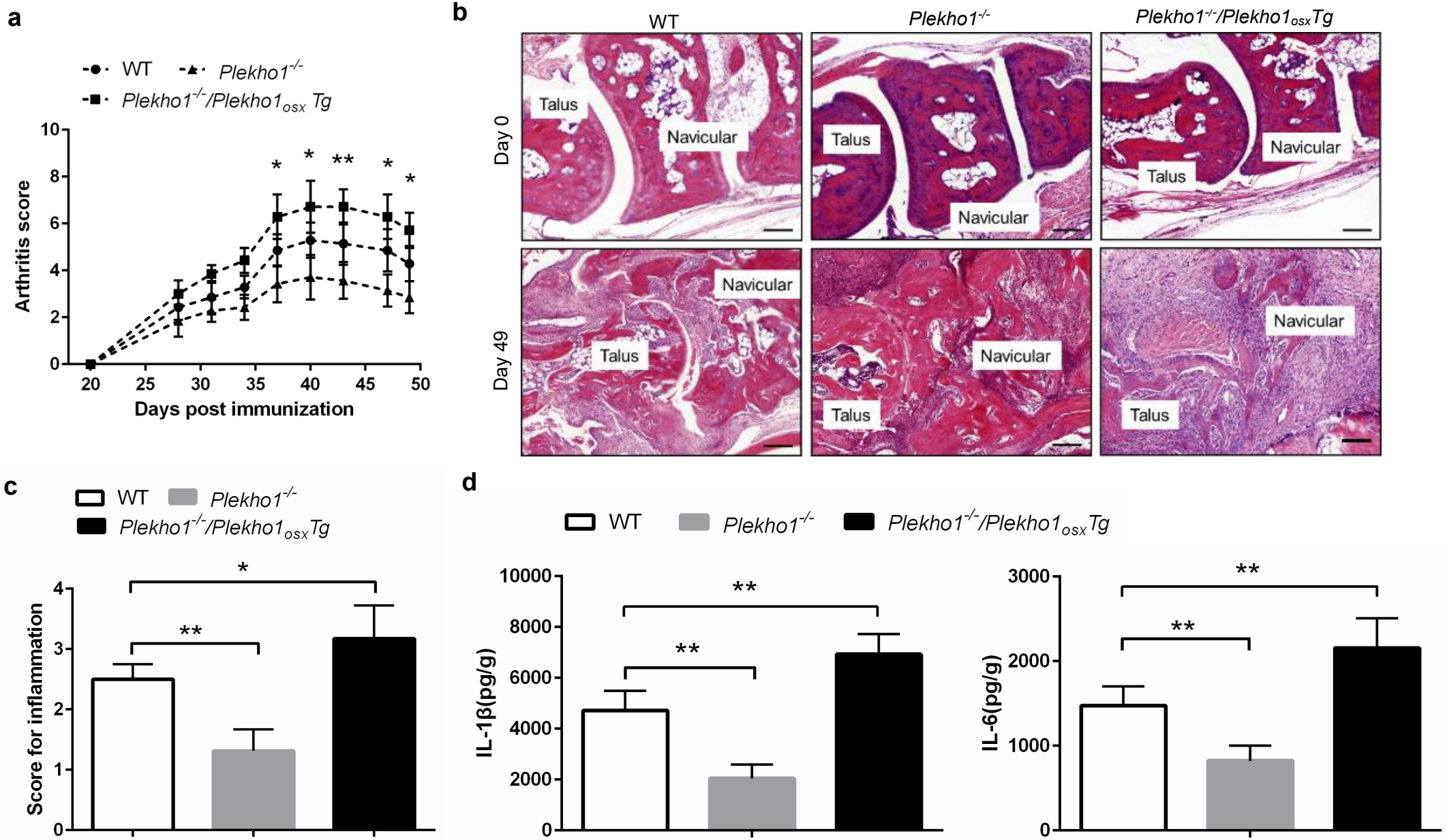
a
WT
Plekho1-/-
Plekho1-/-/Plekho1osx Tg
Arthritis score
Days post immunization
b
WT
Plekho1-/-
Plekho1-/-/Plekho1osxTg
Day 0
Day 49
Talus
Navicular
c
WT
Plekho1-/-
Plekho1-/-/Plekho1osxTg
Score for inflammation
d
WT
Plekho1-/-
Plekho1-/-/Plekho1osxTg
IL-1β(pg/g)
IL-6(pg/g)

Figure 2-7 Overexpressed *Plekho1* in osteoblasts exacerbates inflammation in *Plekho1*$^{-/-}$*/Plekho1*$_{osx}$ *Tg* mice with CIA. (**a**) Disease progression assessed by arthritic score in WT-CIA, *Plekho1*$^{-/-}$-CIA and *Plekho1*$^{-/-}$*/Plekho1*$_{osx}$ *Tg*-CIA mice. *P < 0.05, **P < 0.01，compared to WT-CIA group. (**b**) Representative histological images in the ankle joint of hind paws from WT-CIA, *Plekho1*$^{-/-}$-CIA and *Plekho1*$^{-/-}$*/Plekho1*$_{osx}$ *Tg*-CIA mice. Scale bars, 50μm. (**c**) Histological inflammation score in the ankle joint of hind paws from WT-CIA, *Plekho1*$^{-/-}$-CIA and *Plekho1*$^{-/-}$*/Plekho1*$_{osx}$ *Tg*-CIA mice. (**d**) IL-1β and lL-6 levels in the ankle joint of hind paws from WT-CIA, *Plekho1*$^{-/-}$-CIA and *Plekho1*$^{-/-}$*/Plekho1*$_{osx}$ *Tg*-CIA mice on day 49 after primary immunization by ELISA examination. All data are the mean ± s.d. *n* = 9 per group. *P < 0.05, **P < 0.01. For **a**, a two-way ANOVA with subsequent Bonferroni posttests is performed. For **c & d**, a one-way ANOVA with subsequent Tukey's multiple comparisons test is performed.

2.5 Role of osteoblastic PLEKHO1 in inflammation regulation

2.5.1 Experimental design

The previous studies have demonstrated that joint inflammation progression was mainly caused by the activated FLS and immune cells including infiltrating lymphocytes and neutrophils (Choy, 2012). To study the role of osteoblastic PLEKHO1 in inflammation regulation, the studies of cross-talk between osteoblasts and FLS, $CD4^+$ T lymphocytes, as well as neutrophils by using an *in vitro* co-culture system was essential. The *in vitro* co-culture system could experimentally simulate the temporo-spatial complexity of the *in vivo* cross-talk between osteoblasts and inflammatory cells in the joint.

The osteoblasts were differentiated from the primary osteoblast precursor cells isolated from the calvarial bone of newborn *Plekho1*$_{osx}^{-/-}$ mice, *Plekho1*$_{osx}$ *Tg* mice, and WT littermates in osteogenic medium and confirmed to express osteocalcin. The FLS, $CD4^+$ T lymphocytes, and neutrophils were obtained from WT mice by collagenase digestion and specific magnetic beads-based selection, respectively. Thereafter, the FLSs, $CD4^+$ T lymphocytes or neutrophils were co-cultured with *Plekho1*$_{osx}^{-/-}$, *Plekho1*$_{osx}$ *Tg* or WT osteoblasts, respectively, in the presence and absence of TNF-α **(Fig. 2-8)**. After co-culture, the FLSs and $CD4^+$ T lymphocytes were collected to examine the mRNA levels of IL-1β and IL-6 for real-time PCR analysis. The neutrophils at the bottom of the transwells were stained by chloroacetate esterase and the positive cells were counted.

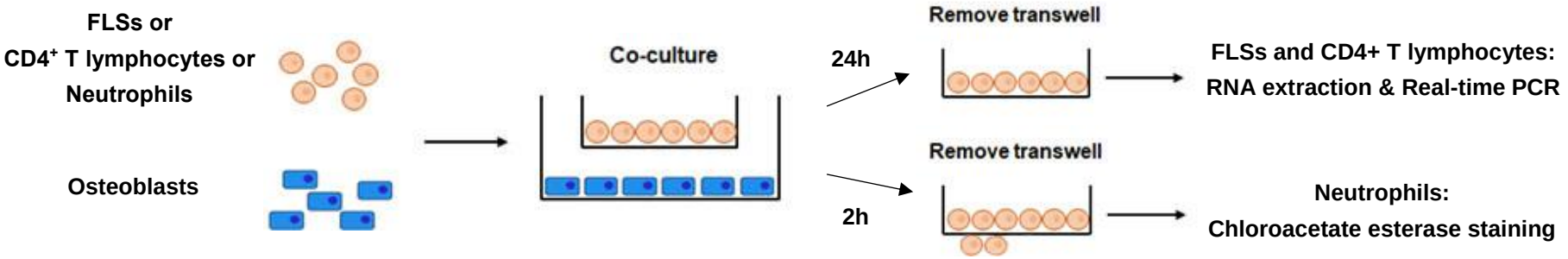

Figure 2-8 A schematic diagram illustrating the design of the co-culture experiments. The $CD4^+$ T lymphocytes or FLSs or neutrophils derived from WT mice are co-cultured with the osteoblasts derived from *Plekho1*$_{osx}^{-/-}$ mice, *Plekho1*$_{osx}$ *Tg* mice or WT mice, with or without the stimulation of TNF-α.

2.5.2 Result

The results showed that under TNF-α stimulation, the IL-1β and IL-6 mRNA levels in the $CD4^+$ T lymphocytes and FLSs were remarkably decreased after co-culture with osteoblasts from *Plekho1*$_{osx}^{-/-}$ mice when compared with the control group **(Fig. 2-9a-b)**. The migration of neutrophils was also inhibited after co-culture with osteoblasts from *Plekho1*$_{osx}^{-/-}$ mice **(Fig. 2-9c)**.

In addition, we also found that under TNF-α stimulation, the IL-1β and IL-6 mRNA levels in $CD4^+$ T lymphocytes and FLSs were higher after co-culture with osteoblasts from *Plekho1*$_{osx}$ *Tg* mice when compared with the control group **(Fig. 2-9d-e)**. The migration of neutrophils was also enhanced after co-culture with osteoblasts from *Plekho1*$_{osx}$ *Tg* mice **(Fig. 2-9f)**. **These novel results pointed to an important role of osteoblastic PLEKHO1 in modulating local inflammatory response in RA.**

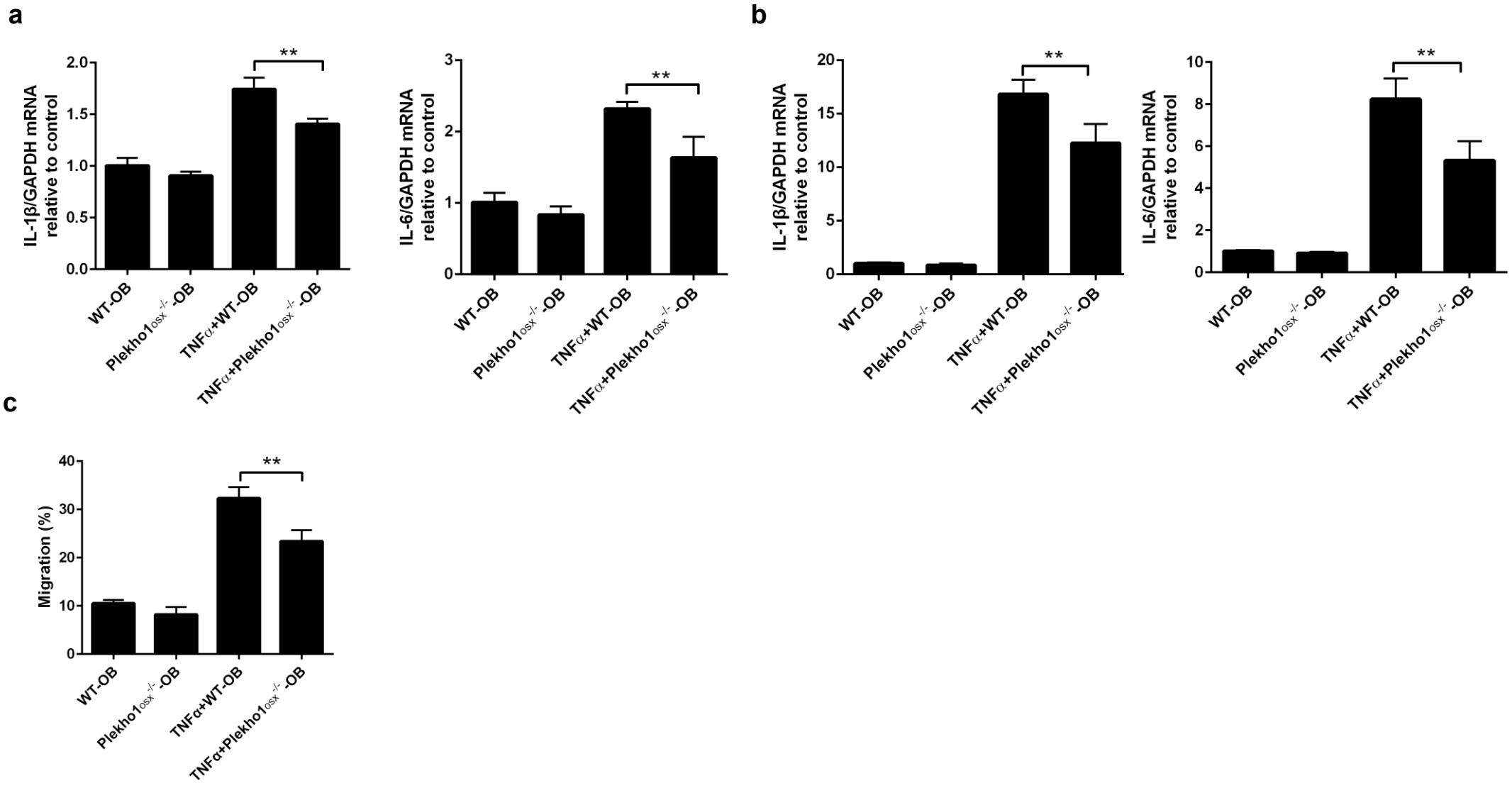
a
IL-1β/GAPDH mRNA relative to control
2.0
1.5
1.0
0.5
0.0
**
WT-OB
Plekho1osx -/- -OB
TNFα+WT-OB
TNFα+Plekho1osx -/- -OB
IL-6/GAPDH mRNA relative to control
3
2
1
0
**
WT-OB
Plekho1osx -/- -OB
TNFα+WT-OB
TNFα+Plekho1osx -/- -OB
b
IL-1β/GAPDH mRNA relative to control
20
15
10
5
0
**
WT-OB
Plekho1osx -/- -OB
TNFα+WT-OB
TNFα+Plekho1osx -/- -OB
IL-6/GAPDH mRNA relative to control
10
8
6
4
2
0
**
WT-OB
Plekho1osx -/- -OB
TNFα+WT-OB
TNFα+Plekho1osx -/- -OB
c
Migration (%)
40
30
20
10
0
**
WT-OB
Plekho1osx -/- -OB
TNFα+WT-OB
TNFα+Plekho1osx -/- -OB

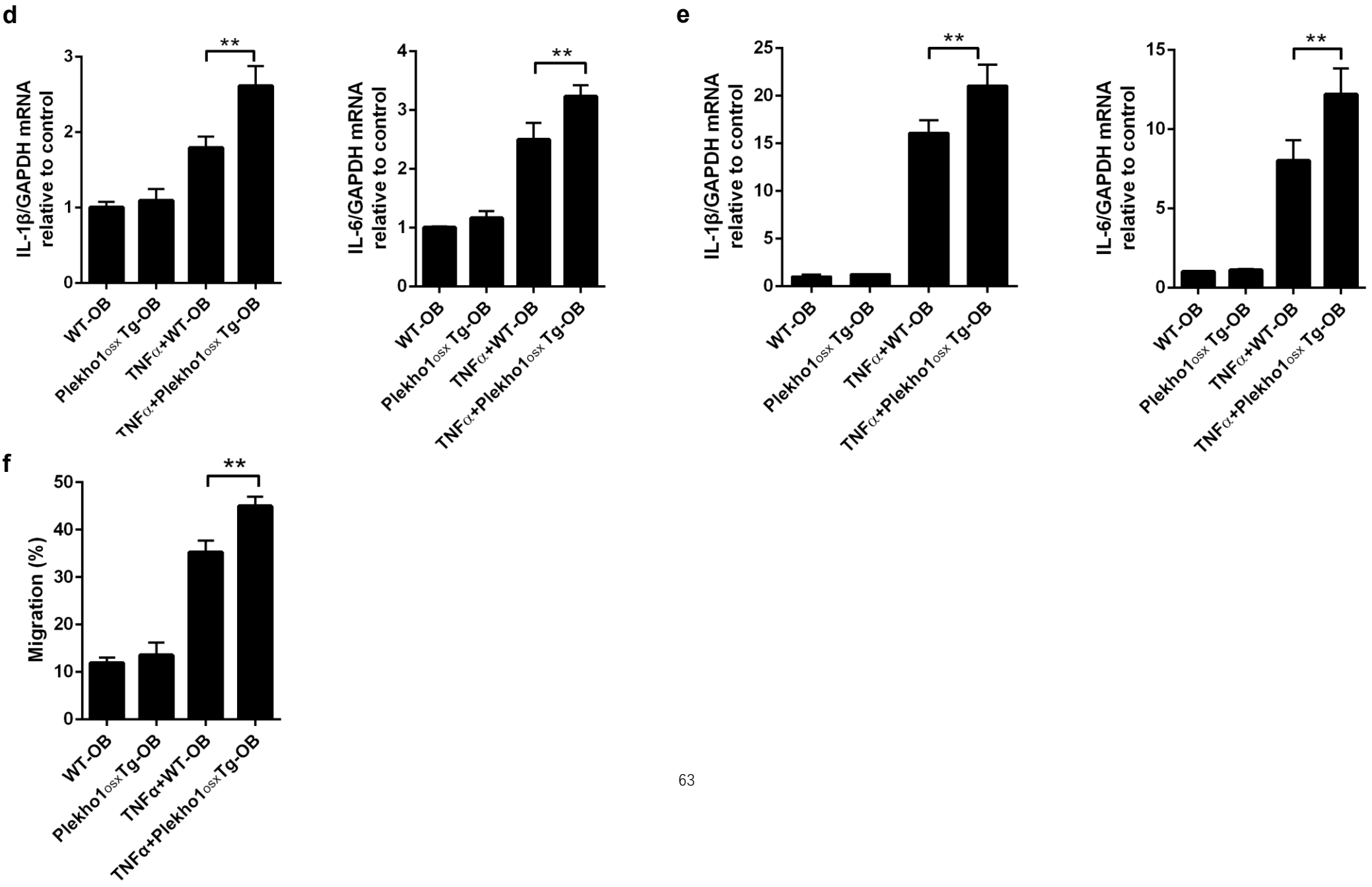
d
IL-1β/GAPDH mRNA relative to control
IL-6/GAPDH mRNA relative to control
e
IL-1β/GAPDH mRNA relative to control
IL-6/GAPDH mRNA relative to control
f
Migration (%)
**
WT-OB
Plekho1osx Tg-OB
TNFα+WT-OB
TNFα+Plekho1osx Tg-OB

Figure 2-9 The co-culture between *Plekho1*$_{osx}^{-/-}$, *Plekho1*$_{osx}$ *Tg* or WT osteoblasts and inflammatory cells in the presence and absence of TNF-α. (**a**) IL-1β and IL-6 mRNA levels in $CD4^+$ T lymphocytes after co-culture with osteoblasts from WT mice and *Plekho1*$_{osx}^{-/-}$ mice. (**b**) IL-1β and IL-6 mRNA levels in FLS after co-culture with osteoblasts from WT mice and *Plekho1*$_{osx}^{-/-}$ mice. (**c**) Migration of neutrophils after co-culture with osteoblasts from WT mice and *Plekho1*$_{osx}^{-/-}$ mice. (**d**) IL-1β and IL-6 mRNA levels in $CD4^+$ T lymphocytes after co-culture with osteoblasts from WT mice and *Plekho1*$_{osx}$ *Tg* mice. (**e**) IL-1β and IL-6 mRNA levels in FLS after co-culture with osteoblasts from WT mice and *Plekho1*$_{osx}$ *Tg* mice. (**f**) Migration of neutrophils after co-culture with osteoblasts from WT mice and *Plekho1*$_{osx}$ *Tg* mice. All data are the mean ± s.d. $n = 9$ per group. **P < 0.01. A one-way ANOVA with subsequent Tukey's multiple comparisons test is performed.

2.6 Influence of osteoblastic PLEKHO1 in the TNF-α-stimulated osteoblast-releasing inflammatory effectors

2.6.1 Experimental design

In *in vitro* studies, we used a mouse osteoblast–like cell line MC3T3E1 to explore the mechanism of osteoblastic PLEKHO1 in inflammation modulation. The cells were seeded and followed by the transfection of *Plekho1* siRNA and random siRNA, respectively. After the incubation with the siRNA, the cells were stimulated with or without TNF-α. The supernatant from MC3T3E1 was collected to detect the protein levels of IL-1β and IL-6 production.

In *in vivo* studies, we crossed hTNFtg mice, which could spontaneously develop arthritis at the age of four week due to the overexpressed human TNF transgene, with *Plekho1*$_{osx}^{-/-}$ mice to obtain *Plekho1*$_{osx}^{-/-}$/hTNFtg mice. The joint swelling assessment was performed in the hTNFtg and *Plekho1*$_{osx}^{-/-}$/hTNFtg mice from week 3 to week 10 for once per week. And the hTNFtg and *Plekho1*$_{osx}^{-/-}$/hTNFtg mice were sequentially sacrificed at week 4 and week 10 (n=10 for each genotype at each time point), respectively. And the ankle joints of hid paws were collected for the histological evaluation of inflammation.

2.6.2 Result

2.6.2.1 The decrease in the releasing inflammatory effectors by the inhibition of osteoblastic PLEKHO1 expression

We found that after *Plekho1* silencing by *Plekho1* siRNA, the IL-1β and IL-6 production in supernatant of TNF-α-stimulated MC3T3E1 cells were remarkably lower than the random siRNA group **(Fig. 2-10)**.

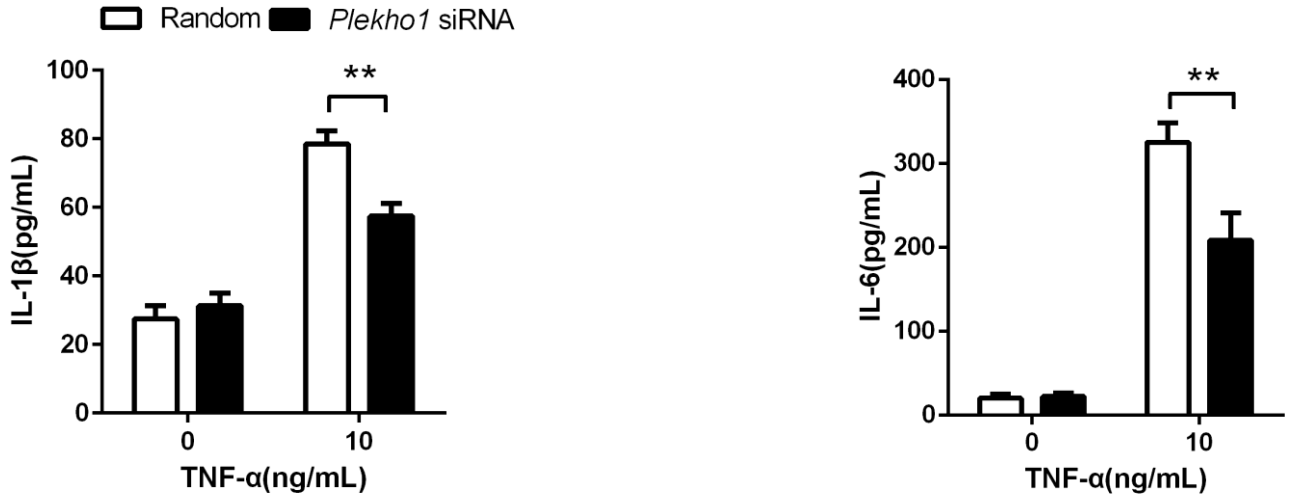

Figure 2-10 The releasing inflammatory effectors after the silence of *Plekho1* within osteoblasts. Levels of inflammatory cytokines (IL-1β, IL-6) produced by MC3T3E1 cells transfected with *Plekho1* siRNA or random siRNA and subjected to TNF-α (10 ng/ml). Data are representative of three independent experiments. **P<0.01. Comparisons between two groups are performed using a Student's t test.

2.6.2.2 The attenuation of joint inflammation by the deficiency of *Plekho1* in *Plekho1*$_{osx}^{-/-}$/hTNFtg mice

In line with the above findings *in vitro*, *Plekho1*$_{osx}^{-/-}$/hTNFtg mice showed a distinct alleviation of disease severity. The arthritis score in *Plekho1*$_{osx}^{-/-}$/hTNFtg mice was significantly lower than that in hTNFtg mice from 7 week to 10 weeks after birth **(Figure 2-11a)**. Histological analysis also indicated that joint inflammation was significantly ameliorated in *Plekho1*$_{osx}^{-/-}$/hTNFtg mice compared to hTNFtg mice, which were reflected by lower histological inflammation score at week 10 **(Figure 2-11b-c)**. **These results implied that osteoblastic PLEKHO1 on joint inflammation regulation might be related with TNF-α involved signal mechanism.**

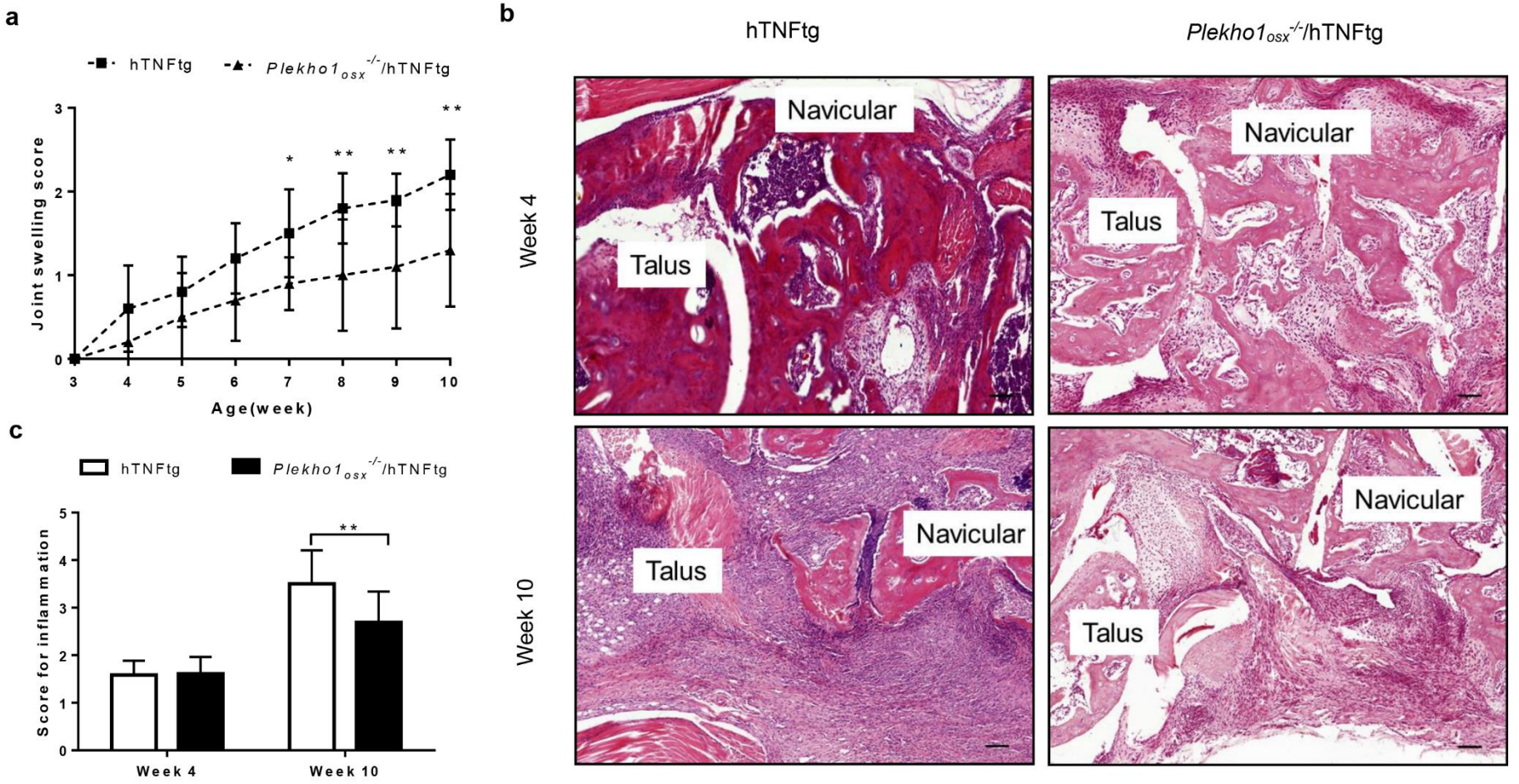
a
hTNFtg
Plekho1osx-/-/hTNFtg
Joint swelling score
Age(week)
b
hTNFtg
Plekho1osx-/-/hTNFtg
Week 4
Week 10
Navicular
Talus
c
hTNFtg
Plekho1osx-/-/hTNFtg
Score for inflammation
Week 4
Week 10

Figure 2-11 Deficiency of *Plekho1* in osteoblasts alleviates joint inflammation in *Plekho1*$_{osx}^{-/-}$/hTNFtg mice. (**a**) Disease progression assessed by joint swelling score in hTNFtg and *Plekho1*$_{osx}^{-/-}$/hTNFtg mice from week 3 to 10. (**b**) Representative histological images in the ankle joint of the hind paws from hTNFtg and *Plekho1*$_{osx}^{-/-}$/hTNFtg mice. Scale bars, 50 μm. (**c**) Histological inflammation score inthe ankle joint of the hind paws of hTNFtg and *Plekho1*$_{osx}^{-/-}$/hTNFtg mice. All data are the mean ± s.d.*P<0.05, **P<0.01. *n*= 10 per group. Two-way ANOVA with subsequent Bonferroni posttests is performed. Comparisons between two groups are performed using a Student's t test.

2.7 The inhibition of RIP1 ubiquitination under TNF-α stimulation in *Plekho1*-silenced osteoblasts

2.7.1 Experimental design

As previous studies have demonstrated that NF-κB signal pathway played an important role in TNF-α induced inflammatory cytokines production (Hayden and Ghosh, 2008). Therefore, the changes of related proteins in this signal pathway were detected after the transfection with *Plekho1* siRNA or random siRNA in MC3T3E1. After the transfection, the cells were stimulated with or without TNF-α. The cell lysis was collected to detect the western blot analysis.

.

2.7.2 Result

We found that IKKα/β and p65 phosphorylation as well as RIP1 ubiquitination were inhibited under TNF-α stimulation in *Plekho1*-silenced MC3T3E1 cells, although no significantly change on production of IKKβ and p65 **(Fig. 2-12a-c)**. **It Indicated that the PLEKHO1 participated in the RIP1 ubiquitination under TNF-α-stimulated inflammatory modulation in osteoblasts.**

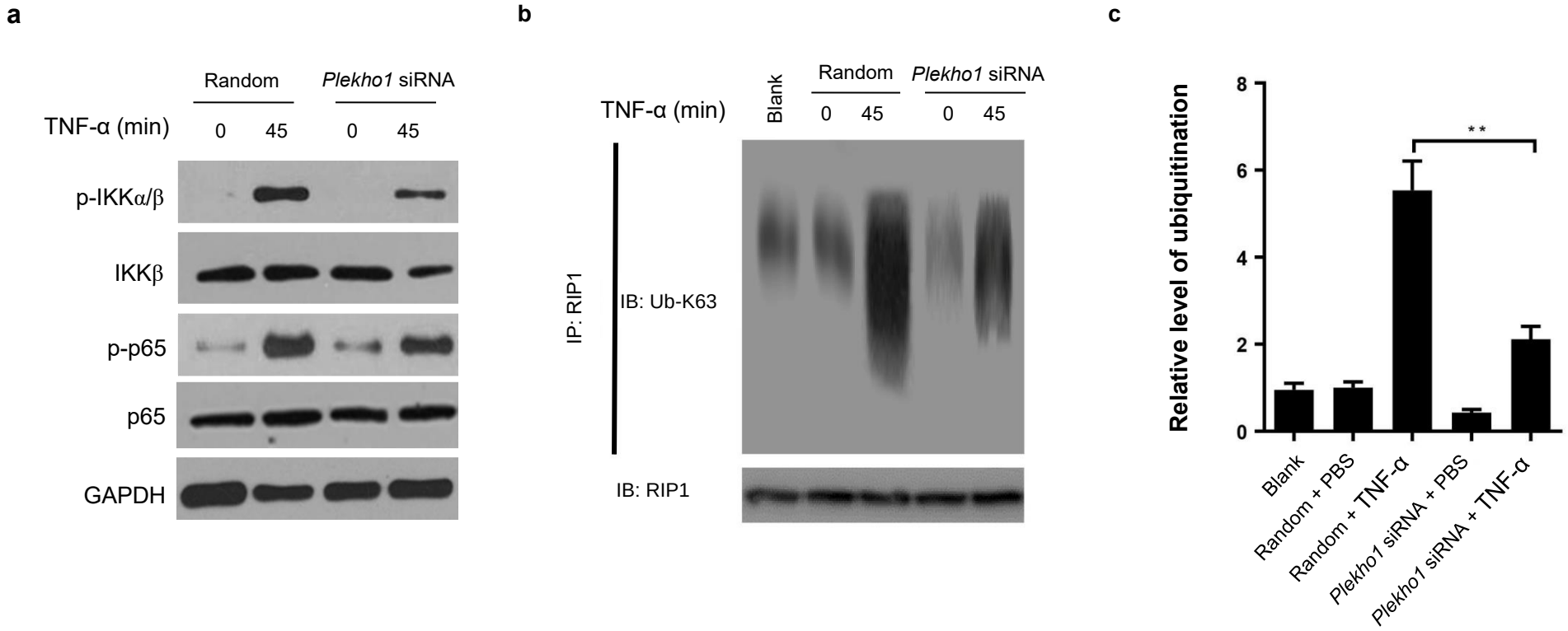

Figure 2-12 The silencing of osteoblastic *Plekho1* inhibited the TRAF2-mediated ubiquitination of RIP1. (a) MC3T3E1 cells transfected with *Plekho1* siRNA or random siRNA are stimulated with TNF-α (10 ng/ml) for 45min, and harvested for detection of IKKα/β and p65 phosphorylation. **(b)** MC3T3E1 cells transfected with *Plekho1* siRNA or random siRNA are stimulated with TNF-α (10 ng/ml) for 45min, and harvested for detection of RIP1 ubiquitination. **(c)** Quantification of relative level of RIP1 ubiquitination. Note: IP, Immunoprecipitation; IB, immunoblotting. Data are representative of three independent experiments. **P<0.01. Comparisons between two groups are performed using a Student's t test.

2.8 Mechanism of PLEKHO1 to mediate RIP1 ubiquitination under TNF-α-stimulated inflammatory modulation in osteoblasts

2.8.1 Experimental design

Previous studies demonstrated that TNF-α upregulated the expression of inflammatory mediators through TRAF2-mediated NF-κB activation in MC3T3E1 cells (Tsai et al., 2014). In addition, PLEKHO1 could interact with the member of TRAF family to regulate the downstream signal (Zhang et al., 2014), we therefore hypothesized that PLEKHO1 might interact with TRAF2 to promote the activation of NF-kB signal pathways for mediating RIP1 ubiquitination. Then, the HEK293T cells were subjected to the following three experiments:

1) To test whether TRAF2 could interact with PLEKHO1 and which domain in TRAF2 was essential for their interaction. HEK293T cells were transfected with Flag-TRAF2 in the full-length proteins or truncated mutants and Myc-PLEKHO1 in the full-length proteins. The cell lysis was collected to subject to immunoprecipitation of TRAF2 protein by western blotting.
2) To identify the key domain in PLEKHO1 that interacted with TRAF2. HEK293T cells were transfected with Flag-TRAF2 in the full-length proteins and Myc-PLEKHO1 in the full-length proteins or truncated mutants. The cell lysis was collected to subject to immunoprecipitation of PLEKHO1 protein by western blotting.
3) To determine whether PLEKHO1 affected TRAF2-mediated RIP1 ubiquitination. HEK293T cells were transfected with Myc-RIP1, HA-Ubiquitin (HA-Ub), Flag-PLEKHO1 or Flag-ΔLZ and Flag-TRAF2 or Flag-ΔTRAF C. The cell lysis was collected to subject to immunoprecipitation of RIP1 proteins for the ubiquitination assay by western blot and quantify the levels of RIP1 ubiquitination.

2.8.2 Result

2.8.2.1 TRAF C domain (ΔTRAF C) in TRAF2 was essential for the interaction between TRAF2 and PLEKHO1.

Because TRAF2 contains a ring finger domain, a zinc finger domain, a TRAF N domain and a TRAF C domain (Aggarwal, 2003, Zheng et al., 2011, Hoeflich et al., 1999). Thus, we constructed Myc-tagged full-length PLEKHO1 (Myc-PLEKHO1), Flag-tagged full-length TRAF2 (Flag-TRAF2) and various TRAF2 truncated mutants including Flag-ΔRing, Flag-ΔRing-Zinc, Flag-TRAF N and Flag-ΔTRAF C **(Fig. 2-13a)**. After immunoprecipitation using anti-Flag antibody, we detected that TRAF2 could interact with PLEKHO1 **(Fig. 2-13b**, Lane 2**)**. However, deletion of TRAF C domain (ΔTRAF C) abolished the interaction between TRAF2 and PLEKHO1 **(Fig. 2-13b**, Lane 6**)**, whereas other truncated mutants (ΔRing, ΔRing-Zinc and TRAF C) maintained the binding with PLEKHO1 as that of full-length TRAF2 **(Fig. 2-13b**, Lane 3-5**)**.

a

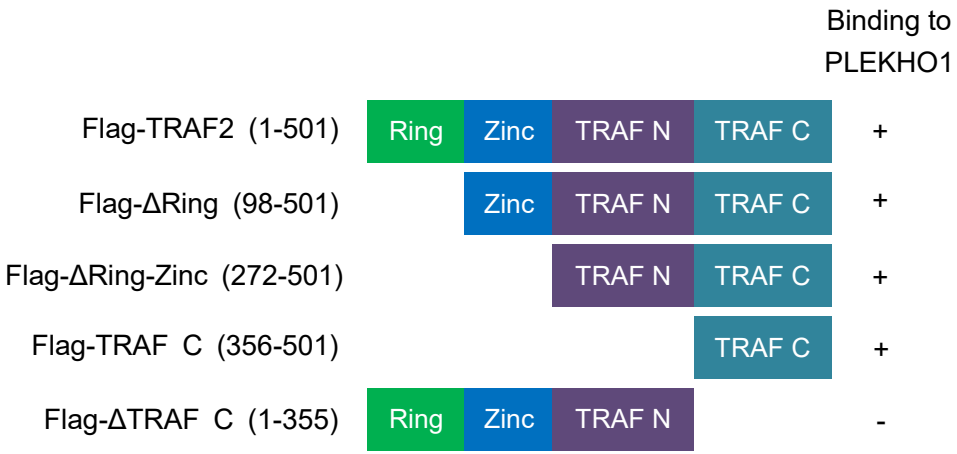
Binding to PLEKHO1
Flag-TRAF2 (1-501)
Ring
Zinc
TRAF N
TRAF C
+
Flag-ΔRing (98-501)
Zinc
TRAF N
TRAF C
+
Flag-ΔRing-Zinc (272-501)
TRAF N
TRAF C
+
Flag-TRAF C (356-501)
TRAF C
+
Flag-ΔTRAF C (1-355)
Ring
Zinc
TRAF N
-

b

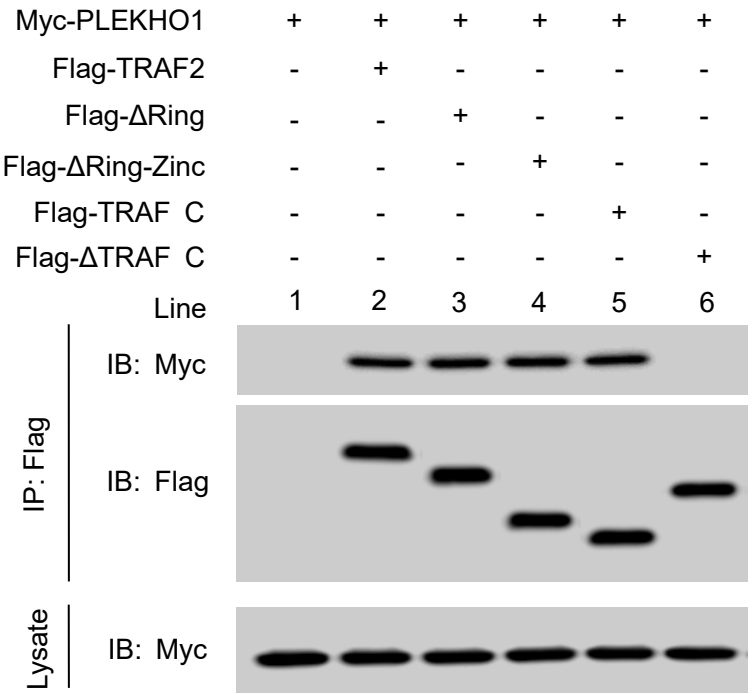
Myc-PLEKHO1 + + + + + +
Flag-TRAF2 - + - - - -
Flag-ΔRing - - + - - -
Flag-ΔRing-Zinc - - - + - -
Flag-TRAF C - - - - + -
Flag-ΔTRAF C - - - - - +
Line 1 2 3 4 5 6
IP: Flag
IB: Myc
IB: Flag
Lysate
IB: Myc

Figure 2-13 Immunoprecipitation using anti-Flag antibody to examine the PLEKHO1-TRAF2 interaction and mapping of the PLEKHO1-interacting domain in TRAF2. (a) The Flag-tagged full-length TRAF2 (Flag-TRAF2) and various truncated mutants (Flag-ΔRing, Flag-ΔRing-Zinc, Flag-TRAF N and Flag-ΔTRAF C) are shown with amino acid numbers. **(b)** HEK293T cells are transfected with Myc-PLEKHO1 and Flag-TRAF2 or truncated mutants as indicated. Full-length TRAF2 or truncated mutants is immunoprecipitated by anti-Flag antibody. PLEKHO1 in immunoprecipitates or whole-cell lysate is detected by anti-Myc antibody. Note: IP, Immunoprecipitation; IB, immunoblotting. Data are representative of three independent experiments.

2.8.2.2 LZ-containing domain (ΔLZ) in PLEKHO1 was important for the interaction between TRAF2 and PLEKHO1.

Because PLEKHO1 is composed of an N-terminal pleckstrin homology (PH)-containing domain and a C-terminal leucine zipper (LZ)-containing domain (Lu et al., 2008, Wang et al., 2012). We also constructed PLEKHO1 truncated mutants (Myc-ΔPH, Myc-LZ and Myc-ΔLZ) **(Fig. 2-14a)**. Data from immunoprecipitation showed that the PLEKHO1 mutant with deletion of LZ-containing domain (ΔLZ) could not interact with TRAF2 **(Fig. 2-14b,** Lane 5**)**, but other PLEKHO1 mutants could still bound to TRAF2 **(Fig. 2-14b,** Lane 2-4**)**.

a

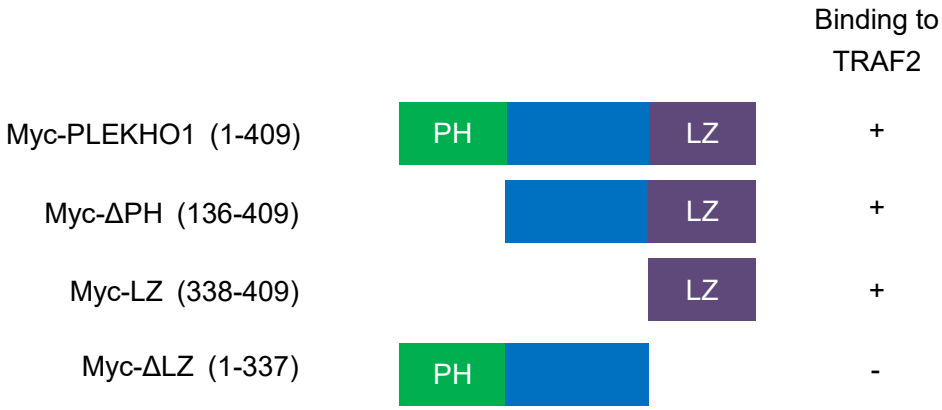
Binding to TRAF2
Myc-PLEKHO1 (1-409)
PH
LZ
+
Myc-ΔPH (136-409)
LZ
+
Myc-LZ (338-409)
LZ
+
Myc-ΔLZ (1-337)
PH
-

b

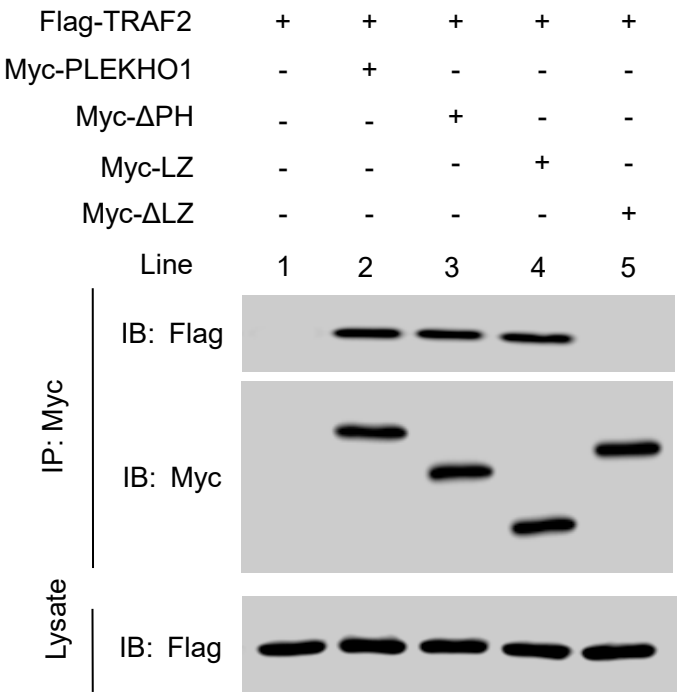
Flag-TRAF2 + + + + +
Myc-PLEKHO1 - + - - -
Myc-ΔPH - - + - -
Myc-LZ - - - + -
Myc-ΔLZ - - - - +
Line 1 2 3 4 5
IP: Myc
IB: Flag
IB: Myc
Lysate
IB: Flag

Figure 2-14 Immunoprecipitation using anti-Myc antibody to examine the PLEKHO1-TRAF2 interaction and mapping of the TRAF2-interacting domain in PLEKHO1. (a) The Myc-tagged full-length PLEKHO1 (Myc-PLEKHO1) and various truncated mutants (Myc-ΔPH, Myc-LZ, and Myc-ΔLZ) are shown with amino acid numbers. **(b)** HEK293T cells are transfected with Flag-TRAF2 and Myc-PLEKHO1 or truncated mutants as indicated. Full-length PLEKHO1 or truncated mutants is immunoprecipitated by anti-Myc antibody. TRAF2 in immunoprecipitates or whole-cell lysate is detected by anti-Flag antibody. Note: IP, Immunoprecipitation; IB, immunoblotting. Data are representative of three independent experiments.

2.8.2.3 The promotion of PLEKHO1 to TRAF2-mediated ubiquitination of RIP1

Our results demonstrated that PLEKHO1 promoted the TRAF2-mediated ubiquitination of RIP1 **(**lane 3 in **Fig. 2-15a,** lane 3 in **Fig. 2-15c, Fig. 2-15b, Fig. 2-15d)**. Nevertheless, PLEKHO1 mutant with deletion of c-terminal LZ-containing domain had no obvious promotive effects on TRAF2-mediated ubiquitination of RIP1 **(**lane 4 in **Fig. 2-15a, Fig. 2-15b)**. Disruption of TRAF2-PLEKHO1 interaction by deletion of ΔTRAF C in TRAF2 also diminished the promotive effect of PLEKHO1 on TRAF2-mediated RIP1 ubiquitination **(**lane 4 in **Fig. 2-15c, Fig. 2-15d).** Because TRAF2 could ubiquitinate RIP1, which is essential for NF-kB activation (Chen, 2005). **All these results indicated that PLEKHO1 could interact with TRAF2 to promote the TRAF2-mediated ubiquitination of RIP1 to activate NF-kB during inflammation modulation in osteoblasts.**

a

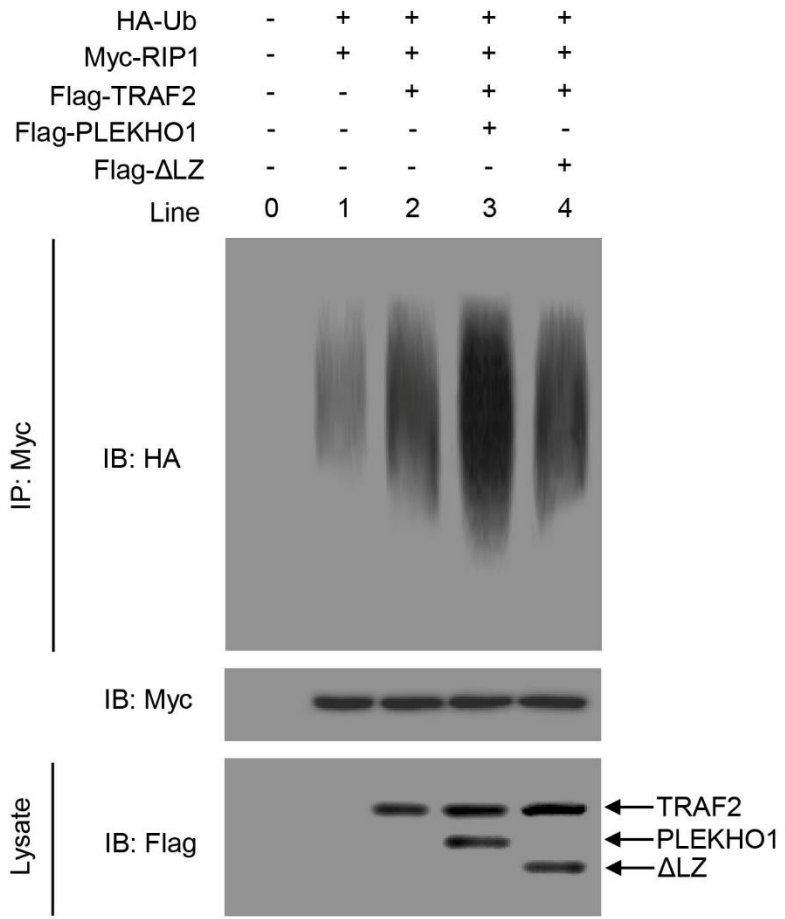
HA-Ub - + + + +
Myc-RIP1 - + + + +
Flag-TRAF2 - - + + +
Flag-PLEKHO1 - - - + -
Flag-ΔLZ - - - - +
Line 0 1 2 3 4
IP: Myc
IB: HA
IB: Myc
Lysate
IB: Flag
TRAF2
PLEKHO1
ΔLZ

b

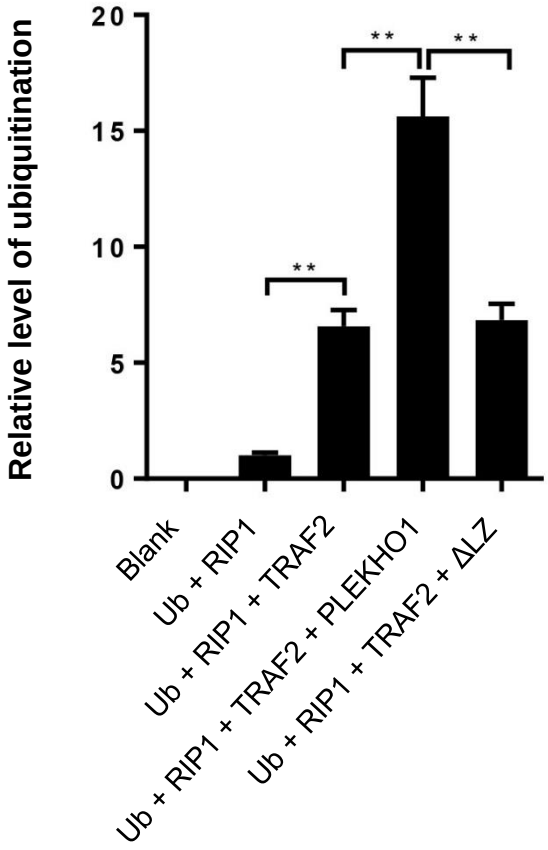
Relative level of ubiquitination
20
15
10
5
0
**
**
**
Blank
Ub + RIP1
Ub + RIP1 + TRAF2
Ub + RIP1 + TRAF2 + PLEKHO1
Ub + RIP1 + TRAF2 + ΔLZ

c

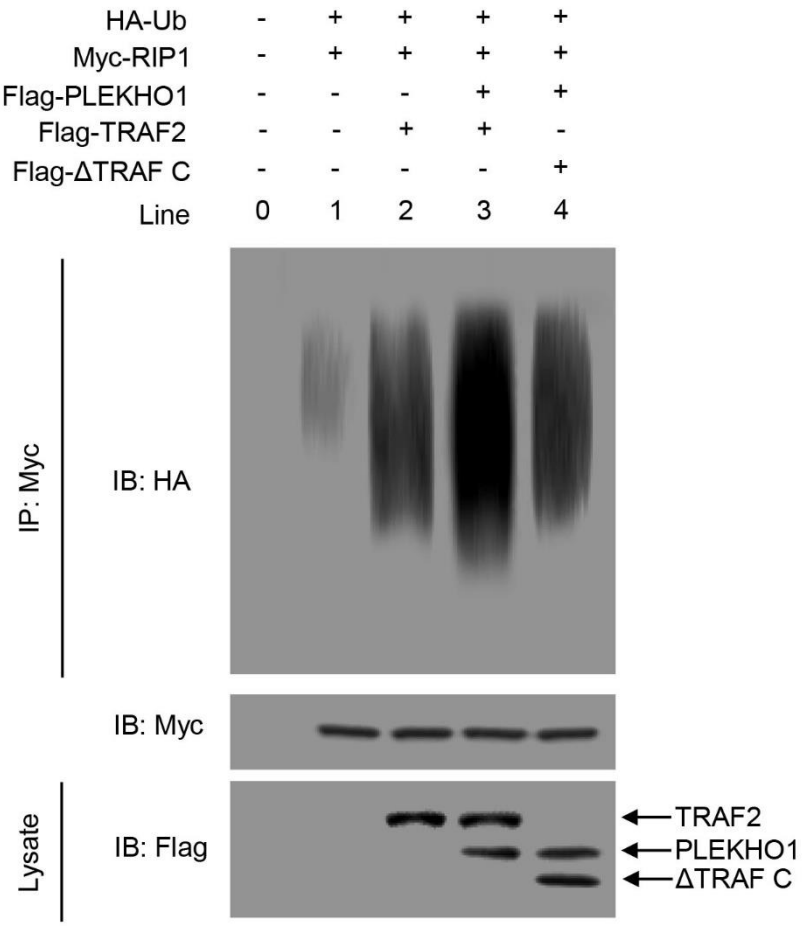
HA-Ub - + + + +
Myc-RIP1 - + + + +
Flag-PLEKHO1 - - - + +
Flag-TRAF2 - - + + -
Flag-ΔTRAF C - - - - +
Line 0 1 2 3 4
IP: Myc
IB: HA
IB: Myc
Lysate
IB: Flag
TRAF2
PLEKHO1
ΔTRAF C

d

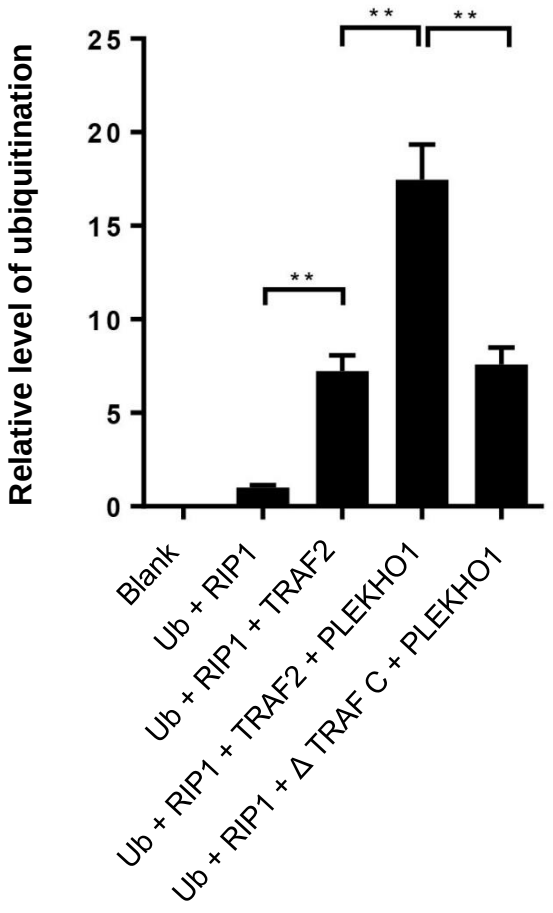
Relative level of ubiquitination
25
20
15
10
5
0
**
**
**
Blank
Ub + RIP1
Ub + RIP1 + TRAF2
Ub + RIP1 + TRAF2 + PLEKHO1
Ub + RIP1 + Δ TRAF C + PLEKHO1

Figure 2-15 The promotion of PLEKHO1 in the TRAF2-mediated ubiquitination of RIP1. (a) *In vitro* ubiquitination assay of RIP1 in HEK293T cells transfected with Myc-RIP1, HA-Ubiquitin (HA-Ub) and Flag-TRAF2, along with Flag-PLEKHO1 or Flag-ΔLZ. Ubiquitination of RIP1 is detected in Myc immunoprecipitates. **(b)** Quantification of relative level of RIP1 ubiquitination. **(c)** *In vitro* ubiquitination assay of RIP1 in HEK293T cells transfected with Myc-RIP1, HA-Ub and Flag-PLEKHO1, along with Flag-TRAF2 or Flag-ΔTRAF C. Ubiquitination of RIP1 is detected in Myc immunoprecipitates. **(d)** Quantification of relative level of RIP1 ubiquitination. Note: IP, Immunoprecipitation; IB, immunoblotting. Data are representative of three independent experiments. **P<0.01. Comparisons between two groups are performed using a Student's t test.

2.9 The attenuation in joint inflammation and bone formation reduction by inhibition of osteoblastic PLEKHO1 in CIA mice

2.9.1 Experimental design

A cross-species *Plekho1* siRNA and a nucleic acid delivery system targeting osteoblasts were used in this study, which was both established by our group (Guo et al., 2014, Zhang et al., 2012). This cross-species *Plekho1* siRNA could target the four species (human, monkey, rat and mouse). *In vivo* studies demonstrated that periodic intravenous injections of this cross-species *Plekho1* siRNA promoted bone formation and reversed bone loss in the osteoporotic mice. On the other hand, to facilitate delivering this cross-species *Plekho1* siRNA to osteoblasts, we have developed a targeted delivery system – $(AspSerSer)_6$-liposome. This targeted delivery system was used to deliver *Plekho1* siRNA specifically achieving high gene knockdown efficiency in osteoblasts in this study.

After CIA was successfully established (day 28 after primary immunization, a mouse with a score of one or above was regarded as arthritic), seven mice were sacrificed before treatment as CIA baseline (CIA-BL). The remaining twenty-eight CIA mice were divided into $(AspSerSer)_6$-liposome-*Plekho1* siRNA group, $(AspSerSer)_6$-liposome-non sense siRNA group, $(AspSerSer)_6$-liposome group, and vehicle control group. The mice in each group received six periodic intravenous injections of $(AspSerSer)_6$-liposome-*Plekho1* siRNA, $(AspSerSer)_6$-liposome-non sense siRNA, $(AspSerSer)_6$-liposome, and PBS, respectively, with a siRNA dose of 5.89 mg/kg at an interval of one week **(Fig. 2-16)**. The clinical severity of arthritis in mice was scored at day 21 after the primary immunization once per week. And after the 6-week treatment, the ankle joints of hid paws from each group were collected for the LCM to examine the mRNA levels of *Plekho1* in OCN^+ cells, then the remaining parts were evaluated by the MicroCT analysis,

dynamic bone histomorphometric analysis, histological evaluation of inflammation, as well as used to examine the protein levels of IL-1β and IL-6 by ELISA.

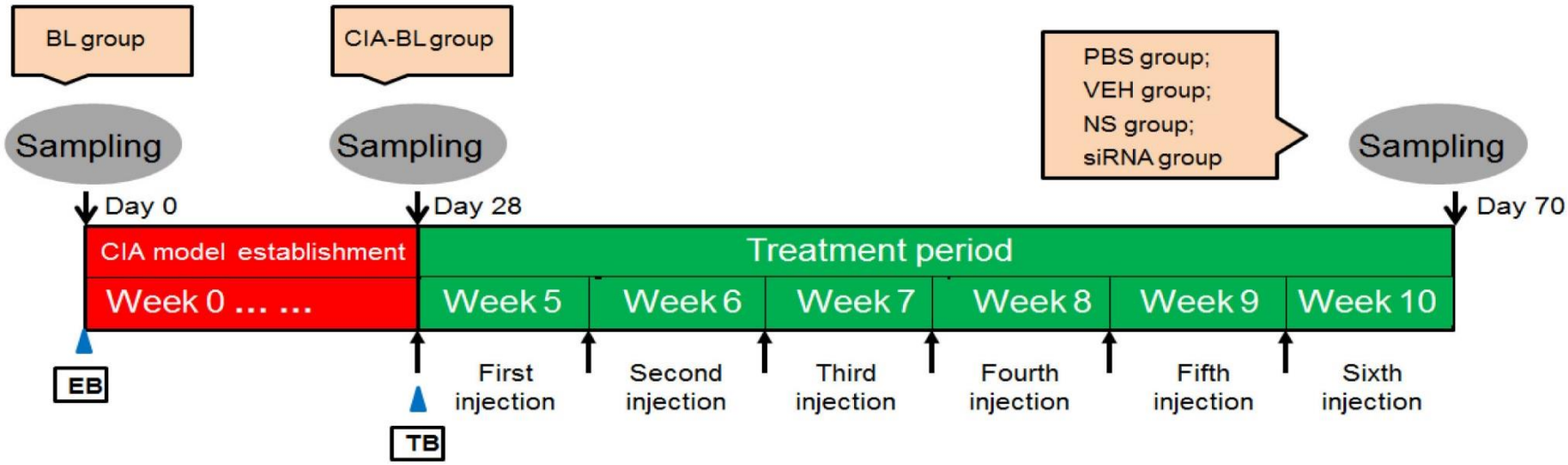

Figure 2-16 A schematic diagram for illustrating the CIA mice treated with osteoblast-targeting delivery system encapsulated *Plekho1* siRNA. Note: BL, baseline; CIA-BL, collagen-induced arthritis baseline; VEH, $(AspSerSer)_6$-liposome; NS, $(AspSerSer)_6$-liposome-NS siRNA; siRNA, $(AspSerSer)_6$-liposome-*Plekho1*siRNA.

2.9.2 Result

We firstly confirmed that the level of *Plekho1* mRNA was significantly downregulated in Ocn^+ cells of siRNA-treated CIA mice after six-week treatment (on day 70 after primary immunization) **(Fig. 2-17)**.

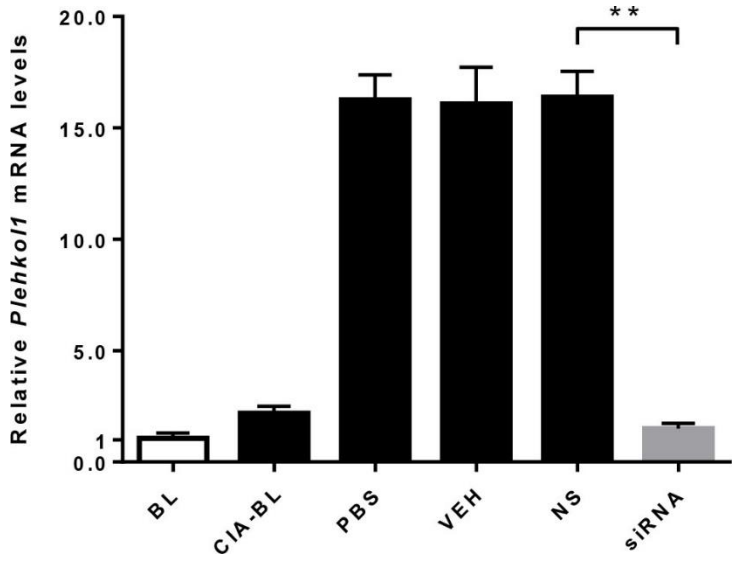

Figure 2-17 Real-time PCR analysis of *Plekho1* mRNA levels in Ocn$^+$ cells from CIA mice treated with osteoblast-targeting delivery system encapsulated *Plekho1* siRNA. The Ocn$^+$ cells are isolated by LCM in the articular bone from the hind paws collected from the groups of mice indicated at day 70 after primary immunization. All data are the mean ± s.d. **P < 0.01. *n*=7 per group. A one-way ANOVA with subsequent Tukey's multiple comparisons test is performed. Notes: BL, baseline; CIA-BL, collagen-induced arthritis baseline; VEH, $(AspSerSer)_6$-liposome; NS, $(AspSerSer)_6$-liposome-NS siRNA; siRNA, $(AspSerSer)_6$-liposome-*Plekho1*siRNA

Thereafter, we found that arthritis score was significantly decreased in siRNA-treated CIA mice when compared to mice treated with $(AspSerSer)_6$-liposome-non sense siRNA (hereafter NS), $(AspSerSer)_6$-liposome (hereafter VEH) or PBS **(Fig. 2-18a)**. Histological evaluation showed that the score of joint inflammation in siRNA-treated CIA mice was also significantly lower when compared to three other control groups after treatment **(Fig. 2-18b-c)**. IL-1β and IL-6 levels in ankle joint of hind paws from siRNA-treated CIA mice were also significantly lower when compared with the three other control groups **(Fig. 2-18d)**. Subsequently, microCT analysis showed better organized microarchitecture and a higher bone mass in tibial bone of siRNA-treated CIA mice compared to mice treated with NS, VEH or PBS after treatment **(Fig. 2-18c)**. The values of BMD, BV/TV, Tb.N and Tb.Th of the tibial bones had remarkable restoration in siRNA-treated CIA mice, whereas such restoration was not observed in CIA mice treated with NS, VEH or PBS **(Fig. 2-18e)**. Similarly, we found a larger width between the xylenol and calcein labeling bands in the mice treated with siRNA compared to the mice treated with NS, VEH or PBS. The values of MAR, BFR/BS and Ob.S/BS were significantly higher, whereas the value of Oc.S/BS were significantly lower in siRNA group when compared with three other control groups after treatment **(Fig. 2-18c, 2-18f)**.

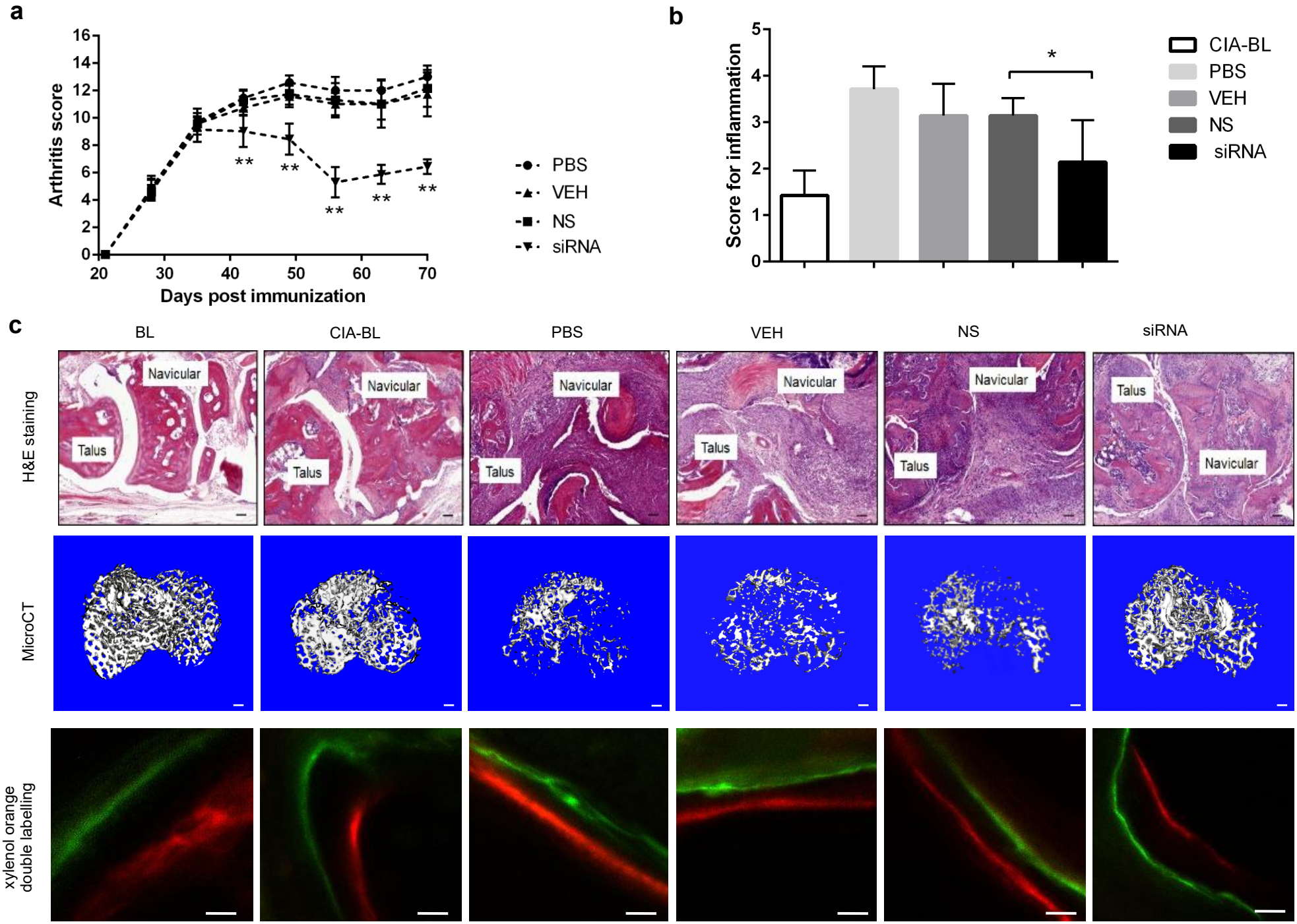
a
Arthritis score
Days post immunization
PBS
VEH
NS
siRNA
b
Score for inflammation
CIA-BL
PBS
VEH
NS
siRNA
c
BL
CIA-BL
PBS
VEH
NS
siRNA
H&E staining
MicroCT
calcein green and xylenol orange double labelling
Navicular
Talus

d

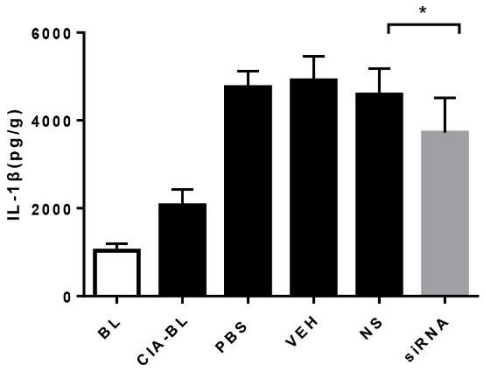
IL-1β(pg/g)
6000
4000
2000
0
*
BL
CIA-BL
PBS
VEH
NS
siRNA

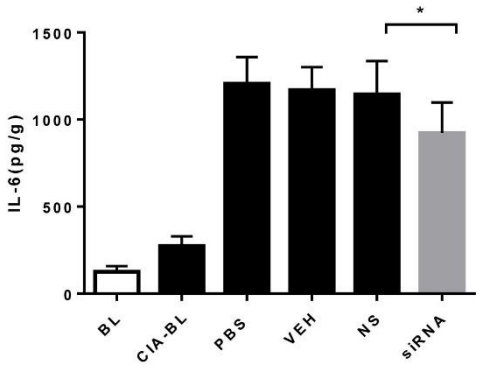
IL-6(pg/g)
1500
1000
500
0
*
BL
CIA-BL
PBS
VEH
NS
siRNA

e

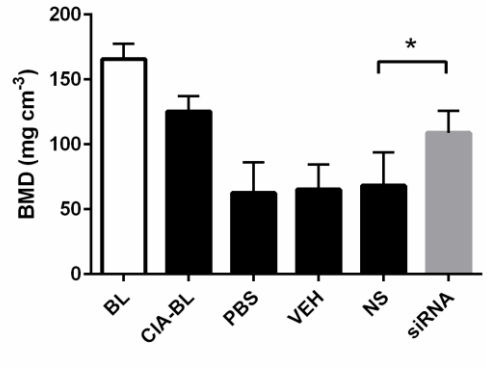
BMD (mg cm-3)
200
150
100
50
0
*
BL
CIA-BL
PBS
VEH
NS
siRNA

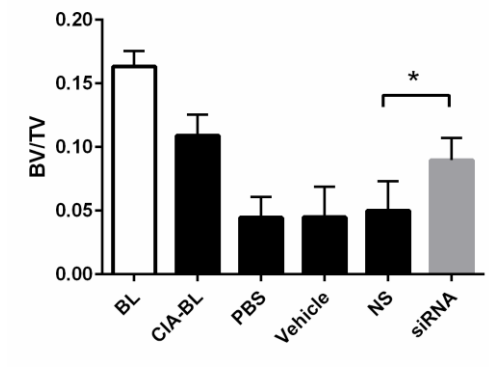
BV/TV
0.20
0.15
0.10
0.05
0.00
*
BL
CIA-BL
PBS
Vehicle
NS
siRNA

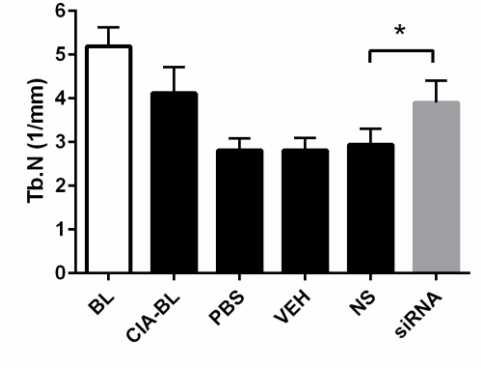
Tb.N (1/mm)
6
5
4
3
2
1
0
*
BL
CIA-BL
PBS
VEH
NS
siRNA

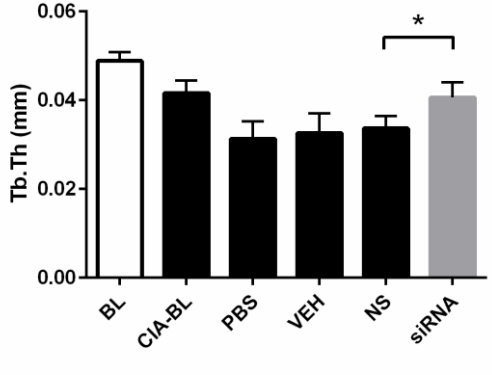
Tb.Th (mm)
0.06
0.04
0.02
0.00
*
BL
CIA-BL
PBS
VEH
NS
siRNA

f

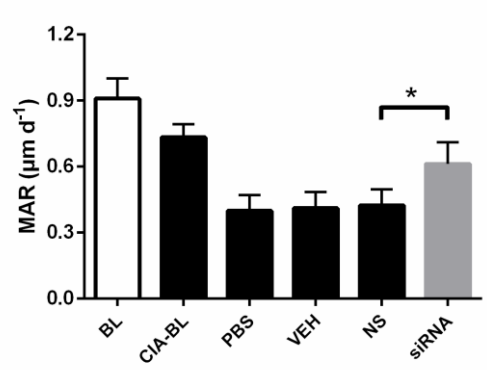
MAR (μm d-1)
1.2
0.9
0.6
0.3
0.0
*
BL
CIA-BL
PBS
VEH
NS
siRNA

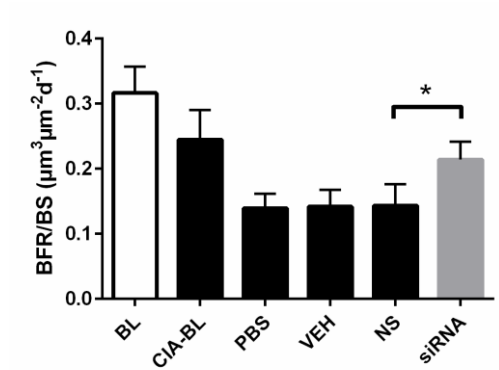
BFR/BS (μm3μm-2d-1)
0.4
0.3
0.2
0.1
0.0
*
BL
CIA-BL
PBS
VEH
NS
siRNA

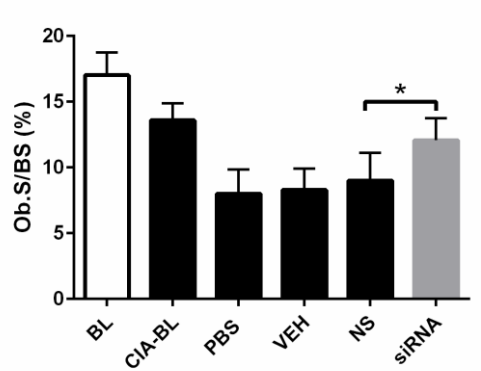
Ob.S/BS (%)
20
15
10
5
0
*
BL
CIA-BL
PBS
VEH
NS
siRNA

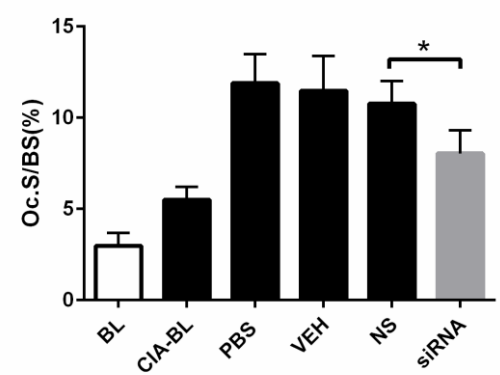
Oc.S/BS(%)
15
10
5
0
*
BL
CIA-BL
PBS
VEH
NS
siRNA

Figure 2-18 Osteoblastic PLEKHO1 inhibition leads to amelioration of articular inflammation and promotion of bone formation in CIA mice. (**a**) Time course changes in arthritis score from CIA mice treated with PBS, VEH, NS, and siRNA, respectively. (**b**) Histological inflammation score in the hind paws from the CIA mice after 6-week treatment in the respective group. (**c**) Representative histological images (Scale bars, 50 μm), microCT images (proximal tibial bones, Scale bars, 100 μm), calcein green and xylenol orange double labelling (Scale bars, 10 μm) from the hind paws of mice in each group at day 70 after primary immunization. (**d**) Levels of IL-1β and IL-6 in ankle joint from the hind paws of the CIA mice after treatment in the respective group. (**e**) The values of microCT parameters (BMD, BV/TV, Tb.N and Tb.Th) of the proximal tibial bones from the CIA mice after treatment in the respective group. (**f**) The values of bone histomorphometric parameters (MAR, BFR/BS, Ob.S/BS and Oc.S/BS) in the hind paws from the CIA mice after treatment in the respective group. All data are the mean ± s.d. *P < 0.05, **P < 0.01. *n* = 7 per group. For **a**, a two-way ANOVA with subsequent Bonferroni posttests is performed. For **b, d, e, & f**, a one-way ANOVA with subsequent Tukey's multiple comparisons test is performed. Note: BL, baseline; CIA-BL, collagen-induced arthritis baseline; VEH, $(AspSerSer)_6$-liposome; NS, $(AspSerSer)_6$-liposome -NS siRNA; siRNA, $(AspSerSer)_6$-liposome -*Plekho1* siRNA.

3. Discussion

This study, for the first time, uncovered a new role of osteoblastic PLEKHO1 in regulating joint inflammation in RA pathogenesis. We further demonstrated that osteoblastic PLEKHO1 inhibition could not only augment bone formation but also inhibit joint inflammation in RA.

Previous views suggest that the joint inflammation in RA is mainly mediated by the activated inflammatory cells such as FLSs and immune cells including infiltrated T lymphocytes and leukocytes (McInnes and Schett, 2011). However, it remains unclear whether other cell populations also contribute to regulate the local joint inflammation. Albeit osteoblasts are among the dominant cell types in the joint, the current perspectives restrict their role in the modulation of bone formation in RA. Interestingly, our study showed that osteoblasts could directly contribute to regulate the local joint inflammation during RA development. The inflammation environment of RA could induce the expression of PLEKHO1 within osteoblasts, as evidenced by the aberrant high levels of PLEKHO1 in osteoblasts of the joint bone samples from both RA patients and CIA mice as well as the increased PLEKHO1 expression in both human and mouse osteoblast-like cells stimulated by various inflammatory cytokines. More surprisingly, we found that genetic deletion of *Plekho1* gene in osteoblasts markedly attenuated the local joint inflammation in inflammatory arthritic mouse models, as supported by the low arthritis scores and histological inflammation scores as well as downregulated inflammatory cytokines (IL-1β and IL-6) in joint samples from the $Plekho1_{osx}^{-/-}$ mice induced by type II collagen. Moreover, conditional overexpression of osteoblastic *Plekho1* in the *Plekho1* systemic knockout mice ($Plekho1^{-/-}/Plekho1_{osx}$ *Tg*) significantly exacerbated the joint inflammation in CIA model. All these findings indicate that the osteoblasts with high PLEKHO1 expression contribute to the joint inflammation in RA.

Despite the regulatory role on BMP signaling, PLEKHO1 has been identified to regulate the cytokine signaling response to inflammation (Zhang et al., 2007a, Sakamoto et al., 2014). A recent study showed that overexpression of PLEKHO1 triggered the activation of pro-inflammatory pathways in the HEK293T model system (Juhasz et al., 2013). Consistently, we found lower levels of inflammatory cytokines (IL-1β and IL-6) in $CD4^+$ T cells and FLSs as well as decreased migration of neutrophils after co-culture with the *Plekho1*-depleted osteoblasts derived from the $Plekho1_{osx}^{-/-}$ mice when compared to those co-cultured with *Plekho1*-intact osteoblasts. Furthermore, the above changes in the inflammatory cells were reversed after co-culture with the *Plekho1*-overexpressed osteoblasts derived from the $Plekho1_{osx}$ *Tg* mice. All these results suggest that the elevated osteoblastic PLEKHO1 could regulate the inflammatory cells that were commonly activated in the local inflammatory environment in RA joint. As well known, the cellular interactions believed to be of importance in the pathogenesis of RA. These interactions are facilitated by the cytokines released from the activated cells that then, through both autocrine and paracrine mechanisms, induce the production of other pro-inflammatory cytokines, which together contribute to the pathogenesis of the disease (Brennan and McInnes, 2008). FLSs, $CD4^+$ T lymphocytes, and neutrophils could be activated by cytokine-driven stimuli, including IL-1β, IL-6, IL-18 and so on (McInnes and Schett, 2007). Moreover, in our study, we further found that silence of osteoblastic *Plekho1* could remarkably decrease the production of IL-1β and IL-6. We thought that PLEKHO1 affecting the secretion of inflammatory cytokines in osteoblasts might be one of the ways in which osteoblasts affected the activities of FLSs, $CD4^+$ T lymphocytes, and neutrophils.

TNF-α plays a pivotal role in regulating the inflammatory response in RA

through inducing pro-inflammatory cytokines release, activating inflammatory cells and promoting leukocytes accumulation (Brennan and McInnes, 2008). Recently, emerging evidence indicated that osteoblasts could respond to the stimulations of TNF-α by secretion of several inflammatory effectors (Shen et al., 2005, Confalone et al., 2010). Our studies showed that silence of osteoblastic *Plekho1* could remarkably decrease the production of the important pro-inflammatory cytokines (IL-1β and IL-6). Moreover, we observed remarkable alleviation of local inflammation in human TNF-α transgenic mice with osteoblastic deficiency of *Plekho1*, implying that osteoblastic PLEKHO1 on joint inflammation regulation might be related with TNF-α involved signal mechanism. Therefore, to further investigate the molecular mechanism of osteoblastic PLEKHO1 modulating the joint inflammation in RA, we performed a series of *in vitro* studies. We found that the phosphorylation of IKKα/β and p65 as well as the ubiquitination of RIP1 in NF-κB signal pathway were remarkably inhibited in TNF-α-stimulated osteoblasts after PLEKHO1 silence. Moreover, we confirmed that PLEKHO1 could bind to TRAF2 and promote TRAF2-mediated RIP1 ubiquitination in TNF-α-stimulated osteoblasts, and the domains for the interaction were LZ-containing domain of PLEKHO1 and C domain of TRAF2 respectively. In contrast to the previous studies which demonstrated that lipid mediator sphingosine-1-phosphate specifically bound to TRAF2 and increased TRAF2-catalyzed ubiquitination of RIP1 (Alvarez et al., 2010), our study found a new cofactor “PLEKHO1” required for TRAF2-mediated RIP1 ubiquitination to activate NF-kB for inducing inflammatory cytokines production **(Fig. 2-19)**.

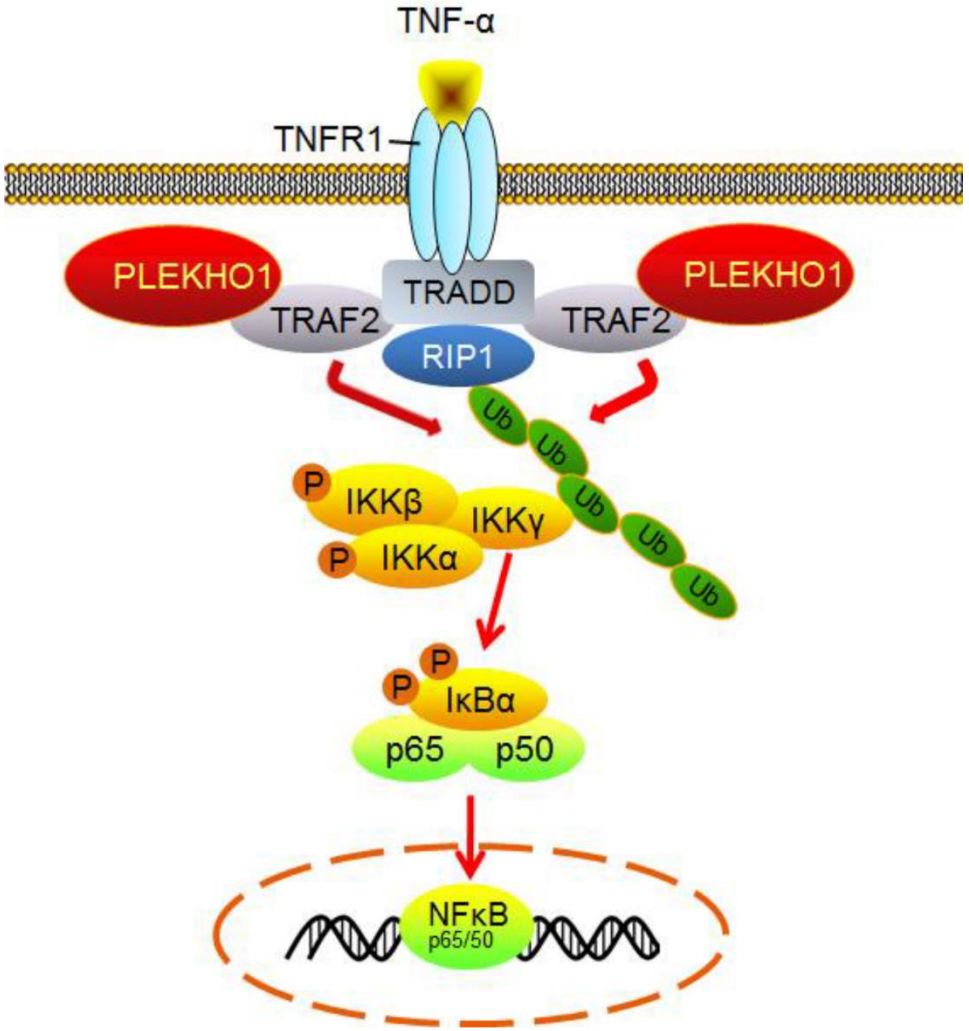
TNF-α
TNFR1
PLEKHO1
TRADD
PLEKHO1
TRAF2
TRAF2
RIP1
Ub
Ub
Ub
Ub
Ub
P
IKKβ
IKKγ
P
IKKα
P
P
IκBα
p65
p50
NFκB
p65/50

Figure 2-19 A model of the role of PLEKHO1 in TRAF2-mediated NF-κB activation initiated by TNF-α. Binding of TNF-α to the trimeric TNFR1 results in the recruitment of TNFR1-associated death domain protein (TRADD), which then recruits TRAF2 and RIP1. PLEKHO1 can interact with TRAF2 to promote TRAF2-mediated RIP1 ubiquitination, which acts as a scaffold to recruit and activate IKK complexes. IKK then phosphorylates IκBα leading to the activation of NF-κB signaling pathway.

In addition, we observed that the osteoblast-specific *Plekho1*-depleted CIA mice showed an apparent attenuation in bone formation reduction and osteoblast-targeted *Plekho1* siRNA treatment could promote bone repair in CIA rodents, which could be explained by the above documented role of PLEKHO1 as a critical ubiquitylation modulator for regulating the BMP signaling (Lu et al., 2008). Certainly, PLEKHO1's effect on local inflammation regulation might also be considered as one of the mechanisms for its bone formation modulation, as the common view regarded that inflammation could impair the function of osteoblasts-mediated bone formation in RA (Baum and Gravallese, 2014).

Considering the role of osteoblastic PLEKHO1 in regulating joint inflammation and bone erosion repair during RA, inhibition of it may exert dual beneficial effect on RA treatment. Thus, to facilitate its clinical translation, we evaluated the effect of osteoblast-targeted PLEKHO1 inhibition by administrating *Plekho1* siRNA encapsulated by our developed osteoblast-targeting delivery system in a CIA mouse model. We demonstrated that osteoblast-targeting *Plekho1* siRNA treatment not only improved arthritis symptoms and but also promoted bone formation in the animal model. Moreover, the siRNA treatment didn't cause any significant side effects. These results will also facilitate clinical translation of RNA interference-based therapeutic strategy in RA (Apparailly and Jorgensen, 2013).

4. Conclusion

Our studies uncovered a previously unrecognized role of osteoblastic PLEKHO1 in mediating the joint inflammation during RA development. The targeted inhibition of osteoblastic PLEKHO1 may be a promising therapeutic strategy with dual action of inflammation inhibition and bone formation augmentation for RA.

Reference

1. ADAMOPOULOS, I. E., CHAO, C. C., GEISSLER, R., LAFACE, D., BLUMENSCHEIN, W., IWAKURA, Y., MCCLANAHAN, T. & BOWMAN, E. P. 2010. Interleukin-17A upregulates receptor activator of NF-kappaB on osteoclast precursors. *Arthritis Res Ther,* 12**,** R29.
2. AGGARWAL, B. B. 2003. Signalling pathways of the TNF superfamily: a double-edged sword. *Nat Rev Immunol,* 3**,** 745-56.
3. AL-HERZ, A., AL-AWADHI, A., SALEH, K., AL-KANDARI & W. 2016. A Comparison of Rheumatoid Arthritis Patients in Kuwait with Other Populations: Results from the KRRD Registry. *British Journal of Medicine & Medical Research,* 14**,** 11.
4. ALUNNO, A., CARUBBI, F., GIACOMELLI, R. & GERLI, R. 2017. Cytokines in the pathogenesis of rheumatoid arthritis: new players and therapeutic targets. *BMC Rheumatol,* 1**,** 3.
5. ALVAREZ, S. E., HARIKUMAR, K. B., HAIT, N. C., ALLEGOOD, J., STRUB, G. M., KIM, E. Y., MACEYKA, M., JIANG, H., LUO, C., KORDULA, T., MILSTIEN, S. & SPIEGEL, S. 2010. Sphingosine-1-phosphate is a missing cofactor for the E3 ubiquitin ligase TRAF2. *Nature,* 465**,** 1084-8.
6. AMANO, T., YAMASAKI, S., YAGISHITA, N., TSUCHIMOCHI, K., SHIN, H., KAWAHARA, K., ARATANI, S., FUJITA, H., ZHANG, L., IKEDA, R., FUJII, R., MIURA, N., KOMIYA, S., NISHIOKA, K., MARUYAMA, I., FUKAMIZU, A. & NAKAJIMA, T. 2003. Synoviolin/Hrd1, an E3 ubiquitin ligase, as a novel pathogenic factor for arthropathy. *Genes Dev,* 17**,** 2436-49.
7. APPARAILLY, F. & JORGENSEN, C. 2013. siRNA-based therapeutic approaches for rheumatic diseases. *Nat Rev Rheumatol,* 9**,** 56-62.
8. ASSIER, E., BOISSIER, M. C. & DAYER, J. M. 2010. Interleukin-6:

from identification of the cytokine to development of targeted treatments. *Joint Bone Spine,* 77**,** 532-6.

9. AUGER, I., BALANDRAUD, N., RAK, J., LAMBERT, N., MARTIN, M. & ROUDIER, J. 2009. New autoantigens in rheumatoid arthritis (RA): screening 8268 protein arrays with sera from patients with RA. *Ann Rheum Dis,* 68**,** 591-4.
10. BAUM, R. & GRAVALLESE, E. M. 2014. Impact of inflammation on the osteoblast in rheumatic diseases. *Curr Osteoporos Rep,* 12**,** 9-16.
11. BAUM, R. & GRAVALLESE, E. M. 2016. Bone as a Target Organ in Rheumatic Disease: Impact on Osteoclasts and Osteoblasts. *Clin Rev Allergy Immunol,* 51**,** 1-15.
12. BERGER, M., HSIEH, C. Y., BAKELE, M., MARCOS, V., RIEBER, N., KORMANN, M., MAYS, L., HOFER, L., NETH, O., VITKOV, L., KRAUTGARTNER, W. D., VON SCHWEINITZ, D., KAPPLER, R., HECTOR, A., WEBER, A. & HARTL, D. 2012. Neutrophils express distinct RNA receptors in a non-canonical way. *J Biol Chem,* 287**,** 19409-17.
13. BESSIS, N., GUERY, L., MANTOVANI, A., VECCHI, A., SIMS, J. E., FRADELIZI, D. & BOISSIER, M. C. 2000. The type II decoy receptor of IL-1 inhibits murine collagen-induced arthritis. *Eur J Immunol,* 30**,** 867-75.
14. BITON, J., BOISSIER, M. C. & BESSIS, N. 2012. TNFalpha: activator or inhibitor of regulatory T cells? *Joint Bone Spine,* 79**,** 119-23.
15. BITON, J., SEMERANO, L., DELAVALLEE, L., LEMEITER, D., LABORIE, M., GROUARD-VOGEL, G., BOISSIER, M. C. & BESSIS, N. 2011. Interplay between TNF and regulatory T cells in a TNF-driven murine model of arthritis. *J Immunol,* 186**,** 3899-910.
16. BIVER, E., BEAGUE, V., VERLOOP, D., MOLLET, D., LAJUGIE, D.,

BAUDENS, G., NEIRINCK, P. & FLIPO, R. M. 2009. Low and stable prevalence of rheumatoid arthritis in northern France. *Joint Bone Spine,* 76**,** 497-500.

17. BOISSIER, M. C., SEMERANO, L., CHALLAL, S., SAIDENBERG-KERMANAC'H, N. & FALGARONE, G. 2012. Rheumatoid arthritis: from autoimmunity to synovitis and joint destruction. *J Autoimmun,* 39**,** 222-8.
18. BRAND, D. D., LATHAM, K. A. & ROSLONIEC, E. F. 2007. Collagen-induced arthritis. *Nat Protoc,* 2**,** 1269-75.
19. BRENNAN, F. M. & MCINNES, I. B. 2008. Evidence that cytokines play a role in rheumatoid arthritis. *J Clin Invest,* 118**,** 3537-45.
20. CARBONELL, J., COBO, T., BALSA, A., DESCALZO, M. A. & CARMONA, L. 2008. The incidence of rheumatoid arthritis in Spain: results from a nationwide primary care registry. *Rheumatology (Oxford),* 47**,** 1088-92.
21. CHABAUD, M., DURAND, J. M., BUCHS, N., FOSSIEZ, F., PAGE, G., FRAPPART, L. & MIOSSEC, P. 1999. Human interleukin-17: A T cell-derived proinflammatory cytokine produced by the rheumatoid synovium. *Arthritis Rheum,* 42**,** 963-70.
22. CHEN, X., BAUMEL, M., MANNEL, D. N., HOWARD, O. M. & OPPENHEIM, J. J. 2007. Interaction of TNF with TNF receptor type 2 promotes expansion and function of mouse CD4+CD25+ T regulatory cells. *J Immunol,* 179**,** 154-61.
23. CHEN, Z. J. 2005. Ubiquitin signalling in the NF-kappaB pathway. *Nat Cell Biol,* 7**,** 758-65.
24. CHOY, E. 2012. Understanding the dynamics: pathways involved in the pathogenesis of rheumatoid arthritis. *Rheumatology (Oxford),* 51 Suppl 5**,** v3-11.
25. COHEN, S. B., DORE, R. K., LANE, N. E., ORY, P. A., PETERFY, C.

G., SHARP, J. T., VAN DER HEIJDE, D., ZHOU, L., TSUJI, W. & NEWMARK, R. 2008. Denosumab treatment effects on structural damage, bone mineral density, and bone turnover in rheumatoid arthritis: a twelve-month, multicenter, randomized, double-blind, placebo-controlled, phase II clinical trial. *Arthritis Rheum,* 58**,** 1299-309.

26. CONFALONE, E., D'ALESSIO, G. & FURIA, A. 2010. IL-6 Induction by TNFalpha and IL-1beta in an Osteoblast-Like Cell Line. *Int J Biomed Sci,* 6**,** 135-40.
27. COSTENBADER, K. H., CHANG, S. C., LADEN, F., PUETT, R. & KARLSON, E. W. 2008. Geographic variation in rheumatoid arthritis incidence among women in the United States. *Arch Intern Med,* 168**,** 1664-70.
28. DIMITROULAS, T., NIKAS, S. N., TRONTZAS, P. & KITAS, G. D. 2013. Biologic therapies and systemic bone loss in rheumatoid arthritis. *Autoimmun Rev,* 12**,** 958-66.
29. DINARELLO, C. A. 1988. Biology of interleukin 1. *Faseb j,* 2**,** 108-15.
30. EKLUND, L. & OLSEN, B. R. 2006. Tie receptors and their angiopoietin ligands are context-dependent regulators of vascular remodeling. *Exp Cell Res,* 312**,** 630-41.
31. FERGUSON, K. L., TAHERI, P., RODRIGUEZ, J., TONAPI, V., CARDELLIO, A. & DECHERT, R. 1997. Tumor necrosis factor activity increases in the early response to trauma. *Acad Emerg Med,* 4**,** 1035-40.
32. FERRARA, N. 2001. Role of vascular endothelial growth factor in regulation of physiological angiogenesis. *Am J Physiol Cell Physiol,* 280**,** C1358-66.
33. FIRESTEIN, G. S. 2003. Evolving concepts of rheumatoid arthritis. *Nature,* 423**,** 356-61.

34. FIRESTEIN, G. S., XU, W. D., TOWNSEND, K., BROIDE, D., ALVARO-GRACIA, J., GLASEBROOK, A. & ZVAIFLER, N. J. 1988. Cytokines in chronic inflammatory arthritis. I. Failure to detect T cell lymphokines (interleukin 2 and interleukin 3) and presence of macrophage colony-stimulating factor (CSF-1) and a novel mast cell growth factor in rheumatoid synovitis. *J Exp Med,* 168**,** 1573-86.

35. FOLKMAN, J. & KLAGSBRUN, M. 1987. Angiogenic factors. *Science,* 235**,** 442-7.

36. FOSSIEZ, F., DJOSSOU, O., CHOMARAT, P., FLORES-ROMO, L., AIT-YAHIA, S., MAAT, C., PIN, J. J., GARRONE, P., GARCIA, E., SAELAND, S., BLANCHARD, D., GAILLARD, C., DAS MAHAPATRA, B., ROUVIER, E., GOLSTEIN, P., BANCHEREAU, J. & LEBECQUE, S. 1996. T cell interleukin-17 induces stromal cells to produce proinflammatory and hematopoietic cytokines. *J Exp Med,* 183**,** 2593-603.

37. FREEMAN & J. 2018. *RA Facts: What are the Latest Statistics on Rheumatoid Arthritis?* [Online]. Rheumatoid Arthritis Support Network. [Accessed].

38. FUJII, H., SHAO, L., COLMEGNA, I., GORONZY, J. J. & WEYAND, C. M. 2009. Telomerase insufficiency in rheumatoid arthritis. *Proc Natl Acad Sci U S A,* 106**,** 4360-5.

39. GOLDRING, S. R. & GRAVALLESE, E. M. 2000. Mechanisms of bone loss in inflammatory arthritis: diagnosis and therapeutic implications. *Arthritis Res,* 2**,** 33-7.

40. GRAVALLESE, E. M., MANNING, C., TSAY, A., NAITO, A., PAN, C., AMENTO, E. & GOLDRING, S. R. 2000. Synovial tissue in rheumatoid arthritis is a source of osteoclast differentiation factor. *Arthritis Rheum,* 43**,** 250-8.

41. GUMA, M., RONACHER, L., LIU-BRYAN, R., TAKAI, S., KARIN, M.

& CORR, M. 2009. Caspase 1-independent activation of interleukin-1beta in neutrophil-predominant inflammation. *Arthritis Rheum,* 60**,** 3642-50.

42. GUO, B., ZHANG, B., ZHENG, L., TANG, T., LIU, J., WU, H., YANG, Z., PENG, S., HE, X., ZHANG, H., YUE, K. K., HE, F., ZHANG, L., QIN, L., BIAN, Z., TAN, W., LIANG, Z., LU, A. & ZHANG, G. 2014. Therapeutic RNA interference targeting CKIP-1 with a cross-species sequence to stimulate bone formation. *Bone,* 59**,** 76-88.
43. GUO, Q., WANG, Y., XU, D., NOSSENT, J., PAVLOS, N. J. & XU, J. 2018. Rheumatoid arthritis: pathological mechanisms and modern pharmacologic therapies. *Bone Res,* 6**,** 15.
44. HARDY, R. S., HULSO, C., LIU, Y., GASPARINI, S. J., FONG-YEE, C., TU, J., STONER, S., STEWART, P. M., RAZA, K., COOPER, M. S., SEIBEL, M. J. & ZHOU, H. 2013. Characterisation of fibroblast-like synoviocytes from a murine model of joint inflammation. *Arthritis Res Ther,* 15**,** R24.
45. HAROON, N., AGGARWAL, A., LAWRENCE, A., AGARWAL, V. & MISRA, R. 2007. Impact of rheumatoid arthritis on quality of life. *Mod Rheumatol,* 17**,** 290-5.
46. HAYDEN, M. S. & GHOSH, S. 2008. Shared principles in NF-kappaB signaling. *Cell,* 132**,** 344-62.
47. HOEFLICH, K. P., YEH, W. C., YAO, Z., MAK, T. W. & WOODGETT, J. R. 1999. Mediation of TNF receptor-associated factor effector functions by apoptosis signal-regulating kinase-1 (ASK1). *Oncogene,* 18**,** 5814-20.
48. INFANTE-DUARTE, C., HORTON, H. F., BYRNE, M. C. & KAMRADT, T. 2000. Microbial lipopeptides induce the production of IL-17 in Th cells. *J Immunol,* 165**,** 6107-15.
49. INGLIS, J. J., CRIADO, G., MEDGHALCHI, M., ANDREWS, M.,

SANDISON, A., FELDMANN, M. & WILLIAMS, R. O. 2007. Collagen-induced arthritis in C57BL/6 mice is associated with a robust and sustained T-cell response to type II collagen. *Arthritis Res Ther,* 9**,** R113.

50. IOBAGIU, C., MAGYAR, A., NOGUEIRA, L., CORNILLET, M., SEBBAG, M., ARNAUD, J., HUDECZ, F. & SERRE, G. 2011. The antigen specificity of the rheumatoid arthritis-associated ACPA directed to citrullinated fibrin is very closely restricted. *J Autoimmun,* 37**,** 263-72.
51. JUHASZ, K., ZVARA, A., LIPP, A. M., NIMMERVOLL, B., SONNLEITNER, A., BALOGI, Z. & DUDA, E. 2013. Casein kinase 2-interacting protein-1, an inflammatory signaling molecule interferes with TNF reverse signaling in human model cells. *Immunol Lett,* 152**,** 55-64.
52. KALLA, A. A. & TIKLY, M. 2003. Rheumatoid arthritis in the developing world. *Best Pract Res Clin Rheumatol,* 17**,** 863-75.
53. KARLSON, E. W., CHIBNIK, L. B., TWOROGER, S. S., LEE, I. M., BURING, J. E., SHADICK, N. A., MANSON, J. E. & COSTENBADER, K. H. 2009. Biomarkers of inflammation and development of rheumatoid arthritis in women from two prospective cohort studies. *Arthritis Rheum,* 60**,** 641-52.
54. KARMAKAR, S., KAY, J. & GRAVALLESE, E. M. 2010. Bone damage in rheumatoid arthritis: mechanistic insights and approaches to prevention. *Rheum Dis Clin North Am,* 36**,** 385-404.
55. KAWAGUCHI, M., ADACHI, M., ODA, N., KOKUBU, F. & HUANG, S. K. 2004. IL-17 cytokine family. *J Allergy Clin Immunol,* 114**,** 1265-73; quiz 1274.
56. KIM, K. W., KIM, H. R., KIM, B. M., CHO, M. L. & LEE, S. H. 2015. Th17 cytokines regulate osteoclastogenesis in rheumatoid arthritis.

Am J Pathol, 185**,** 3011-24.

57. KLARESKOG, L., RONNELID, J., LUNDBERG, K., PADYUKOV, L. & ALFREDSSON, L. 2008. Immunity to citrullinated proteins in rheumatoid arthritis. *Annu Rev Immunol,* 26**,** 651-75.
58. KLARESKOG, L., STOLT, P., LUNDBERG, K., KALLBERG, H., BENGTSSON, C., GRUNEWALD, J., RONNELID, J., HARRIS, H. E., ULFGREN, A. K., RANTAPAA-DAHLQVIST, S., EKLUND, A., PADYUKOV, L. & ALFREDSSON, L. 2006. A new model for an etiology of rheumatoid arthritis: smoking may trigger HLA-DR (shared epitope)-restricted immune reactions to autoantigens modified by citrullination. *Arthritis Rheum,* 54**,** 38-46.
59. KNUPFER, H. & PREISS, R. 2008. sIL-6R: more than an agonist? *Immunol Cell Biol,* 86**,** 87-91.
60. KOCH, A. E. 1998. Review: angiogenesis: implications for rheumatoid arthritis. *Arthritis Rheum,* 41**,** 951-62.
61. KONG, Y. Y., FEIGE, U., SAROSI, I., BOLON, B., TAFURI, A., MORONY, S., CAPPARELLI, C., LI, J., ELLIOTT, R., MCCABE, S., WONG, T., CAMPAGNUOLO, G., MORAN, E., BOGOCH, E. R., VAN, G., NGUYEN, L. T., OHASHI, P. S., LACEY, D. L., FISH, E., BOYLE, W. J. & PENNINGER, J. M. 1999. Activated T cells regulate bone loss and joint destruction in adjuvant arthritis through osteoprotegerin ligand. *Nature,* 402**,** 304-9.
62. KOTAKE, S., UDAGAWA, N., TAKAHASHI, N., MATSUZAKI, K., ITOH, K., ISHIYAMA, S., SAITO, S., INOUE, K., KAMATANI, N., GILLESPIE, M. T., MARTIN, T. J. & SUDA, T. 1999. IL-17 in synovial fluids from patients with rheumatoid arthritis is a potent stimulator of osteoclastogenesis. *J Clin Invest,* 103**,** 1345-52.
63. KOYAMA, T. & TANAKA, S. 2016. [Mechanism of bone destruction in rheumatoid arthritis and perspectives of the treatment]. *Clin Calcium,*

26, 735-41.

64. LAINER-CARR, D. & BRAHN, E. 2007. Angiogenesis inhibition as a therapeutic approach for inflammatory synovitis. *Nat Clin Pract Rheumatol,* 3, 434-42.

65. LAM, J., TAKESHITA, S., BARKER, J. E., KANAGAWA, O., ROSS, F. P. & TEITELBAUM, S. L. 2000. TNF-alpha induces osteoclastogenesis by direct stimulation of macrophages exposed to permissive levels of RANK ligand. *J Clin Invest,* 106, 1481-8.

66. LEE, D. M., KIENER, H. P., AGARWAL, S. K., NOSS, E. H., WATTS, G. F., CHISAKA, O., TAKEICHI, M. & BRENNER, M. B. 2007. Cadherin-11 in synovial lining formation and pathology in arthritis. *Science,* 315, 1006-10.

67. LEFEVRE, S., KNEDLA, A., TENNIE, C., KAMPMANN, A., WUNRAU, C., DINSER, R., KORB, A., SCHNAKER, E. M., TARNER, I. H., ROBBINS, P. D., EVANS, C. H., STURZ, H., STEINMEYER, J., GAY, S., SCHOLMERICH, J., PAP, T., MULLER-LADNER, U. & NEUMANN, E. 2009. Synovial fibroblasts spread rheumatoid arthritis to unaffected joints. *Nat Med,* 15, 1414-20.

68. LI, P., SCHWARZ, E. M., O'KEEFE, R. J., MA, L., BOYCE, B. F. & XING, L. 2004. RANK signaling is not required for TNFalpha-mediated increase in CD11(hi) osteoclast precursors but is essential for mature osteoclast formation in TNFalpha-mediated inflammatory arthritis. *J Bone Miner Res,* 19, 207-13.

69. LIAO, K. P., ALFREDSSON, L. & KARLSON, E. W. 2009. Environmental influences on risk for rheumatoid arthritis. *Curr Opin Rheumatol,* 21, 279-83.

70. LIU, J., LIANG, C., GUO, B., WU, X., LI, D., ZHANG, Z., ZHENG, K., DANG, L., HE, X., LU, C., PENG, S., PAN, X., ZHANG, B. T., LU, A. & ZHANG, G. 2017. Increased PLEKHO1 within osteoblasts

suppresses Smad-dependent BMP signaling to inhibit bone formation during aging. *Aging Cell,* 16**,** 360-376.

71. LOI, F., CORDOVA, L. A., PAJARINEN, J., LIN, T. H., YAO, Z. & GOODMAN, S. B. 2016. Inflammation, fracture and bone repair. *Bone,* 86**,** 119-30.
72. LU, K., YIN, X., WENG, T., XI, S., LI, L., XING, G., CHENG, X., YANG, X., ZHANG, L. & HE, F. 2008. Targeting WW domains linker of HECT-type ubiquitin ligase Smurf1 for activation by CKIP-1. *Nat Cell Biol,* 10**,** 994-1002.
73. LUDVIGSSON, J. F., NORDENVALL, C. & JARVHOLM, B. 2014. Smoking, use of moist snuff and risk of celiac disease: a prospective study. *BMC Gastroenterol,* 14**,** 120.
74. MARRIOTT, I., GRAY, D. L., TRANGUCH, S. L., FOWLER, V. G., JR., STRYJEWSKI, M., SCOTT LEVIN, L., HUDSON, M. C. & BOST, K. L. 2004. Osteoblasts express the inflammatory cytokine interleukin-6 in a murine model of Staphylococcus aureus osteomyelitis and infected human bone tissue. *Am J Pathol,* 164**,** 1399-406.
75. MCCARTY & D. 1980. *The Joints and Synovial Fluid*.
76. MCINNES, I. B., BUCKLEY, C. D. & ISAACS, J. D. 2016. Cytokines in rheumatoid arthritis - shaping the immunological landscape. *Nat Rev Rheumatol,* 12**,** 63-8.
77. MCINNES, I. B. & SCHETT, G. 2007. Cytokines in the pathogenesis of rheumatoid arthritis. *Nat Rev Immunol,* 7**,** 429-42.
78. MCINNES, I. B. & SCHETT, G. 2011. The pathogenesis of rheumatoid arthritis. *N Engl J Med,* 365**,** 2205-19.
79. MOSMANN, T. R., CHERWINSKI, H., BOND, M. W., GIEDLIN, M. A. & COFFMAN, R. L. 2005. Two types of murine helper T cell clone. I. Definition according to profiles of lymphokine activities and secreted proteins. 1986. *J Immunol,* 175**,** 5-14.

80. NADKARNI, S., MAURI, C. & EHRENSTEIN, M. R. 2007. Anti-TNF-alpha therapy induces a distinct regulatory T cell population in patients with rheumatoid arthritis via TGF-beta. *J Exp Med,* 204**,** 33-9.

81. NEUNABER, C., ZECKEY, C., ANDRUSZKOW, H., FRINK, M., MOMMSEN, P., KRETTEK, C. & HILDEBRAND, F. 2011. Immunomodulation in polytrauma and polymicrobial sepsis - where do we stand? *Recent Pat Inflamm Allergy Drug Discov,* 5**,** 17-25.

82. NIE, J., LIU, L., HE, F., FU, X., HAN, W. & ZHANG, L. 2013. CKIP-1: a scaffold protein and potential therapeutic target integrating multiple signaling pathways and physiological functions. *Ageing Res Rev,* 12**,** 276-81.

83. OKADA, H. & MURAKAMI, S. 1998. Cytokine expression in periodontal health and disease. *Crit Rev Oral Biol Med,* 9**,** 248-66.

84. PEDERSEN, J. K., KJAER, N. K., SVENDSEN, A. J. & HORSLEV-PETERSEN, K. 2009. Incidence of rheumatoid arthritis from 1995 to 2001: impact of ascertainment from multiple sources. *Rheumatol Int,* 29**,** 411-5.

85. PETTIT, A. R., JI, H., VON STECHOW, D., MULLER, R., GOLDRING, S. R., CHOI, Y., BENOIST, C. & GRAVALLESE, E. M. 2001. TRANCE/RANKL knockout mice are protected from bone erosion in a serum transfer model of arthritis. *Am J Pathol,* 159**,** 1689-99.

86. PLENGE, R. M. 2009. Rheumatoid arthritis genetics: 2009 update. *Curr Rheumatol Rep,* 11**,** 351-6.

87. POLIACHIK, S. L., BAIN, S. D., THREET, D., HUBER, P. & GROSS, T. S. 2010. Transient muscle paralysis disrupts bone homeostasis by rapid degradation of bone morphology. *Bone,* 46**,** 18-23.

88. RANTAPAA-DAHLQVIST, S., DE JONG, B. A., BERGLIN, E., HALLMANS, G., WADELL, G., STENLUND, H., SUNDIN, U. & VAN

VENROOIJ, W. J. 2003. Antibodies against cyclic citrullinated peptide and IgA rheumatoid factor predict the development of rheumatoid arthritis. *Arthritis Rheum,* 48**,** 2741-9.

89. REDLICH, K., HAYER, S., MAIER, A., DUNSTAN, C. R., TOHIDAST-AKRAD, M., LANG, S., TURK, B., PIETSCHMANN, P., WOLOSZCZUK, W., HARALAMBOUS, S., KOLLIAS, G., STEINER, G., SMOLEN, J. S. & SCHETT, G. 2002a. Tumor necrosis factor alpha-mediated joint destruction is inhibited by targeting osteoclasts with osteoprotegerin. *Arthritis Rheum,* 46**,** 785-92.
90. REDLICH, K., HAYER, S., RICCI, R., DAVID, J. P., TOHIDAST-AKRAD, M., KOLLIAS, G., STEINER, G., SMOLEN, J. S., WAGNER, E. F. & SCHETT, G. 2002b. Osteoclasts are essential for TNF-alpha-mediated joint destruction. *J Clin Invest,* 110**,** 1419-27.
91. RIOJA, I., BUSH, K. A., BUCKTON, J. B., DICKSON, M. C. & LIFE, P. F. 2004. Joint cytokine quantification in two rodent arthritis models: kinetics of expression, correlation of mRNA and protein levels and response to prednisolone treatment. *Clin Exp Immunol,* 137**,** 65-73.
92. ROMAS, E., SIMS, N. A., HARDS, D. K., LINDSAY, M., QUINN, J. W., RYAN, P. F., DUNSTAN, C. R., MARTIN, T. J. & GILLESPIE, M. T. 2002. Osteoprotegerin reduces osteoclast numbers and prevents bone erosion in collagen-induced arthritis. *Am J Pathol,* 161**,** 1419-27.
93. ROUVIER, E., LUCIANI, M. F., MATTEI, M. G., DENIZOT, F. & GOLSTEIN, P. 1993. CTLA-8, cloned from an activated T cell, bearing AU-rich messenger RNA instability sequences, and homologous to a herpesvirus saimiri gene. *J Immunol,* 150**,** 5445-56.
94. SAKAMOTO, T., KOBAYASHI, M., TADA, K., SHINOHARA, M., IO, K., NAGATA, K., IWAI, F., TAKIUCHI, Y., ARAI, Y., YAMASHITA, K., SHINDO, K., KADOWAKI, N., KOYANAGI, Y. & TAKAORI-KONDO,

A. 2014. CKIP-1 is an intrinsic negative regulator of T-cell activation through an interaction with CARMA1. *PLoS One,* 9**,** e85762.

95. SATO, K., SUEMATSU, A., OKAMOTO, K., YAMAGUCHI, A., MORISHITA, Y., KADONO, Y., TANAKA, S., KODAMA, T., AKIRA, S., IWAKURA, Y., CUA, D. J. & TAKAYANAGI, H. 2006. Th17 functions as an osteoclastogenic helper T cell subset that links T cell activation and bone destruction. *J Exp Med,* 203**,** 2673-82.

96. SEMERANO, L., CLAVEL, G., ASSIER, E., DENYS, A. & BOISSIER, M. C. 2011. Blood vessels, a potential therapeutic target in rheumatoid arthritis? *Joint Bone Spine,* 78**,** 118-23.

97. SFIKAKIS, P. P. 2010. The first decade of biologic TNF antagonists in clinical practice: lessons learned, unresolved issues and future directions. *Curr Dir Autoimmun,* 11**,** 180-210.

98. SHEN, F., RUDDY, M. J., PLAMONDON, P. & GAFFEN, S. L. 2005. Cytokines link osteoblasts and inflammation: microarray analysis of interleukin-17- and TNF-alpha-induced genes in bone cells. *J Leukoc Biol,* 77**,** 388-99.

99. SHIGEYAMA, Y., PAP, T., KUNZLER, P., SIMMEN, B. R., GAY, R. E. & GAY, S. 2000. Expression of osteoclast differentiation factor in rheumatoid arthritis. *Arthritis Rheum,* 43**,** 2523-30.

100. SMOLEN, J. S., ALETAHA, D., KOELLER, M., WEISMAN, M. H. & EMERY, P. 2007. New therapies for treatment of rheumatoid arthritis. *Lancet,* 370**,** 1861-74.

101. SMOLEN, J. S. & STEINER, G. 2003. Therapeutic strategies for rheumatoid arthritis. *Nat Rev Drug Discov,* 2**,** 473-88.

102. SONDARVA, G., KUNDU, C. N., MEHROTRA, S., MISHRA, R., RANGASAMY, V., SATHYANARAYANA, P., RAY, R. S., RANA, B. & RANA, A. 2010. TRAF2-MLK3 interaction is essential for TNF-alpha-induced MLK3 activation. *Cell Res,* 20**,** 89-98.

103. STEINMAN, L. 2007. A brief history of T(H)17, the first major revision in the T(H)1/T(H)2 hypothesis of T cell-mediated tissue damage. *Nat Med,* 13**,** 139-45.

104. SVOBODA, P., KANTOROVA, I. & OCHMANN, J. 1994. Dynamics of interleukin 1, 2, and 6 and tumor necrosis factor alpha in multiple trauma patients. *J Trauma,* 36**,** 336-40.

105. SYMMONS, D., TURNER, G., WEBB, R., ASTEN, P., BARRETT, E., LUNT, M., SCOTT, D. & SILMAN, A. 2002. The prevalence of rheumatoid arthritis in the United Kingdom: new estimates for a new century. *Rheumatology (Oxford),* 41**,** 793-800.

106. SZEKANECZ, Z. & KOCH, A. E. 2005. Endothelial cells in inflammation and angiogenesis. *Curr Drug Targets Inflamm Allergy,* 4**,** 319-23.

107. SZEKANECZ, Z. & KOCH, A. E. 2008. Vascular involvement in rheumatic diseases: 'vascular rheumatology'. *Arthritis Res Ther,* 10**,** 224.

108. TAKAYANAGI, H., IIZUKA, H., JUJI, T., NAKAGAWA, T., YAMAMOTO, A., MIYAZAKI, T., KOSHIHARA, Y., ODA, H., NAKAMURA, K. & TANAKA, S. 2000. Involvement of receptor activator of nuclear factor kappaB ligand/osteoclast differentiation factor in osteoclastogenesis from synoviocytes in rheumatoid arthritis. *Arthritis Rheum,* 43**,** 259-69.

109. TAKEUCHI, M., ROTHE, M. & GOEDDEL, D. V. 1996. Anatomy of TRAF2. Distinct domains for nuclear factor-kappaB activation and association with tumor necrosis factor signaling proteins. *J Biol Chem,* 271**,** 19935-42.

110. TSAI, C. L., CHEN, W. C., HSIEH, H. L., CHI, P. L., HSIAO, L. D. & YANG, C. M. 2014. TNF-alpha induces matrix metalloproteinase-9-dependent soluble intercellular adhesion molecule-1 release via

TRAF2-mediated MAPKs and NF-kappaB activation in osteoblast-like MC3T3-E1 cells. *J Biomed Sci,* 21**,** 12.

111. VAN DEN HOEK, J., BOSHUIZEN, H. C., ROORDA, L. D., TIJHUIS, G. J., NURMOHAMED, M. T., VAN DEN BOS, G. A. & DEKKER, J. 2017. Mortality in patients with rheumatoid arthritis: a 15-year prospective cohort study. *Rheumatol Int,* 37**,** 487-493.
112. VEALE, D. J. & FEARON, U. 2006. Inhibition of angiogenic pathways in rheumatoid arthritis: potential for therapeutic targeting. *Best Pract Res Clin Rheumatol,* 20**,** 941-7.
113. WALSH, N. C., REINWALD, S., MANNING, C. A., CONDON, K. W., IWATA, K., BURR, D. B. & GRAVALLESE, E. M. 2009. Osteoblast function is compromised at sites of focal bone erosion in inflammatory arthritis. *J Bone Miner Res,* 24**,** 1572-85.
114. WANG, Y., NIE, J., WANG, Y., ZHANG, L., LU, K., XING, G., XIE, P., HE, F. & ZHANG, L. 2012. CKIP-1 couples Smurf1 ubiquitin ligase with Rpt6 subunit of proteasome to promote substrate degradation. *EMBO Rep,* 13**,** 1004-11.
115. WEI, S., KITAURA, H., ZHOU, P., ROSS, F. P. & TEITELBAUM, S. L. 2005. IL-1 mediates TNF-induced osteoclastogenesis. *J Clin Invest,* 115**,** 282-90.
116. WEYAND, C. M., HICOK, K. C., CONN, D. L. & GORONZY, J. J. 1992. The influence of HLA-DRB1 genes on disease severity in rheumatoid arthritis. *Ann Intern Med,* 117**,** 801-6.
117. WEYAND, C. M., KURTIN, P. J. & GORONZY, J. J. 2001. Ectopic lymphoid organogenesis: a fast track for autoimmunity. *Am J Pathol,* 159**,** 787-93.
118. YAO, Z., FANSLOW, W. C., SELDIN, M. F., ROUSSEAU, A. M., PAINTER, S. L., COMEAU, M. R., COHEN, J. I. & SPRIGGS, M. K. 2011. Herpesvirus saimiri encodes a new cytokine, IL-17, which

binds to a novel cytokine receptor. *J Immunol,* 187**,** 4392-402.

119. ZHANG, G., GUO, B., WU, H., TANG, T., ZHANG, B. T., ZHENG, L., HE, Y., YANG, Z., PAN, X., CHOW, H., TO, K., LI, Y., LI, D., WANG, X., WANG, Y., LEE, K., HOU, Z., DONG, N., LI, G., LEUNG, K., HUNG, L., HE, F., ZHANG, L. & QIN, L. 2012. A delivery system targeting bone formation surfaces to facilitate RNAi-based anabolic therapy. *Nat Med,* 18**,** 307-14.

120. ZHANG, G., SHENG, H., HE, Y. X., XIE, X. H., WANG, Y. X., LEE, K. M., YEUNG, K. W., LI, Z. R., HE, W., GRIFFITH, J. F., LEUNG, K. S. & QIN, L. 2009. Continuous occurrence of both insufficient neovascularization and elevated vascular permeability in rabbit proximal femur during inadequate repair of steroid-associated osteonecrotic lesions. *Arthritis Rheum,* 60**,** 2966-77.

121. ZHANG, L., TANG, Y., TIE, Y., TIAN, C., WANG, J., DONG, Y., SUN, Z. & HE, F. 2007a. The PH domain containing protein CKIP-1 binds to IFP35 and Nmi and is involved in cytokine signaling. *Cell Signal,* 19**,** 932-44.

122. ZHANG, L., TIE, Y., TIAN, C., XING, G., SONG, Y., ZHU, Y., SUN, Z. & HE, F. 2006. CKIP-1 recruits nuclear ATM partially to the plasma membrane through interaction with ATM. *Cell Signal,* 18**,** 1386-95.

123. ZHANG, L., WANG, Y., XIAO, F., WANG, S., XING, G., LI, Y., YIN, X., LU, K., WEI, R., FAN, J., CHEN, Y., LI, T., XIE, P., YUAN, L., SONG, L., MA, L., DING, L., HE, F. & ZHANG, L. 2014. CKIP-1 regulates macrophage proliferation by inhibiting TRAF6-mediated Akt activation. *Cell Res,* 24**,** 742-61.

124. ZHANG, Z., GORMAN, C. L., VERMI, A. C., MONACO, C., FOEY, A., OWEN, S., AMJADI, P., VALLANCE, A., MCCLINTON, C., MARELLI-BERG, F., ISOMAKI, P., RUSSELL, A., DAZZI, F., VYSE, T. J., BRENNAN, F. M. & COPE, A. P. 2007b. TCRzetadim lymphocytes

define populations of circulating effector cells that migrate to inflamed tissues. *Blood,* 109**,** 4328-35.

125. ZHENG, C., YIN, Q. & WU, H. 2011. Structural studies of NF-kappaB signaling. *Cell Res,* 21**,** 183-95.

126. ZHOU, X., ZHANG, Z., FENG, J. Q., DUSEVICH, V. M., SINHA, K., ZHANG, H., DARNAY, B. G. & DE CROMBRUGGHE, B. 2010. Multiple functions of Osterix are required for bone growth and homeostasis in postnatal mice. *Proc Natl Acad Sci U S A,* 107**,** 12919-24.

127. ZWERINA, J., REDLICH, K., POLZER, K., JOOSTEN, L., KRONKE, G., DISTLER, J., HESS, A., PUNDT, N., PAP, T., HOFFMANN, O., GASSER, J., SCHEINECKER, C., SMOLEN, J. S., VAN DEN BERG, W. & SCHETT, G. 2007. TNF-induced structural joint damage is mediated by IL-1. *Proc Natl Acad Sci U S A,* 104**,** 11742-7.

CURRICULUM VITAE

Academic qualifications of the thesis author, Ms. DANG Lei:

- Received the degree of Bachelor of Science (Honours) from Guangzhou University of Chinese Medicine, June 2011.

- Received the degree of Master of Philosophy from Hong Kong Baptist University, November 2016.

June 2019